Investigation of the North Atlantic Heinrich events using molecular approach

Oksana Viktorovna Kornilova

Investigation of the North Atlantic Heinrich Events using molecular approach

Volume I: Text and Tables

University of Durham

Oksana Viktorovna Kornilova

A thesis submitted to the University of Durham in accordance with the requirements of the degree of Doctor of Philosophy in the Faculty of Science

Department of Geography

April 2005

DECLARATION

I hereby certify that the work described in this thesis is my own, except where otherwise acknowledged, and has not been submitted previously for a degree at this or any other university.

Oksana Kornilova

CONTENTS

TABLE OF CONTENTS

ACKNOWLEDGEMENTS

I would like to thank my supervisors Prof. Antoni Rosell-Melé and Dr. Ian Evans for their support, scientific guidance and patience over the years leading to the submission of this thesis. Special thanks to:
- Toni for devising this very challenging and exciting PhD project and for providing a great deal of support and encouragement.
- To Ian for looking after my interests in Durham, for help with statistics, and for his willingness to insert all those missing "thes" into the thesis.
The completion of this thesis would not have been possible without Dr Marie Russell (now at FRS Marine Laboratory). This project was started together with Marie who ordered and analysed the North American and ODP 609 samples. Special thanks to Marie for great pains she took in setting up the "Dawson lab" and organising work in it. I would like to thank James Bendle and Erin McClymont for sharing long laboratory hours, ideas and occasional frustrations.

Thanks to the scientific party and crew of the RRS *James Clark Ross* (cruise JR51) for 35 amazing days at sea, for providing great work environment and good company. Especially, the Master (C. Elliot) and PSO (Prof. J. Dowdeswell) for leading the campaign, the Deck Engineer Simon Wright for tying the lab down, Neil Campbell (BGS) for fishing up the cores and Dr Cólm Ó Cofaigh for providing core descriptions and to Toni for "fighting our corner".

I would like to thank ARCICE NERC thematic programme, British Council ORS award scheme and Department of Geography for funding my PhD.

Many thanks to Dr Francis Grousset for providing data and samples from core SU90-09, which was the focus of Chapter 4. ODP, Canadian Geological Survey and Dr H. Rashid are thanked for sediment samples. Thanks to Dr D.Gunn (SOC) for logging the ARCICE cores and to Dr Nick Cox for his help with statistics.

I also wish to acknowledge the technical support of members of the Department of Geography, Durham. Particular thanks go to Frank, Brian, Derek, Eddie and Neil for assistance in the lab and to Freda for making orders.

Finally, I would like to express my eternal gratitude to my husband Anton for his love, unconditional support, and most of all patience; to my daughter Marina for some added excitement in the writing up of the theses, to my parents and in-laws who made it all possible by taking turns at the cradle and making sure that we have the most walked baby in the neighbourhood; and to all family and friends for their support and encouragement.

ABSTRACT

The aim of this thesis is to investigate the application of biomarkers to study the provenance of allochthonous organic matter deposited in the North Atlantic during the last glacial period mainly as ice rafted debris (IRD) in Heinrich Layers (HLs). Two novel approaches are used in this work:

- *The biomarker composition of sedimentary organic matter is used to characterise and compare possible sources and sinks of IRD*
- *Glacigenic debris flows (GDFs) are used as proxies for possible sources of IRD in the deep ocean.*

The distribution of photosynthetic pigments, n-alkanes, highly branched aliphatic hydrocarbons (unresolved complex mixture (UCM) in the gas chromatogram) and long-chain alkenones in the sediments from the possible sources and sinks of IRD is analysed. Sources of IRD are represented by GDF deposits from the Nordic Seas and the western Atlantic margins. Sinks are represented by deep-sea cores containing HLs: cores SU90-09 and ODP 609 are from the main area of IRD deposition, "IRD belt", and cores MD95-2024 and HU87-025-07P are from Labrador Sea.

GDF and HL sediments generally contain a very high proportion of biodegraded and thermally mature organic matter originating from ancient outcrops eroded by former ice streams. Most hemipelagic sediments overlying GDFs or HLs in the deep-sea cores contain signatures of less reworked organic matter.

GDF sediments at the North Atlantic margins are largely homogenous in their biomarker composition; they contain biomarker distributions that are characteristic and unique to each GDF deposit and thus significantly different from those of the overlying hemipelagic sediments. It was concluded that the biomarker fingerprints of the organic matter in each GDF can be considered as combined signatures of a variety of organic-rich outcrops eroded by a particular ice stream and therefore can be used to constrain the sources of IRD in the North Atlantic.

"Typical" HLs 1, 2, 4 & 5 can be identified in the sedimentary records on the basis of the biomarker composition of sedimentary organic matter. Biomarker compositions of sediments from "untypical" HLs 3 and 6 in the two cores from the "IRD belt" differ significantly from those of the "typical" HLs 1, 2, 4 & 5 and are similar to the overlying ambient sediments. In contrast, all HL samples from the Labrador Sea core MD95-2024 are similar. A shift in oceanic Polar Front location is reflected in the biomarker composition of ambient sediments deposited after HL3 in core SU90-09. These contain highly degraded organic matter of ice rafted origin whose biomarker composition differs from that of the "typical" HLs but not from that of HL3.

The biomarker composition of the HL sediments from core SU90-09 varies both between and within HLs. All HLs in core SU90-09 can be distinguished from one another based on their biomarker composition. For the most part, the biomarker compositions of the sediments in the older HLs 4 and 5 are more similar to one another than to those in the younger HLs 1 and 2. Precursor events are recognised in the sedimentary record of HLs 1 and 2 but not HLs 4 and 5. Three steps can be distinguished in the deposition of HLs 4 and 5, with the narrow middle step different from the periods above and below it. HL1 and possibly HL2 contain two steps.

With regard to source-sink correlation, IRD in the HLs in core MD95-2024 contains a combined signal from North American and West Greenland sources. Similar signatures are present in the "typical" HLs from cores SU90-09 and ODP 609. A contribution from an additional unidentified source or sources is present in both cores, substantial in the former and minor in the latter. However, no significant input from the European ice sheets was detected. The variability between and within HLs is probably a result of variability in the relative input from different IRD sources. The biomarker composition of the "untypical" HLs 3 and 6 from ODP 609 is more consistent with aeolian rather than IRD input.

Biomarker analysis provides a potentially more detailed and more specific approach than analysis of bulk properties of sediments to characterize sources and sinks of IRD.

1. Introduction

Cover image: Terrestrial sediments frozen into ice are transported into the ocean. Photo: J. Dowdeswell.

CONTENTS

TABLES

(See volume II for figures).

1.1 The Heinrich Events

The climate of our planet is characterised by periods of rapid change. Such variability is recorded, for example, in the marine sediments and glacial archives of the Quaternary (e.g. Adams *et al.*, 1999; Alley *et al.*, 1993; Dansgaard *et al.*, 1993; Taylor *et al.*, 1993). Understanding the causes, mechanisms and consequences of climatic changes that occurred in the past is important because they provide an analogy for possible future environmental change associated, for instance, with the effects of ice cap melting in response to global warming. An important area of research is focused on the past relationships between the different ice sheets of the Northern Hemisphere and their influence on dynamics of the ocean and atmosphere systems and global climate (e.g. Broecker, 1994; Chapman *et al.*, 2000; Cortijo, 2000).

During the last glacial period, there have been several episodes of quasi-periodic iceberg discharge from the ice sheets into the North Atlantic (Heinrich Events (HEs)) (e.g. Broecker *et al.*, 1992; Grousset *et al.*, 1993; Heinrich, 1988). These episodes are recorded in Quaternary sediments as Heinrich layers (HLs), compared with ambient sediment, typically characterised by increased levels of ice rafted debris (IRD), grey reflectance, grain size and magnetic susceptibility and low abundance of foraminifera relative to IRD (Bond *et al.*, 1992; Broecker *et al.*, 1992; Heinrich, 1988). Another feature are the high sediment accumulation rates during HEs, calculated using ^{230}Th chronology (Francois & Bacon, 1994; McManus *et al.*, 1998) and ^{14}C ages (Huon *et al.*, 2002), and estimated to be higher than 4-15 cm ka^{-1} for HLs1, 2, 4 & 5 (Bond *et al.*, 1993; Bond *et al.*, 1992; Cortijo *et al.*, 1997; Grousset *et al.*, 2001; Vidal *et al.*, 1997). The main area of the IRD deposition, referred to as the "IRD belt", spreads for more than 3,000 km across the Northern Atlantic between ~40°N and 55°N (**Fig. 1.1**) (Ruddiman, 1977) with the thickness of HLs increasing westwards from a few centimetres to a meter or more towards the Labrador Sea (e.g. Bond *et al.*, 1992; Grousset *et al.*, 1993; Heinrich, 1988; Rashid *et al.*, 2003c). Outside the main "IRD belt", HLs have been recorded from the northwestern Labrador Sea (e.g. Andrews & Tedesco, 1992) to the Iberian margin (e.g. Lebreiro *et al.*, 1996). Numerous ice rafting events have also been identified in the Nordic Seas (e.g. Koç & Jansen, 1994), some of which were synchronous with the HEs.

HEs are thought to have resulted from brief periods of massive iceberg discharge primarily from the Laurentide Ice Sheet approximately every 7000 years (Andrews & Tedesco, 1992; Heinrich, 1988; MacAyeal, 1993). Six such events (HE6-HE1) lasting about 495 ±255(one standard deviation) years (Hemming, 2004 and references therein) have been recognised in the interval between past 60 and 10.5 ka. Recently, there has been a claim for an additional HL, identified between HLs 5 and 6 in the Labrador Sea (Rashid *et al.*, 2003b).

Heinrich Events correlate with shifts in other climate records such as for example Greenland ice cores (Bond *et al.*, 1993), Florida vegetation (Grimm *et al.*, 1993), Colorado lake sediments (Anderson *et al.*, 2000), corals of Papua New Guinea (Yokoyama *et al.*, 2001), Lake Baikal sediments (Prokopenko *et al.*, 2001), South-American salar (Baker *et al.*, 2001), Chinese loess (Heslop *et al.*, 1999; Porter & An, 1995) and South China Sea sediments (Chen *et al.*, 1999; Lin *et al.*, 1999). Estimations of sea surface temperatures (SST) and sea surface salinity (SSS) during HEs indicate considerable drop in both parameters (Bard *et al.*, 2000; Bond *et al.*, 1992; Cayre *et al.*, 1999; Chapman *et al.*, 2000; Cortijo *et al.*, 1997; Maslin *et al.*, 1995; Rosell-Mele *et al.*, 2002) apparently caused by fresh water release from the melting icebergs. That is thought to have resulted in a disruption of deep-water formation in the North Atlantic (Bond *et al.*, 1992; Broecker, 1994; Maslin, 1995; Maslin *et al.*, 1995; Paillard & Labeyrie, 1994). Change in thermohaline circulation is likely to have affected global climate. With no northward transportation of water and thus heat from the western tropical North Atlantic, a warming of the Southern Hemisphere should have occurred. This view is supported by the model developed by Paillard & Cortijo (1999) for HE4 and Crucifix & Berger (2002) for HE1. Comparison between marine and ice records in both hemispheres, although it should be considered with caution, suggests correlation between climatic changes of the two hemispheres (Charles *et al.*, 1996; Cortijo, 2000).

The cause of HEs still remains a mystery. The main schools of thought argue that either the internal dynamics of the Laurentide Ice Sheet, or externally forced climate change (e.g. rapid changes in sea level), influenced the ice sheet or its environment and gave rise to the events. Key to the discussion is to explain whether and why the timing of the iceberg discharges from the Laurentide Ice Sheet were synchronous with those from other ice sheets, i.e. in Europe and Iceland. Thus, an external forcing would affect

all ice sheets simultaneously and produce their simultaneous response, whereas internal failure of the Laurentide Ice Sheet would lead any responses of the other ice sheets.

The proposed external causes for the HEs are insolation changes brought about by variations in the eccentricity of the Earth's orbit (Heinrich, 1988; Mienert & Chi, 1995) or orbital inclination (Muller & MacDonald, 1995). However, the response of 3km thick ice sheets to external climate forcing is likely to be very slow (in the order of thousands of years), which does not fit with the evidence for very rapid deposition of HLs (Dowdeswell *et al.*, 1995; McCave, 1995). In addition, no correlation has been found between the timing of deposition of the HLs and any component of the Milankovitch insolation cycles (Broecker et al., 1992; Bond et al., 1993).

An alternative cause of HEs is internal collapse of the Laurentide Ice Sheet. According to MacAyeal's 'binge-purge' theory (1993), accumulation of ice in the Laurentide Ice Sheet (binge phase) and discharge of icebergs (purge) occur according to changes in basal temperature. MacAyeal (1993) based his calculations on the assumption that the release of icebergs occurred through the Hudson Strait. However, IRD from Europe, followed by that from the Gulf of St. Lawrence, precede carbonates from Northern Canada in HLs from several cores studied by Bond & Lotti (1995) and Grousset *et al.*, (2001; 2000).

As a third possible cause of HEs, sea level rise as a result of melting of European ice sheets in response to global temperature changes induced by 1,500 year Dansgaard-Oeschger cycles (Bond & Lotti, 1995) has been suggested by van Kreveld (2000). Periods of cooling preceding HEs (Bond *et al.*, 1993) and the presence of European IRD in sediment records prior to Laurentide material (Grousset *et al.*, 2001; Scourse *et al.*, 2000) support this point of view. If HEs are considered together with frequent minor ice rafting episodes between them, there is good correlation between these events and cooling episodes recorded in the Greenland ice cores (Bond & Lotti, 1995; Bond *et al.*, 1999; Thouveny *et al.*, 2000).

However, it remains unclear if this mechanism could account for the sharp onset of IRD from the Laurentide Ice Sheet and the copious amounts of icebergs necessary to explain the thickness of HLs and the consequences on oceanic circulation implied from proxy records and modelling. Recently, another hypothesis has been put forward, based

on a combination of external climate forcing and a newly observed glaciological process (Hulbe *et al.*, 2004). This proposes the existence of ice shelves along the eastern Canadian seaboard that could rapidly disintegrate as a result of climate-controlled meltwater infilling of surface crevasses.

1.1.1 Aim and objectives

The aim of this thesis is to investigate the application of biomarkers to the study of provenance of allochthonous organic matter deposited in the North Atlantic during the last glacial period.

The objectives are:

- To describe the characteristic biomarker signatures of the possible sources of IRD by using Glacigenic Debris Flows (GDF) as a source proxy of IRD in HLs
- To determine the spatial and temporal variability of allochthonous and autochthonous inputs of organic matter in deep sea glacigenic and hemipelagic sediments from several cores in the North Atlantic
- To compare the allochthonous biomarker signatures in deep-sea sediments with those described in the possible source areas to ascertain the provenance of IRD during HEs.

Key aspects of the research, which are considered testable hypotheses, are:

- That the composition of biomarkers in glacigenic sediments in the North Atlantic can be used to find out the provenance of IRD in HLs. That implies that IRD in HLs carries a biomarker signature characteristic of each source, and therefore that each source has a distinct biomarker signature or fingerprint.

- That the organic matter in the debris flow deposits in the margins of the North Atlantic has a distinct and characteristic composition, which is analogous to that of the IRD originating from the ice sheet that gave rise to the debris flows.

In addition, another goal will be to set up the appropriate analytical methodology for the rapid and routine characterisation of broad biomarker fingerprints in deep-sea sediments.

1.2 Current views on provenance of IRD in the glacial North Atlantic

In order to understand the causes of HEs, it is important to determine the source regions of IRD in different HLs, and the timing of each depositional event. Provenance studies so far have been based mostly on mineralogical (e.g. Bond & Lotti, 1995; Grousset *et al.*, 2000), petrographic (e.g. Piper & DeWolfe, 2003), isotopic (e.g. Grousset *et al.*, 1993; Gwiazda *et al.*, 1996a; 1996b; Hemming *et al.*, 1998; 2000) and elemental (e.g. Thomson *et al.*, 1995) composition of the lithic fraction of HLs, and comparison of IRD in HLs with material from various potential terrestrial sources. Other methods include study of magnetic parameters (e.g. Stoner *et al.*, 1996; 1998), micropalaeontological composition (e.g. Rahman, 1995) and bulk properties of organic matter (e.g. Huon *et al.*, 2002). Some of the results produced by these methods are contradictory. One of the reasons for this may be that different grain size fractions are used for provenance studies by different authors. Although the <63 μm fraction is more abundant in glacial sediments than the >63 μm (Andrews, 2000), it could have been transported by means other than ice rafting. Many studies concentrated on the >150 μm fraction because of its definitely ice rafted origin. However, that leads to under-representation of some of the rock types, e.g. shale (Hemming, 2004).

1.2.1 Overview of current methods used in provenance studies

1.2.1.1 Mineralogical and petrographic analysis of lithic fraction

The mineralogical composition of terrigenous grains has been used to determine the sources or IRD. Three groups of rocks are usually considered: (i) volcanic glass from Iceland, (ii) hematite coated quartz and feldspar from Proterozoic and Phanerozoic red beds of the Gulf of St. Lawrence, and (iii) detrital carbonate mainly from Palaeozoic deposits of eastern and northern Canada (Bond & Lotti, 1995; de Abreu *et al.*, 2003; Grousset *et al.*, 2001). In addition to this, Scourse (2000) proposed detrital chalk as evidence of the British Ice sheet collapse.

1.2.1.2 Analysis of magnetic parameters

Increase in magnetic susceptibility (MS) is associated with continental input into the ocean. Magnetic susceptibility measurements have been used to identify HLs (Grousset *et al.*, 1993). In that work, the peaks on MS records coincided with detrital carbonate increases and thus were interpreted as an indication of North American provenance. Detrital layers in the Labrador Sea are characterised by increased magnetic susceptibility supporting this interpretation (e.g. Stoner *et al.*, 1996). At the same time, the increase in this parameter north of 52°N is several times lower than in the "IRD belt" (Robinson *et al.*, 1995).

1.2.1.3 Isotopic analysis of mineral particles

Detailed analysis of various potential source areas showed that most of them could be distinguished on the basis of their isotopic composition. The Nd-Sr-Pb isotopic composition of bulk IRD of individual grains is widely used in provenance studies in order to constrain the basement terrain of the IRD source areas (Benson *et al.*, 2003; Grousset *et al.*, 2000; Hemming *et al.*, 1998; Innocent *et al.*, 2000). Broadly speaking, European sources are characterised by radiogenic Nd ($-15<\varepsilon_{Nd}[0]<-10$), unradiogenic Sr ($0.710<{}^{87}Sr/{}^{86}Sr<0.725$) and young Rb-Sr model (<0.5 Ga), whereas Canadian province materials (Canadian Shield, Baffin Bay & Greenland) contain unradiogenic Nd ($-45<\varepsilon_{Nd}[0]<-17$), more radiogenic Sr ($0.72<{}^{87}Sr/{}^{86}Sr<0.733$) & old Rb-Sr model (~2-3 Ga) (Grousset *et al.*, 2000).

Variation in Pb isotopes ratios were used as proxy for different IRD sources by Gwiazda *et al.*(1996a; 1996b). Hemming *et al.* (1998; 2000; 2002) used ${}^{40}Ar/{}^{39}Ar$ ages of hornblende grains, Farmer *et al.* (2003) studied Sr-Nd-Pb composition of fine sediment fraction, Fagel *et al* (2002) and Innocent *et al.*, (2000; 1997) used Sm-Nd signatures. The shortcoming of this method lies in the similar geological histories of the major landmasses surrounding North Atlantic which makes it difficult to distinguish between different potential source areas (e.g. Farmer *et al.*, 2003; Gwiazda *et al.*, 1996b). For instance, detailed analysis of the isotopic compositions of the ice-proximal glacimarine sediments and IRD in the North Atlantic (Farmer *et al.*, 2003) suggest that higher $\varepsilon_{Nd}[0]$ (>-15) could have been delivered to the North Atlantic not only from the

Fennoscandian Ice Sheet (Grousset *et al.*, 2000), but from the southeastern margin of the Laurentide Ice Sheet.

1.2.1.4 Elemental analysis

Thomson *et al.* (1995) used increases in Mg/Al ratio as a proxy for detrital dolomite from Canada. Rare-earth elemental composition was used to constrain IRD source in HL2 from the Labrador Sea (Benson *et al.*, 2003). Increase in Zr/Al, Si/Al and Ti/Al ratios in HLs was interpreted by Hinrichs *et al.*(2001) as a result of aeolian input of loess.

1.2.1.5 Micropalaeontological analysis

Use of concentration of reworked nannofossils was proposed as a proxy for input from Cretaceous chalks originating in Northern Europe (Rahman, 1995). Zaragosi *et al.* (2001) recorded dynocist assemblages of European origin preceding Canadian signature in HL from the Bay of Biscay. Reworked palynomorphs were used by Hiscott *et al.* (2001) to determine IRD sources in the Labrador Sea.

1.2.1.6 Bulk properties of organic matter

Concentrations of organic carbon (OC), total nitrogen (TN) and stable isotope ratios ($\delta^{13}C$ and $\delta^{15}N$) of fine-sized (<50 μm) organic matter in the North Atlantic core SU90-09 were used by Huon *et al.* (2002) to demonstrate a change in the sources of organic matter over the past 50 ka. The authors report contrasts in sedimentary organic matter supply between earlier (HE4 & HE5) and younger (HE1 & HE2) HEs.

1.2.2 IRD events in different areas of the North Atlantic

Based on magnetic susceptibility records, Grousset *et al.* (1993) demonstrated that the thickness of HLs 1, 2, 4 & 5 decreases from west to east, with gradients elongated around ~45°N. Similar findings were reported by Dowdeswell *et al.* (1995) for HLs 1 and 2. That indicates predominantly Hudson Strait provenance and similar pathways of icebergs for these events (Dowdeswell *et al.*, 1995; Grousset *et al.*, 1993). The distribution of HL3 shows decreasing thickness from north-west to south-east and may indicate change in the source and pathways of icebergs for this layer (Grousset *et al.*,

1993). Another indicator of a Hudson Strait source, the presence of detrital carbonate, was detected within but not outside the "IRD belt" (Bond *et al.*, 1992). Carbonates were present in all HLs from the southwestern North Atlantic but absent from HLs 3 and 6 towards the northeastern part (Bond *et al.*, 1992). Bond and Lotti (1995), however, distinguished a narrow carbonate peak in HL3 not only in core ODP 609 (49°53'N, 24°14'W) but also in the north-eastern core VM23-81 (54°15'N, 16°50'W). Absence or near absence of carbonate in some of the HLs was interpreted by Bond *et al.* (1992) as a result of melting of icebergs before reaching eastern locations. As an alternative explanation, input from the European sources of IRD was proposed (Grousset *et al.*, 1993). Although Hudson Strait appears to be the predominant source area, the existence of multiple sources of IRD, European as well as American, in the North Atlantic HLs is supported by mineralogical (Bond & Lotti, 1995; de Abreu *et al.*, 2003; Grousset *et al.*, 2001; Scourse *et al.*, 2000), isotopic (Grousset *et al.*, 2000; Revel *et al.*, 1996) and palynological data (Rahman, 1995).

Labrador Sea

Locations proximal to former ice sheets, such as the Labrador Sea and Nordic Seas, preserve more detailed sedimentary records of ice sheet instability. Detrital layers in the Labrador Sea are thought to have been deposited not only by ice rafting but also by nepheloid flow and turbidites (Andrews & Tedesco, 1992; Hesse & Khodabakhsh, 1998; Hillaire-Marcel *et al.*, 1994; Rashid *et al.*, 2003c). Andrews & MacLean (2003) suggest that meltwater discharge rather than ice rafting was the dominant process in HL formation in the Labrador Sea. Several detrital layers have been recognised based on magnetic properties of the sediments (Hillaire-Marcel *et al.*, 1994; Stoner *et al.*, 1996). Hillaire-Marcel *et al.* (1994) noted that both carbonate and coarse fraction are not consistently present in all Heinrich layers in the Labrador Sea, suggesting variability in the sources of IRD. Heinrich layers, some with high detrital carbonate content (DC) and others with low (LDC) corresponding to North Atlantic HEs were identified on the basis of ^{14}C AMS dates on *Neogloboquadrina pachyderma* (Andrews *et al.*, 1994; Andrews & Tedesco, 1992) and geomagnetic palaeointensity (Stoner *et al.*, 1998). A predominantly North American Precambrian Shield source was reported for HLs in several Labrador Sea cores from Sm-Nd isotope data (Innocent *et al.*, 1997).

Nordic Seas

Input from European ice sheets is recorded in the sediments of the Nordic Seas; increase in the IRD content and other indicators of climate change correlate well with $\delta^{18}O$ in Greenland ice cores (e.g. Andrews *et al.*, 1998; Baumann *et al.*, 1995; Dokken & Hald, 1996; Elliot *et al.*, 1998; Fronval *et al.*, 1995). Baumann *et al.* (1995) linked IRD peaks on the Vøring Plateau in the Norwegian Sea to HE2, HE3, HE4 and HE5. Fronval *et al.* (1995) also identified detrital layers, some of which correlate in time with North Atlantic HEs, in a sediment core from the Norwegian Sea. Their mineralogical composition suggested a Fennoscandian origin. A core from the continental slope south of the Denmark Strait sill, analysed by Andrews *et al.* (1998), contained two layers approximately coeval with HL1 and HL2 in the North Atlantic.

However, Dowdeswell *et al.* (1999) argue that there is insufficient evidence for such correlation since only a few IRD peaks in the Nordic Seas match HLs unambiguously and because of age uncertainty of ±2,000 years. What is more, the findings of Baumann *et al.* (1995) contradict those of Fronval *et al.* (1995). Lack of correlation between IRD layers in the North Atlantic and Norwegian-Greenland Sea was also reported by Mienert & Chi (1995) on the basis of magnetic susceptibility and density analysis of sediment cores. Based on the study of three cores from the continental slope of the Spitsbergen margin, Lloyd *et al.* (1996) maintain that IRD events in the Nordic Seas could not have correlated with HEs due to the different mechanisms of their formation.

According to Lloyd *et al.* (1996), IRD production in the Norwegian-Greenland Sea is mostly determined by moisture supply that controls ice cap accumulation and thus iceberg calving. The main source of moisture in that region is evaporation of sea surface waters. During glacial periods, sea surface temperatures in the region would be low, reducing evaporation and thus growth of Arctic ice sheets. In warmer periods, when the arctic front retreats, the inflow of Atlantic waters into the Norwegian-Greenland Sea would produce moisture supply for expansion of Arctic ice masses. The build up and collapse of ice sheets in mid-latitudes (e.g. the Laurentide Ice Sheet) would have a similar effect, leading to an antiphase relationship between ice masses in mid and

high altitudes (Boulton *et al.*, 1985). This view is supported by the fact that the Spitsbergen margin IRD peaks occur during interstadials as well as glacial periods.

Four IRD events coeval with HE1-4 were recorded in the sediments from the Fram Strait (Darby *et al.*, 2002) indicating input from Arctic sources.

1.2.3 Variability of sedimentary characteristics between HLs

Variability in the properties of sediments between so-called "typical" HE1, HE2, HE4 & HE5 and "untypical" HE3 and HE6 events in the North Atlantic is well established. HLs 3 and 6 from the cores within the "IRD belt" are characterised by lower peaks in magnetic susceptibility than HLs 1, 2, 4 & 5 (Grousset *et al.*, 2001; 1993; Robinson *et al.*, 1995) and lower mass fluxes of total sediment as calculated using U-Th isotope data (McManus *et al.*, 1998). They differ from the "typical" HLs also in their isotopic composition (e.g. Grousset *et al.*, 2000; Gwiazda *et al.*, 1996b). On the basis of Nd and Sr isotopic analysis of sediments in HLs 1, 2, 4 and 5, Grousset *et al.* (1993) named Baffin Bay as a source area of IRD in these layers. Lead isotope composition of HL2 in the "IRD belt" (Gwiazda *et al.*, 1996b) points at Churchill province of the Canadian Shield (Hudson Bay, Hudson Strait and Baffin Island) as a provenance area for this layer. Similar findings were reported by Snoeckx *et al.* (1999) for HE4 using Sr-Nd data and by Hemming et al. (1998) on the basis of $^{40}Ar/^{39}Ar$ ages of individual hornblende grains as well as Nd-Sr-Pb isotopic analysis of HLs1, 2, 4 & 5 in core V28-82 (49°27'N, 22°16'W) from the northeastern Atlantic. Pb isotope composition of these layers matches that of Baffin Island except for one isotope ratio (Hemming *et al.*, 2000). In contrast, IRD in HL3 appears to have originated primarily from Scandinavia and Greenland (Gwiazda *et al.*, 1996a). Revel *et al.* (1996) reported systematic increase eastwards in contribution from European sources in HLs 3 & 6 based on Sr-Nd isotopic composition. HL3 from the Northeastern core T88-9P, also differs from HLs 1, 2, 4 & 5 in terrigenous biomarker characteristics (Madureira *et al.*, 1997). Abreu *et al* (2003) attributed the provenance of HL3 IRD in a core from the Iberian margin (MD95-2040) to mostly Icelandic source as indicated by the presence of volcanic glass. HL4 at this location is thicker than the rest of HLs and its IRD accumulation record has a double-peaked structure (Thomson *et al.*, 1999).

There is a possibility, however, that HLs 3 and 6 in the northeastern part of the North Atlantic do not contain IRD and changes in the sedimentary records associated with these events reflect changes in sea surface temperatures and foraminifera productivity in response to iceberg release from the Laurentide Ice Sheet (Bond *et al.*, 1992). The isotopic signature (Sr, Nd & Pb) of HL3 sediments is similar to that of the background sediments (Gwiazda *et al.*, 1996a; Revel *et al.*, 1996). In the ODP 609 core (49°53'N, 24°14'W), the abundance of lithic fragments per gram of sediment in HL3 is practically indistinguishable from the ambient sediments, in contrast to HLs 1, 2, 4 & 5 (Bond & Lotti, 1995; Broecker *et al.*, 1992).

The unusual character of the North Atlantic HE3 is recorded also in the Labrador Sea. Kirby & Andrews (1999) reported absence of HL3 from the northwestern Labrador Sea and proposed a different source area (across rather than along the Hudson Strait) for this event. Based on sedimentological evidence from a number of cores, Rashid *et al.* (2003a) argue that HL3 in the Labrador Sea is similar to the other HLs and was not detected previously in some locations due to its deep burial or erosion. U/Th isotopic analysis of the HLs 0-4 in the south-eastern Labrador Sea core HU91-045-094 by Veiga-Pires & Hillaire-Marcel (1999) did not reveal significant differences in sedimentation rates between the HLs in that location. This data is supported by geomagnetic palaeointensity records (Stoner *et al.*, 1998). These results indicate a Hudson Strait provenance of IRD in HL3. However, during this event, icebergs probably did not reach as far east as during prominent HEs 1, 2, 4 and 5 (Grousset *et al.*, 1993).

1.2.4 Source variability within HEs

Bond and Lotti (1995) recorded variable input from different IRD sources within HLs 1, 2 & 4 in cores ODP 609 (49°53'N, 24°14'W) and VM23-81 (54°15'N, 16°50'W) with detrital carbonate input lagging behind basaltic glass (Iceland (Voelker *et al.*, 1998) and Irminger Basin (Elliot *et al.*, 1998; van Kreveld, 2000)) and hematite-coated quartz (East Greenland (Bond *et al.*, 1999; van Kreveld, 2000)). In a more detailed study of the northeastern Atlantic core MD95-2002, Grousset *et al.* (2000) showed that HLs 1, 2, 4 & 5 can be divided into three parts on the basis of their isotopic composition: the bottom and top parts display European origin but the middle part is of North American

derivation. A similar three-step structure was found in HL4 from the Iberian margin (SU92-28). Snoeckx *et al.* (1999) report a European signal at the beginning of HL4 in several North Atlantic cores. Scourse (2000) presents evidence of detrital chalk from the Celtic continental shelf preceding and coinciding with lithic fragments of Laurentide origin in HL2 but not HL1 from two Northeastern Atlantic cores. Based on the mineralogical and isotopic composition of IRD, Grousset *et al.* (2001) identified three phases of IRD deposition in HLs 1 and 2 in central North Atlantic core SU90-09: a European precursor event recorded by volcanic glass, a Laurentide step dominated by quartz, and finally detrital carbonate from Hudson and Baffin Bays. These results are supported by evidence from other locations, e.g. ODP 609 and VM23-81 (Bond *et al.*, 1999). What is more, source areas for precursor events to HL2 and HL4 from ODP 609 appear different from one another according to radiogenic isotope data (Vance & Archer, 2002). Piper & Skene (1998) report iceberg discharge from the continental margin of Nova Scotia as recorded by brick-red sandy mud deposits in several southwestern Labrador Sea cores, immediately preceding release of carbonate-rich IRD corresponding to HE1. Based on detailed petrographic analysis, Piper & DeWolfe (2003) report dilution of the Hudson Strait (carbonate) signal in HLs 1 and 2 in the southwestern Labrador Sea by IRD from numerous sources in Newfoundland and Nova Scotia.

High resolution isotopic analysis of lithic fraction and organic matter in HLs from North Atlantic core SU90-09 revealed that IRD deposition, and therefore iceberg discharge from the Laurentide Ice Sheet, took place in a series of pulses lasting 200-500 years (Grousset *et al.*, 2001) with short periods of hemipelagic sedimentation between them. Similar thin layers were reported in the Barra Fan recording instability of the British ice sheet (Knutz *et al.*, 2001).

1.3 Application of a novel approach to reconstruct IRD provenance

1.3.1 Debris flows as a source proxy of IRD

Provenance studies so far have been based on comparison of various properties (e.g. isotopic, mineralogical *etc.*) of IRD in the HLs with the characteristics of basement or detrital rocks exposed in the regions surrounding North Atlantic (e.g. Gwiazda *et al.*, 1996b; Hemming *et al.*, 1998; Piper & DeWolfe, 2003). The shortcoming of this approach is that properties of individual outcrops in the circum-North Atlantic area do not necessarily reflect the nature of the IRD actually transported into the ocean by icebergs. Ice-proximal sediment may present a more accurate proxy for a source of IRD. For instance, on the basis of petrographic analysis, Scourse *et al.* (2000) linked glacimarine sediments from the Irish Sea ice stream across the Celtic shelf to sediments preceding HL2 in two Northeast Atlantic cores. Farmer *et al.* (2003) used isotopic characteristics of ice proximal sediments to infer provenance of HL sediments. We propose using glacigenic debris flows (GDF) as a proxy for the source of IRD in the North Atlantic. GDF consist of sediments delivered to the continental shelf by ice streams during periods of iceberg discharge and therefore represent an integrated input of materials underlying the ice streams.

1.3.1.1 Palaeo ice streams and sedimentation at ice stream termini

During episodes of ice sheet instability, large masses of icebergs were discharged into the ocean through a series of ice streams (Stokes & Clark, 2001). Existence of these palaeo ice streams is often recorded on the continental shelf as wide bathymetric troughs containing streamlined subglacial bedforms (e.g. O Cofaigh *et al.*, 2002). When overlying readily deformable sediment, ice streams eroded and delivered to the shelfbreak large volumes of sediments (Alley *et al.*, 1989). A large proportion of sediment was deposited on the shelf break and then transported down slope by mass flow processes, mainly debris flows (GDF), forming fan-shaped, diamict-dominated sediment accumulations, Trough Mouth Fans (TMF) (e.g. Vorren & Laberg, 1997; Vorren *et al.*, 1989). TMFs are recognised as useful indicators of former ice streams (Dowdeswell & Siegert, 1999). At the same time, some of the sediment incorporated in ice was transported into the ocean by icebergs and precipitated as ice rafted debris forming HLs. Composition of the sediments in TMF deposits reflects that of the

outcrops eroded by ice streams and of IRD in the detrital layers in the deep ocean. TMF deposits consist of highly mixed, often homogenous sediments representative of large source areas that fed ice streams (e.g. King *et al.*, 1998; 1996; Vorren & Laberg, 1997). That is why we propose to use TMF sediments as a source proxy for IRD in HLs.

1.3.1.2 Major TMF deposits in the North Atlantic

Nordic Seas margins TMFs. Classical TMF model

Several well-defined TMFs are situated around the margins of the Polar North Atlantic (**Fig. 1.1**). Based on the study of these deposits, a classical TMF model was developed (Dowdeswell *et al.*, 1996; Laberg & Vorren, 2000; Vorren & Laberg, 1997). According to this model, when the ice-streams reached the shelf break, large masses of glacigenic diamict-rich sediments accumulated on the upper continental slope at the edge of cross-shelf troughs. These sediments were subsequently remobilised and transported downslope as debris flows. This resulted in fan-shaped deposits dominated by stacked debris flows (**Fig. 1.2**). Eight TMFs have been identified at the margins of the Nordic Seas (**Fig. 1.1**), ranging in size from 2,700 km^2 (Kongsfijord TMF) to 215,000 km^2 (Bear Island TMF) (Vorren & Laberg, 1997).

It is important to note that the size and architecture of debris flow deposits do not necessarily reflect the intensity of the ice streams. Specific geological conditions, such as low gradient (<1°) of continental slope, abundant readily erodible shelf sediment and a wide continental shelf facilitate TMF development (O Cofaigh *et al.*, 2003).

TMF deposits on the North American margin

The morphology and sedimentary architecture of continental slope environments in front of palaeo-ice streams on the North American margin presents a more complicated picture of sedimentary deposition than a classical TMF model suggests (O Cofaigh *et al.*, 2003). In contrast to TMF deposits around the Nordic Seas, where each TMF was formed at the mouth of a single large ice stream, glacigenic deposits in the Baffin Bay and Labrador Sea basins were fed from several ice streams along the continental margin, resulting in heterogeneity of debris flow deposits across these basins (e.g. Aksu, 1984; Hesse *et al.*, 1990). Also, in the Labrador Sea, only part of the sediment was deposited as debris flows. The predominant mechanism of sedimentation is thought to

have been suspension settling from meltwater. Direct discharge from Hudson Strait is recorded as a sandy braid-plain in the North Atlantic Mid-Ocean Channel (NAMOC) (Hesse *et al.*, 1997). On the upper slope, fine muds were deposited by meltwater plumes and subsequently remobilised by turbidites (Hesse *et al.*, 1999b).

1.3.2 Biomarker approach to infer origin of IRD in HLs

Biological marker compounds (biomarkers) are geologically occurring organic compounds with chemical structures that can be unambiguously linked to natural product precursors (Eglinton & Calvin, 1967). They are molecular fossils that preserve information regarding the contribution from different sources of biomass to sedimentary organic matter. Analysis of the abundance and distribution of biomarkers provides information on the operation of the biochemical processes in the geological past, and their response to environmental change (Eglinton *et al.*, 1992). This information cannot always be gained by geologically based measurements.

Analysis of autochthonous (formed during a period of deposition) biomarkers is used to determine variations in palaeoceanographic conditions. For instance, the relative abundance of a group of long-chain alkenones, present in marine sediments, is used to reconstruct past variations in sea surface temperatures through the U^{K}_{37} and $U^{K'}_{37}$ indexes (e.g. Brassell *et al.*, 1986a; Eglinton *et al.*, 1992; Rühlemann *et al.*, 1999). The sedimentary abundance of various phytoplanktonic biomarkers can be related to changes in primary productivity (e.g. Summerhayes *et al.*, 1995). Photosynthetic conditions can be reconstructed by analysing the presence of certain bacteriochlorophylls or their diagenetic counterparts, $>C_{33}$ porphyrins (e.g. Repeta *et al.*, 1992).

With regards to IRD sources, research has been focused on allochthonous (ancient) biomarkers. Rosell-Melé & Koç (1997) and Rosell-Melé *et al.* (1997) reported the presence of metalloporphyrins in North Atlantic sediments associated with late Quaternary deglaciation episodes. These compounds occur widely in ancient sedimentary rocks and petroleum and represent products of long-term diagenesis of chlorophyll (cf. Callot, 1991). The existing data indicate that the porphyrins were

transported with the IRD by way of erosion and advection of organic-rich sedimentary material (Rosell-Melé *et al.*, 1997).

It has been hypothesised that possible source regions of IRD possess unique compositions of allochthonous biomarkers (biomarker fingerprints). Similar fingerprints should be discovered in IRD layers originating from them (Rosell-Melé *et al.*, 1997). The existence of such fingerprints in Heinrich layers has been recorded by the same authors. HLs 2 and 4 from core BOSF 5K (50°41.3' N, 21°51.9' W) from East Thulean Rise and Norwegian Sea core M23260 were characterised by the presence of an abundant homologous series of aryl isoprenoids and two C_{40} diaromatic components with a caratenoid carbon skeleton. What is more, the distribution of components in the HLs of core BOSF 5K compares favourably with those reported for a number of Palaeozoic North American sediments (Requejo *et al.*, 1992).

1.3.3 Photosynthetic pigments

Photosynthetic organisms, such as higher plants and algae, produce a variety of pigments that undergo diagenetic transformation in the water column or at the sediment/water interface forming green sedimentary chlorins and red metalloporphyrins (e.g. Baker & Lauda, 1986; Baker & Palmer, 1979).

The early diagenetic products, chlorins, occur ubiquitously in recent sediments (Callot, 1991). The stratigraphic variations of chlorin concentration in marine sediments have been used as a proxy for changes in palaeoproductivity and preservational efficiency in the highly productive upwelling areas of the Atlantic Ocean (Brassell & Eglinton, 1986; Harris *et al.*, 1996; Summerhayes *et al.*, 1995) and in the North Atlantic and Nordic Seas (Rosell-Melé & Koç, 1997; Rosell-Melé *et al.*, 1997). Previous research shows a drop in SST during the HEs (Chapman *et al.*, 2000; Rosell-Melé *et al.*, 1997). At the same time, these events are characterised by significantly increased concentrations of chlorins. In view of the postulated low productivity during the HEs, high chlorin values were interpreted to be a result of enhanced preservation due to a reduction in the thermohaline circulation during the HEs. According to Rosell-Melé *et al.* (1997), the sudden appearance and disappearance of pigments from the

sediment record may illustrate rapid change in oceanographic conditions triggered by these events, and rapid switch between two states (on/off) of deep water circulation.

Porphyrins, on the other hand, are formed as a result of long-term degradation of chlorophyll (e.g. Baker & Lauda, 1986; Callot *et al.*, 1990). They are widely present in ancient sedimentary rocks and petroleum and the most predominant species, nickel (Ni) and vanadyl (VO) are used as a source parameter in oil-to-source rock correlation (Peters & Moldowan, 1993). Copper and nickel porphyrins are present in terrestrial accumulations of peat and coals (Sundararaman *et al.*, 1984). The presence of porphyrins in Heinrich Layers sediments has been reported for North Atlantic core BOSF 5K. The origin of these pigments was attributed to ice rafted debris from terrestrial sources (Rosell-Melé *et al.*, 1997) since no indigenous porphyrins had been observed in sediments younger than the Late Pliocene (Keely *et al.*, 1994).

Sedimentary metalloporphyrins occur predominantly as vanadium (IV) and nickel (II) complexes, *i.e.* as vanadyl (VO^{2+}) and nickel (Ni^{2+}) species. The relative proportions of these species are related to specific depositional environments. Under oxic conditions, nickel is favoured by the higher equilibrium constant for reaction with free-base porphyrins. However, under low Redox conditions, Ni^{2+} is precipitated as sulphide, leaving VO^{2+} to chelate free-base porphyrins (Lewan, 1984). Thus high *VO/(VO+Ni)* reflects anoxic conditions and vice versa (Peters & Moldowan, 1993). Also, high *VO/(VO+Ni)* has been associated with a marine origin of organic matter, and low – with terrestrial or lacustrine derivation (Peters & Moldowan, 1993).

Stratigraphic variations and relative abundances of photosynthetic pigments can be analysed using UV-visible spectrophotomentry. With a few exceptions, pigments containing a tetrapyrrolic ring have electronic spectra maximum in the near UV-visible range (350-850 nm). The Soret band (S) is the one with the highest extinction in the near UV range (350-420 nm) (Dolphin, 1978). Chlorins are characterised by the additional absorbance maximum at 665 nm (I satellite band) (Baker & Lauda, 1986). In porphyrins, this satellite band shifts to 550 nm (Ni) and 570 nm (VO). Often, an absorbance maximum at the next satellite band is visible – 510 and 530 nm respectively (Eglinton *et al.*, 1985). Photosynthetic pigments can be classified using the ratio of extract absorbance at the Soret band (410 nm) to that at a satellite band (I, 665 nm).

Due to the shift in the satellite band, this ratio (*S/I*) is higher (>10) for porphyrins than for chlorins (1-5) (Rosell-Melé *et al.*, 1997).

1.3.4 N-alkanes

Normal alkanes (n-alkanes) are straight-chain saturated hydrocarbons. They are commonly present in organic-matter-bearing sediments and usually constitute the most abundant compound class in the saturated fraction (Miles, 1994). N-alkanes are produced by higher plants as well as by bacteria and algae (Tissot & Welte, 1984). It is generally accepted that high molecular weight n-alkanes (n-C_{27-31}) originate from epicuticular waxes of higher terrestrial plants (Eglinton & Hamilton, 1967). High abundance of low molecular weight n-alkanes (n-C_{15-19}) is associated with input from marine or lacustrine algae (Gelpi *et al.*, 1970; Tissot & Welte, 1984). Bacterial input (nC_{10-29}) is usually insignificant (Comet & Eglinton, 1987). The presence of n-alkanes in marine sediments has often been associated with aeolian dust inputs (Simoneit, 1977). Madureira *et al.* (1997) interpreted the presence of n-alkanes in Heinrich layers in the northeast Atlantic core T88-9P as a result of such input as well as ice rafting. Villanueva *et al.* (1997), demonstrated the ice rafted origin of n-alkanes in HLs from two cores (SU90-08 and SU90-39).

Long-chain n-alkanes were found to be more resistant to oxic degradation in the water column than some other biomarkers, e.g. sterols and alkenones (Damste *et al.*, 2002). That should have allowed n-alkanes from IRD to be deposited in HLs with little or no alteration. Therefore, they may present a valuable proxy for IRD sources in HLs. In the work of Madureira *et al.* (1997) HL3 differed from HLs1, 2 & 4 in the concentration of n-alkanes and in their relative distribution. That could reflect a different source of IRD in this layer. Gas chromatographic fingerprints are often used in the petroleum industry for correlation purposes (Peters & Moldowan, 1993; Tissot & Welte, 1984). The distribution of n-alkanes reflects both the depositional environment and the degree of reworking of organic matter. They are often present in higher abundance than other compound classes and are easily recognised on a gas chromatogram, therefore they do not require any additional analytical procedures such as for instance mass spectrometry. It was hypothesised that different potential sources

of IRD could be distinguished on the basis of the absolute and relative abundances of n-alkanes. Below, the parameters that can be used to distinguish between different n-alkane sources are discussed.

1.3.4.1 Relative abundance of high molecular weight n-alkanes

The ratio of high molecular weight n-alkanes to low molecular weight ones (**Table 1.1**) can be used to estimate relative input from terrestrial (higher plant) vs. marine (algal) sources of *n*-alkanes in recent sediments. In ancient sediments, however, the abundance of short chain compounds in terrestrially derived organic matter increases with maturation, and n-alkane envelope (in a chromatographic trace) becomes displaced towards lower molecular weight homologues (Peters & Moldowan, 1993). A high concentration of the short-chain n-alkanes in ancient sediments may be a result of biodegradation, e.g. diagenetic transformation of functionalised aliphatic precursors such as n-carboxylic acids of the sediment's organic matter (Tissot & Welte, 1984). The presence of allochthonous organic matter of predominantly terrigenous and reworked (mature and biodegraded) nature in the glacial deposits in the Nordic Seas has been reported previously (Wagner & Henrich, 1994). The ratio of high molecular weight to low molecular weight n-alkanes can be used to distinguish between different potential sources of IRD. In HLs, however, the values could be biased due to the allochthonous input of low molecular weight components. That input reflects productivity which is decoupled from glacial-interglacial processes (Villanueva *et al.*, 1997) and preservation of organic matter that may be enhanced during HEs (Rosell-Melé & Koç, 1997). Hence this parameter may prove less useful when analysing HL sediments.

1.3.4.2 Relative abundances or the long-chain n-alkanes (n-C_{27}, n-C_{29} and n-C_{31})

The relative abundance of the long-chain n-alkanes (n-C_{27}, n-C_{29} and n-C_{31}) is thought to reflect the source of organic matter, n-C_{31} originating from grass and n-C_{27}, n-C_{29} from woodlands (Cranwell, 1973; McCaffrey *et al.*, 1991). Brault *et al.* (1988) attributed predominance of n-C_{29} to a marine background signal, and that of n-C_{31} to terrigenous. The relative abundance of n-C_{27} was shown to increase with change in the type of the source vegetation as a result of the climatic warming (Brincat *et al.*, 2000). In HL sediments, the relative abundance of the long-chain n-alkanes also reflects the degree of

reworking of ice rafted ancient organic matter (Peters & Moldowan, 1993; Tissot & Welte, 1984).

1.3.4.3 Carbon Preference Index (CPI)

Carbon preference index (CPI) is a ratio of abundances of n-alkanes with odd carbon numbers to those with even carbon numbers (Bray & Evans, 1961) (**Table 1.1**). The low molecular weight n-alkanes of algal origin show an odd carbon number predominance with maximum at nC_{17}, whereas terrestrial n-alkanes demonstrate no predominance in that range. In contrast, terrestrial high molecular weight n-alkanes are characterised by high CPI while those derived from algae show no preference or a slight even-carbon predominance at high molecular weight (e.g. Brassell, 1993; Brassell *et al.*, 1978). For sediments with reworked organic matter, high CPI values (>3) are associated with younger organic matter (Fahl & Stein, 1999). CPI <3 is attributed to fossil sources. With maturity, CPI tends to approach 1 (Peters & Moldowan, 1993).

1.3.4.4 Average Chain Length (ACL)

Average chain length (ACL) (**Table 1.1**) is also thought to reflect variability in the source of organic matter (Madureira *et al.*, 1995) with shorter values characteristic of organic matter formed in cooler climates (Poynter *et al.*, 1989). Lower ACL values are expected for ancient sediments as a result of reworking of organic matter (Peters & Moldowan, 1993).

1.3.4.5 Pristane to phytane and isoprenoid/n-alkane ratios

Pristane (C_{19}) and phytane (C_{20}) are isoprenoids derived from phytol, a diagenetic product of chlorophyll. They are easily recognised on the gas chromatogram as eluting after nC_{17} and nC_{18}. Their ratio (*Pr/Ph*) <0.6 is thought to indicate degradation of phytol under anoxic conditions, and >3 is indicative of an oxic depositional environment of terrestrial organic matter (Peters & Moldowan, 1993). However, many other factors may affect the *Pr/Ph* ratio such as input from archaeal lipids (Goosens et al., 1984 in Peters & Moldowan, 1993), coelution on a chromatographic trace (Volkman & Maxwell, 1986 in Peters & Moldowan, 1993) and maturity of organic matter (Ten Haven et al., 1987 in Peters & Moldowan, 1993). Pristane/C_{17} and phytane/C_{18} are also used in correlation studies. Higher values of these ratios are associated with higher

degree of biodegradation and low maturity (Peters & Moldowan, 1993 and references therein). For the purposes of this study, the interpretation of *Pr/Ph* and isoprenoid/n-alkane ratios is less important than the fact that they reflect depositional conditions, organic input and maturity, and therefore may be used to distinguish between different sources of organic matter in the ocean.

1.3.4.6 Unresolved Complex Mixture (UCM)

Unresolved complex mixture (UCM) appears on a gas chromatogram as a hump rising from the baseline, and presents a mixture of various branched and cyclic compounds that could not be separated by gas chromatography. It is a result of biodegradation of the organic matter in the original sediment source (Peters & Moldowan, 1993). UCM found in marine sediments is often associated with petroleum contamination (e.g. Volkman *et al.*, 1992). It may also signify the presence of reworked terrestrial organic matter such as was reported by Wagner and Henrich (1994) to be present in glacigenic sediments of the Nordic Seas.

1.3.5 Other biomarkers

More detailed information on the source of organic matter can be derived from the analysis of other classes of biomarkers, e.g. terpanes, steranes, aromatic and polar compounds (Peters & Moldowan, 1993; Peters *et al.*, 2000). Specific biomarkers diagnostic of a particular source and absent from other sources may be identified. These biomarkers cannot be identified using gas chromatography alone and gas chromatography-mass spectrometry (GC-MS) or gas chromatography-mass spectrometry - mass spectrometry GC-MS-MS is required to determine the structure of individual compounds.

Table 1.1 List of variables used for comparison of biomarker composition of different potential sources and sinks or IRD in the North Atlantic.

Variable	Description	Reference
S/I	Ratio of absorbance in Soret band (410 nm) to a satellite band (665 nm)	(Baker & Lauda, 1986)
$\frac{VO}{VO+Ni}$	Relative abundance of vanadyl porphyrins	(Lewan, 1984)
TNA (ng/g)	Total amount of n-alkanes per gram dry weight	
$\frac{\sum C_{29-31}}{\sum C_{29-31}+\sum C_{17-19}}$	Relative abundance of long-chain n-alkanes	(Peters *et al.*, 2000)
C_{27}/C_{29}	Ratio of n-C_{27} alkane to n-C_{31} alkane	(Cranwell, 1973; McCaffrey *et al.*, 1991)
C_{29}/C_{31}	Ratio of n-C_{27} alkane to n-C_{29} alkane	
$CPI_{17\text{-}23}$	Carbon preference index (n-$C_{17\text{-}23}$ and n-$C_{23\text{-}31}$)	(Bray & Evans, 1961)
$CPI_{24\text{-}31}$	$CPI = \frac{1}{2}\left(\frac{\sum C_n}{\sum C_{n-1}} + \frac{\sum C_n}{\sum C_{n+1}}\right)$	
$ACL_{25\text{-}33}$	Average chain length $ACL_{25-33} = \frac{25C_{25}+27C_{27}+29C_{29}+31C_{31}+33C_{33}}{C_{25}+C_{27}+C_{29}+C_{31}+C_{33}}$	(Poynter *et al.*, 1989) (Ternois *et al.*, 2001),
UCM/g (ng/g)	Unresolved complex mixture per gram dry weight	(Simoneit & Mazurek, 1982; Volkman *et al.*, 1992)
UCM/TNA	Ratio of UCM amount to that of total n-alkanes	
Pr/Ph	Pristane to phytane ratio	(Peters & Moldowan, 1993)
Pr/C_{17}	Pristane to nC_{17} alkane ratio	(Lijmbch, 1975 in Peters & Moldowan, 1993)
Ph/C_{18}	Phytane to nC_{18} alkane ratio	

2. Experimental Methodology

Cover image: MARS 5 microwave accelerated reaction system. A method was developed for rapid extraction of sediment samples.

CONTENTS

TABLES

(See volume II for figures).

2.1 Introduction

The overview of methods used for sample preparation and analysis is shown in **Fig. 2.1**. All samples underwent comparable treatment. Blank analyses were routinely carried out to check for contamination of solvents, utensils or apparatus prior to and during the analysis of samples.

In the course of this study, a method for microwave assisted extraction of biomarkers from marine sediments was developed (Kornilova & Rosell-Melé, 2003). It is presented in Section 2.5.

2.2 Wet-chemistry

2.2.1 Chemicals and preparative equipment

Glassware

Prior to the first use, disposable and reusable glassware was cleaned by firing at 450 °C for 12 hours. Reusable glassware was cleaned between uses by soaking in a solution of nitric acid (1%) for at least 8 hours, followed by rinsing with tap water, and at least 8 hour soaking in a solution of Decon soap (Decon Laboratories Ltd, Hove, UK) (5%). It was rinsed with tap water and then deionised water, dried and fired at 450 °C for 12 hours.

Reagents and Solvents

Details of general-purpose solvents and reagents used for sample preparation and analysis are listed in **Table 2. 1.** Anhydrous crystalline Na_2SO_4 (drying agent), was extracted with dichloromethane (DCM) in batches (100g) in a Soxhlet apparatus and fired at 450 °C for 12 hours.

Table 2. 1 Notation, source and properties of solvents and reagents used in experimental procedures. Source notes: (1) Fisher Chemicals Ltd, Loughborough, UK; (2) BDH Chemical Ltd, Poole, UK; (3) Sigma Aldrich, Gillingham, UK.

Name	Abbreviation	Provider	Grade
Acetone	---	1	Certified® 99.84 by GC
2,2,4-trimethylpentane	iso-Octane	1	Specified® 99.99 by GC
N-hexane	---	1	Distol®
Methanol	MeOH	1	Distol®
Methylene chloride	DCM	1	Certified®
NN-Bis (trimethylsilyl) trifluoracetamide	BSTFA	3	98%
Nitric acid	HNO_3	2	Analar® 69-70.5%
Sodium Sulphate (anhydrous)	Na_2SO_4	1	Certified® 99.50%
Urea	---	1	Certified® 99.70%

Standards

Compounds used as internal and recovery standards are listed in Table 2. 2. Standards were prepared as *iso*-Octane solutions in glass volumetric flasks. A "mixed sediment standard" was used for measuring preparative and analytical precision. This consisted of a homogenised mixture of oceanic sediments collected from a number of locations in the Nordic Seas. One sample of this standard was extracted and analysed with each batch of samples in order to monitor the reproducibility of the processing of samples and analytical procedures. A "sediment blank" was used to monitor for contamination during the preparative and analytical procedures. It was prepared from a homogenised mixture of oceanic sediments by combustion in a furnace at 800 °C to remove all organic matter.

Table 2. 2 Notation and properties of standards used in experimental procedures. Source notes: all standards were obtained from Sigma-Aldrich, Gillingham, UK.

Name	Notation	Properties
Dotriocontane	n-C_{32}	97%
Hexatriocontane	n-C_{36}	97%
Cholestane	---	98%
Cholesterol	---	99+%
5α-Cholestane-3-one	Cholestanone	97%
2-Octyldodecanoic acid	---	96%

2.2.2 Sample workup

Lipid extraction

- The freeze-dried sediments were homogenised to a fine powder in their glass storage vials with a spatula and glass pestle (both implements were rinsed with DCM and dried between samples).
- Weighed aliquots of the crushed samples (0.2-5g) were transferred to pre-weighed Teflon™ microwave vessels. A known concentration of internal standard and 10 ml of DCM/MeOH (3:1) was added.
- Batches of 12 vessels (10 validation samples, 1 blank and 1 "mixed sediment standard") were loaded into the MARS 5 microwave and extracted at 70°C for 5 minutes. See **App.1** for a list of preparative equipment.
- After extraction, the solvent/sediment mixture was transferred from the microwave vessels to test tubes and centrifuged (3000rpm for 5min). The solvent supernatant containing lipid extracts was decanted to a 15 ml Pyrex test-tube.
- To increase recovery, an additional 3ml of DCM/MeOH (3:1) was added to the extracted sediment and the mixture was shaken. The solvent/sediment mixture was again centrifuged (3000rpm for 5min) and the 2nd supernatant product was added to the test tube containing the first.
- The combined solvent extract was concentrated to dryness in a centrifugal evaporator or with nitrogen blow-down.
- To remove residual water, the dry extract was redissolved in 300μl of DCM and eluted through a glass pipette containing extracted cotton wool and anhydrous crystalline sodium sulphate. This operation was repeated three times.
- The dried extracts were placed in a vacuum manifold and the solvent was removed under a gentle stream of nitrogen and a light vacuum, and subsequently stored (sealed) at -20°C until pigment analysis or fractionation.
- The organic extracts were re-dissolved in 500-2000μl of acetone. An aliquot of 30μl from each vial was injected on the HPLC for pigment analysis,

collected and combined with the total sample, taken to dryness with nitrogen and stored (sealed) at -20°C ready for fractionation.

Compound class fractionation and sample cleanup using high performance liquid chromatography (HPLC)

Sediment extract clean-up and fractionation was necessary to remove polar compounds that may interfere during GC analysis of the sample and to separate the total extract into fractions containing the analytes of interest (*n*-alkanes, alkenones, nickel and vanadyl porphyrins). Previously, asphaltenes were precipitated with excess n-hexane and the remaining fraction (maltene) was used for further analysis. The latter was separated into 4 fractions using high performance liquid chromatography (HPLC) adapting the method by Schulz *et al.* (2000). The system used consisted of quaternary pump (Dionex), connected to a guard column (5mm) and ThermoQuest/Hypersil column (250X4.6 mm) packed with LiChrospher Si 100 (5 μm silica). Total extracts (maltenes) were re-dissolved in 30 µl of n-hexane and injected via a 20 µl loop into the HPLC system with a flow rate of 2 ml/min. Four fractions were obtained, which were collected using the Foxy Jr. fraction collector (ISCO, Inc.). The details are presented in the **Table 2. 3**.

The reproducibility of the fractionation procedure was tested with a mixture of standards (hexatriacontane, cholestane, 2-nonadecanone, $C_{37:2}$ alkenone, $C_{37:3}$ alkenone, 5αcholestan-3-one, cholesterol, 1-docosanol) at a concentration of ~100ng/μl for all standards except for the alkenones, which had a combined concentration of ~20ng/μl. Recoveries of the fraction classes were greater than 90-98% for all standards with a precision of ±3.3% (at 95% confidence). The U^{K}_{37}' value of the synthetic alkenone standards (~0.2) was not significantly altered by the procedure. The accuracy at 2σ being 0.008 U^{K}_{37}' units (by GC-FID), or 0.11°C using the Muller *et al* (1998) calibration. The system was controlled with the Chromeleon software (Dionex).

Table 2. 3 Solvents and elution volumes used to fractionate maltene extract by HPLC.

Fraction	Solvent	Volume	Compounds classes
1	n-hexane	5.5 ml	aliphatic hydrocarbons
2	n-hexane/ DCM (90:10; v/v)	14 ml	aromatic hydrocarbons
3	DCM	9 ml	aliphatic ketones (alkenones) and some alcohols
4	acetone	9 ml	"polars" (e.g. sterols, and fatty acids)

Derivatisation

Fractions containing polar compounds (total sample and fractions 3 & 4) were sylilated with BSTFA (NN-Bis (trimethylsilyl) trifluoracetamide). Dry fractionated extracts were dissolved in 100 μl DCM and 40 μl of BSTFA in a GC vial, which was sealed and left overnight at room temperature, or alternatively for 1 hour at 80°C. The solution was spiked with a recovery/GC standard of a known concentration, dried (vacuum manifold or Centrivap@) and stored in a fridge until GC analysis. Prior to this, the dry, fractionated and silylated extracts were redissolved in iso-Octane (10-500μl).

2.3 Instrumental analysis

2.3.1 Total Organic Carbon

Total organic carbon (TOC) content was determined on a CHN elemental analyser (EA1108, Carlo Erba Instruments). Silver cups (4x3.2 mm; Cat. #D2000) were cleaned by Soxhlet extraction with an acetone/hexane mixture (1:1) for 8 hours, dried in a fume cupboard and heated at 250°C for 12 hours. Approximately 1 mg of the dry sediment was placed into each silver cup. The cups were placed on a Teflon plate and left overnight in a desiccator to eliminate moisture. To remove inorganic carbon (i.e. carbonate), samples were saturated with deionised water (1-2 drops were added to each cup using a syringe) and placed in a 2500 ml desiccator containing ~250 ml concentrated hydrochloric acid for 5 hours. The acid in the desiccator was replaced with each new batch of samples (~ 80 samples in a batch). In some of the samples, the carbonate content was very high which resulted in decarbonation reaction being too rapid risking spillage and cross contamination. For those samples, the removal of carbonate was performed in the refrigerator overnight. HCl and water were removed by placing samples in an oven at ~50°C for 1.5 hours. After that procedure, the caps were closed and left overnight in a desiccator.

2.3.2 Photosynthetic pigments

To determine the total content of tetrapyrrolic photosynthetic pigments, (i.e. chlorins and porphyrins), sample extracts were redissolved in 0.03-1 ml of acetone and analysed by visible spectrophotometry using an HPLC system, consisting of Dionex P 580 series pump attached to a Dionex PDA-100 photodiode array detector with a 20 μl injection loop. 30 μl of extract was injected. Acetone was used as a mobile phase. An absorbance spectrum was generated for a range of UV-visible wavelengths (λ = 380-800 nm). Total photosynthetic pigments content was estimated by measuring the absorbance of the extracts in the Soret band (the band with the highest extinction coefficient in the near-UV range, i.e. 360-420 nm). Absorbance in the satellite bands was also recorded for the quantification of specific pigment classes, namely chlorins (665 nm) and porphyrins (510 & 550 nm for nickel and 530 & 570 nm for vanadyl species) (Eglinton *et al.*, 1985).

The relative magnitude of an absorbance for a given wavelength (A_λ) and dilution faction (DF) per gram dry sediment (M) was expressed as P_λ and calculated by:

$$P_\lambda = \frac{(A_\lambda \times DF)}{M}$$

Analytical precision was determined by triplicate analysis of most samples analysed. The relative standard deviation was consistently <5%. The spectrophotometer light source was allowed to stabilise for one hour prior to analysis and blanks and mixed sediment standard samples were analysed with each batch to account for errors from any systematic day-to-day shifts in instrumental response. The analysis of pigments was a non-destructive procedure and the samples were retained for subsequent analysis.

Abundances of Ni and VO porphyrins were calculated by integrating absorbance peaks at 550 and 570 nm from UV-VIS spectra. Then, relative abundance of vanadyl porphyrins in each sample was calculated as a ratio of VO porphyrins to total Ni and VO porphyrins.

2.3.3 Lipid hydrocarbons

Identification of GC amenable compounds was made by comparison with authenticated standards and relative retention times whenever possible. Quantification of lipids was performed on a gas chromatograph fitted with a flame ionisation detector (FID) (CP-3800, Varian Ltd.) with a temperature programmable split-splitless injector. Injector temperature was held at 85°C for 0.1 minute and then rapidly increased to 250°C. Separation was performed using a BP1 fused silica capillary column (50m length x 0.32mm internal diameter, 0.25 μm film thickness). Hydrogen was used as carrier gas (12 psi) and the oven temperature program was 50°C to 140°C at 10°C/min, 140°C to 310°C at 6°C/min and 310°C for 5-35 min.

Data acquisition and compound quantification was performed on Chromeleon software (Dionex). The internal standard used for the quantification of the aliphatic fraction was hexatriacontane (nC_{36}), for aromatic fraction Cholestane was used, Cholestanone was a standard for alkenones and other ketones, and Cholesterol and 2-

Octyldodecanoic acid were used for all other compounds. Where an internal standard was not already present (i.e. added as a recovery standard before extraction) it was added prior to the HPLC separation step or the derivatisation step.

When necessary, chemical structure of the individual compounds was confirmed by mass spectrometry (MS). Gas chromatography mass spectrometry (GC-MS) was performed using HP6890 Gas Chromatograph coupled to MS5973 Mass Spectrometer (HP/Agilent). Injector temperature was 300°C (splitless mode). Separation was achieved with an HP-5MS capillary column (30 m x 0.25 mm internal diameter, film thickness 0.25 μm). Helium was used as a carrier gas (10.58 psi) and the oven-temperature program was 80°C to 150°C at 15°C/min, 150°C to 300°C at 6°C/min and 300°C for 30 minutes. The mass spectrometer was operated in electron impact mode (ionising energy of 70 eV); ion source temperature of 250°C), mass range m/z 40-800. Individual compounds were identified by comparing mass spectra with that in literature sources.

2.4 Data Analysis

Biomarker composition of different samples was compared using a set of parameters borrowed from oil exploration/geochemical research (e.g. Ficken & Farrimond, 1995; Peters *et al.*, 2000). In order to reduce dimensionality of the dataset, principal component analysis (PCA (Davis, 1986)) was used. PCA summarizes the bulk of the variability in the multivariate data set in a small number of "principal components" (PC) which are linear combinations of the original variables (Meglen, 1992). That allows graphic display of the data using 2-4 variables (PC) that represent most of the variability from the original dataset. Biomarker composition of different types of samples was conducted using multivariate analysis of variance (MANOVA) with PC1, PC2, and PC3 as dependent variables. Analysis of variance (ANOVA) of individual variables was conducted when necessary to obtain more detailed information. In order to assess the contribution of individual variables in the overall variability of the biomarker fingerprints of different samples, multinomial logistic regression (mlogit) was used. All the above-mentioned analyses of data were performed using the Stata statistics package.

2.5 Application of microwave-assisted extraction to the analysis of biomarker climate proxies in marine sediments

2.5.1 Introduction

Microwave assisted extraction (MAE) is based on the direct application of electromagnetic radiation to a material (e.g. organic solvent, plant tissue) which has the ability to absorb electromagnetic energy (microwaves) and to transform it into heat. Unlike conventional heating by infrared energy or thermal conductivity, the increase in temperature occurs simultaneously in the whole volume of solvent. This process is caused by the multiple collisions of the solvent molecules as they realign in the oscillating electromagnetic field, generating energy in the form of heat (Letellier & Budzinski, 1999). Compared with conventional methods, such as ultrasonic extraction and Soxhlet extraction, the advantages of MAE are reported to be a higher recovery of the analyte, shorter extraction times and the use of smaller quantities of solvent (e.g. Blanco *et al.*, 2000; Jayaraman *et al.*, 2001; Pastor *et al.*, 1997; Tomaniová *et al.*, 1998).

MAE can be performed in open or closed vessels (see review in LeBlanc, 1999). In open systems, the extraction occurs at atmospheric pressure and with variable energy input. In closed systems, extraction takes place at controlled pressure (up to 5 atm) and a temperature that may exceed the boiling point of the solvent under atmospheric conditions, to increase extraction efficiency. In commercially-available closed systems, a large number of samples can be processed simultaneously.

Since the introduction of MAE of organic compounds by Ganzler et al. (1986), the application of open systems has been reported for the extraction of a wide range of components, including polyaromatic hydrocarbons (PAHs), phenols, total petroleum hydrocarbons, pesticides, polychlorinated biphenyls (PCBs), triazines and fats from a variety of matrices, e.g. soils, sediments and biological tissues (see Camel, 2000; Eskilsson & Björklund, 2000; Kaufmann & Christen, 2002; Letellier & Budzinski, 1999; Letellier *et al.*, 1999 and references therein). Nonetheless, to our knowledge, MAE in closed vessels has not been previously employed in biomarker studies.

Here, the optimisation of MAE of biomarkers belonging to two distinct compound classes, namely chlorins and long-chain C37 alkenones, used as

palaeoclimate proxies in marine sediments, is presented and appraised. Sedimentary abundance of chlorins can be related to past changes in primary productivity in the depositional environments (e.g. Rosell-Melé, 1994, Sumerhayes et al., 1995 and Harris et al., 1996). For example, the presence of certain bacteriochlorophylls or their diagenetic counterparts (>C33 porphyrins, e.g. Repeta et al. (1989) can be used to reconstruct the occurrence of anoxygenic photosynthesis. Alkenones in sediments are used to calculate the U^{K}_{37}' index, a proxy for past sea surface temperatures (Brassell et al., 1986 and Prahl and Wakeham, 1987), which is calculated from the relative abundance of C37:2 [heptatriaconta-(15E,22E)-dien-2-one] and C37:3 [heptatriaconta-(8E,15E,22E)-trien-2-one] unsaturated ketones. Reconstruction of sea surface temperatures is based on the linear relationship between U^{K}_{37}' and temperature (Prahl and Wakeham, 1987 and Müller et al., 1998).

In order to produce a detailed and meaningful palaeoclimatic record, it is necessary to process a large number of samples usually characterised by small size (~1 g) and low organic matter content. Ultrasonic extraction is often the preferred method of sample preparation in palaeoclimate studies (e.g. for the alkenones, see Rosell-Melé et al., 2001). It is a relatively inexpensive procedure, although arguably, both time- and labour-consuming since repeated extraction of the sediment is required to extract the analytes with a recovery close to 99%. A fast alternative is accelerated solvent extraction (ASE), based on applying high temperature and pressure to the sample in a relatively low amount of solvent. Commercial systems are expensive and completely dedicated to the operation. As an alternative, MAE, which is widely employed in the acid digestion of sediments and minerals, was examined. The commercial options are cheaper for MAE than ASE while allowing the simultaneous extraction of multiple samples. The tests have been performed in a commercially available device, and the results are compared with those from the extraction of the same samples using an ultrasonic bath.

2.5.2 Experimental

2.5.2.1 Ultrasonic extraction

Approximately 1 g of freeze-dried and homogenised sediment was extracted using 4 ml of dichloromethane/methanol mixture (3:1) in an ultrasonic bath (Decon Lab Ltd.). Each sample was extracted three times for 15 min. The supernatant was separated from the sediment by centrifuging at 3000 rpm for 5 min in a Mistral 2000 centrifuge (MSE) and then decanted. The solvent from the combined supernatant was removed using a CentriVap Vacuum Concentrator (Labconco).

2.5.2.2 MAE

As in the ultrasonic method, ~1 g of freeze-dried sediment was extracted with dichloromethane/methanol (3:1). The method is described in Section 2.2.2.

2.5.2.3 Quantification of biomarkers

See Sections 2.3.2 and 2.3.3.

2.5.3 Results and discussion

2.5.3.1 Influence of key parameters

Previous studies have established that the efficiency of the recovery of the analyte depends on the extraction conditions, although there is no complete agreement on the significance of the various potentially key factors such as temperature, volume of solvent and extraction time. Most studies show increase in extraction efficiency with increase in temperature due to improved desorption of the analytes from the matrix and higher analyte solubility (e.g. Chee *et al.*, 1996; Llompart *et al.*, 1997; Lopez-Avila *et al.*, 1995). Also, at higher temperatures, solvent viscosity and surface tension decrease, facilitating penetration of the matrix (e.g. sediment). Other researchers, however, report no significant influence of temperature on recovery (e.g. Barnabas *et al.*, 1995; Silgoner *et al.*, 1998). Reduced yields have been reported in some cases, probably due to degradation of thermolabile compounds (e.g. Font *et al.*, 1998; Lopez-Avila *et al.*, 1996). Most researchers have found that a change in the volume of solvent employed does not lead to a significant variation in the recovery of analytes (e.g. Barnabas *et al.*, 1995; Hasty & Revetz, 1995). A few studies, however, did

observe that the amount of solvent employed varied with extraction efficiency. For instance, (Chee et al., 1996) reported decreased recovery of PAHs with an increase in solvent volume. A common observation, however, is that it is necessary for the whole sample to be immersed in solvent to avoid electrical arcing (Barnabas et al., 1995). Finally, extraction time (time interval after the extraction temperature is reached) of 5 min or less is often reported as sufficient for an extraction efficiency similar to or higher than that achieved using traditional methods (e.g. (e.g. Carro *et al.*, 1999; Chee *et al.*, 1996). Others, however, found it necessary to employ longer extraction times to obtain maximum recovery of analytes (e.g. Font *et al.*, 1998; Molins *et al.*, 1997; Silgoner *et al.*, 1998).

The significance of the potentially three key factors (temperature, volume of solvent and extraction time) identified by previous workers and the interaction between them were studied in a screening factorial design. To simplify the procedure, only yields of chlorins were analysed in this part of the study. A set of eight experiments was carried out with each factor at two levels, usually known as 'high' and 'low' (**Table 2.4 and Table 2.5**; (Miller & Miller, 1993 p.185). The conditions chosen for MAE were as similar as possible to those for ultrasonic extraction to facilitate comparison between both methods. The temperatures employed were lower than those reported by previous workers in order to shorten cooling times and prevent possible decomposition of some of the analytes at higher temperatures. To evaluate the precision of the method, each experiment was performed in triplicate.

Table 2. 4 Levels of factors for the screening design.

Factor	Low (-)	High (+)
Volume of solvent (V), ml	4	16
Temperature (t°), °C	40	80
Extraction time (τ), min	5	15

Table 2. 5 Design matrix and response values in factorial design. Yield of pigments is normalised to the highest value (80°C, 16 ml solvent and 5 minutes holding time). Results for ultrasonic extraction (US) are included for comparison

run no.		temperature (T)	volume of solvent (v)	extraction time (t)	relative yield of pigments, %	RSD, %
1	-	-	-	-	73	4.4
2	t	-	-	+	74	1.5
3	v	-	+	-	81	2.4
4	tv	-	+	+	65	2.0
5	T	+	-	-	91	4.5
6	tT	+	-	+	89	3.6
7	vT	+	+	-	100	4.0
8	vtT	+	+	+	97	1.0
9	US				90	3.1

The results of the significance study are shown in **Table 2.5** and **Fig. 2.2** (note that the that relative standard deviation, RSD, did not exceed 4.5%). The effect of each individual factor was assessed by calculating the average difference in response (recovery of chlorins) between the experiments when the levels of the other factors remained fixed. This and the interaction between each pair of factors (e.g. temperature plus volume, volume plus time, etc. — first order interactions) and between all three factors (second order interaction) were calculated according to the procedure outlined in (Miller and Miller, 1993, p. 181). An analysis of variance (ANOVA) was carried out to test the statistical significance of each factor and interaction.

In this design, only the effect of temperature appears to be significant (**Fig. 2.3**). Therefore, only this parameter was optimised to maximise extraction efficiency. It was also evident that MAE at 80 °C produced chlorin recoveries comparable to those obtained by ultrasonication (**Table 2.5** and **Fig. 2.2**). In addition, when using MAE, it was found to be sufficient to extract each sample only once to obtain yields equivalent to those obtained using ultrasonication with three extractions (**Table 2.5** and **Fig. 2.2**). It is apparent that our results show that MAE is a faster and less labour-

consuming method than ultrasonication. Arguably, the higher temperature used in MAE may lead to alteration in the original composition of individual chlorins in the sediment. However, the wavelength of 410 nm used for measurement of chlorin abundance here and in other palaeoclimate investigations only accounts for the presence of the ring structure of the chlorins, not the substituents (Jeffrey *et al.*, 1997). Hence, structural alteration of the chlorins would be irrelevant to these results.

Table 2. 6 Relative recovery of biomarkers using ultrasonic extraction (US) and microwave assisted extraction (MAE) at different temperatures, normalised to MAE at 70°C for alkenones ($C_{37:2}$+$C_{37:3}$) and at 110°C for chlorins. RSD - relative standard deviation, STDEV - standard deviation. U^{K}_{37}' is expressed as the mean and, in parentheses, standard deviation.

		yield of alkenones, %	RSD, %	yield of chlorins, %	RSD, %	U^{K}_{37}'	STDEV
US		60	6.0	80	3.1	0.538	0.011
MAE	50°C	72	4.1	81	5.0	0.554	0.013
	60°C	77	0.4	78	3.3	0.525	0.014
	70°C	100	3.1	83	5.2	0.539	0.012
	80°C	91	4.5	81	4.2	0.529	0.011
	90°C	69	2.0	93	6.8	0.562	0.005
	100°C	71	3.4	97	1.4	0.523	0.015
	110°C	58	2.4	100	7.7	0.558	0.012

2.5.3.2 Optimisation of extraction temperature

A set of seven MAE experiments was conducted at temperatures ranging from 50 to 110 °C using 10 ml of solvent. This volume of solvent is recommended by the manufacturer for the most efficient performance of the temperature probe. An extraction time of 5 min was adopted. The influence of temperature on the yields of total chlorins, di- and tri-unsaturated C37 alkenones and their relative concentrations (expressed as U^{K}_{37}'; Prahl and Wakeham, 1987) was assessed. Results of MAE were also compared with those obtained by ultrasonication (**Table 2.6** and **Fig. 2.4**).

Biomarker yields

MAE at temperatures from 50 to 80 °C produced recoveries of chlorins similar to those obtained using ultrasonication. A further increase in temperature resulted in greater recoveries for MAE. The maximum recovery was achieved at 110 °C (**Table 2.6** and **Fig. 2.4a**). For alkenones, however, microwave extraction efficiency in the 50–80 °C interval was significantly higher than that of ultrasonication. Also, alkenone yields rose by 39% when the temperature increased from 50 to 70 °C. Further increase in temperature, however, caused alkenone yields to decrease. One explanation is that at higher temperatures a large part of the dichloromethane remains in gaseous form and does not participate in the extraction. Although gases do not absorb microwave energy and therefore solvent vapour should quickly cool and condense, the large volume of the extraction vessel (100 ml) may allow a significant proportion of the solvent to remain vaporized. This probably has a stronger effect on dichloromethane than on methanol because of the lower boiling point of the former. Chlorins are more soluble in methanol than in dichloromethane because the polarity of methanol is higher. That may explain why an increase in temperature from 70 to 100 °C did not cause a decrease in extraction efficiency of chlorins, while impairing that of alkenones.

A temperature of 70 °C was chosen as the optimal value for the joint MAE of chlorins and alkenones. The rationale behind this is two-fold. The recovery of alkenones is more sensitive to temperature than that of chlorins and it is a maximum at this temperature.

Moreover, the abundance of alkenones in marine sediments is often close to the detection limit because of the small samples available in these studies. In this work, the highest yield of alkenones (315 ng/g) was reached using MAE at 70 °C compared with 188 ng/g for ultrasonic extraction, a 68% increase. In contrast, chlorin yields at this temperature were as high as those for ultrasonication (**Table 2.6** and **Fig. 2.4a**). This relatively low temperature (most applications cited in the literature use temperatures higher than 100 °C) also allows a shorter cooling time, which further expedites the processing of samples.

Effects of using MAE in the measurement of U^{K}_{37}'

MAE has been reported previously as a method with low selectivity (e.g. Camel, 2000 and references therein). It is not surprising, therefore, that a change in extraction temperature did not influence significantly the relative recovery of C37:2 and C37:3 alkenones. Comparison of between- and within- experiment standard deviations for U^{K}_{37}' values gave F(1.98)<Fcrit(2.46) at =0.05 (Miller and Miller, 1993, p. 60). Comparison between MAE and ultrasonication using a t-test (Miller and Miller, 1993, p. 55) showed that both extraction methods were statistically similar (F(2.25)<Fcrit(4.46) at =0.05 and t(0.35)<tcrit(2.85) at =0.01). This shows that MAE did not introduce a bias in U^{K}_{37}' determination compared with the traditional ultrasonic method and that MAE can be used as an alternative in alkenone extraction and analysis.

Based on the empirical relationship for estimating sea surface temperature from U^{K}_{37}', an error of 1% in the measurement of U^{K}_{37}' translates to an error in the estimate of sea surface temperature of 0.3 °C (Prahl and Wakeham, 1987 and Müller et al., 1998). Given that surface ocean temperatures can vary between 1 and several degrees Celsius over a range of timescales of hundreds to thousands of years (e.g. Rosell-Melé *et al.*, 1998), an analytical error of less than 0.5 °C (or lower than 0.0165 in the standard deviation of U^{K}_{37}') may be considered acceptable. This study reports a standard deviation in the mean of all MAE experiments of 0.016, over the whole range of temperatures, and an average standard deviation in each experiment of 0.011, which implies that this technique is suitable for future U^{K}_{37}' studies.

2.5.4 Conclusions

The use of closed-vessel, microwave-assisted extraction has been appraised for the analysis of biomarkers in marine sediments. Three parameters (temperature, volume of solvent and extraction time) were investigated which, according to previous research, could influence extraction efficiency. Temperature was found to be the only parameter that had a significant influence on yields of the biomarkers. Equivalent values of U^{K}_{37}' were obtained using either MAE or ultrasonication. The use of MAE

does not introduce any bias in the measurement of the alkenone palaeotemperature proxy. MAE was found to be a faster, less laborious and more efficient extraction procedure than ultrasonication. The technique represents a viable alternative to traditional ultrasonic extraction for the analysis of chlorins and long chain alkenones and, therefore, probably other biomarker lipids in marine sediments.

3. Debris Flows as a proxy for sources of IRD in the North Atlantic

Cover image: Gravity core containing glacigenic debris flow sediments from Bear Island Fan is raised onboard RRS James Clark Ross.

CONTENTS

TABLES

(See volume II for figures).

3.1 Introduction

In this chapter, the potential of glacigenic debris flow (GDF) deposits on the North Atlantic continental margins as a source proxy for ice rafted debris (IRD) in the Heinrich Layers (HLs) based on their biomarker composition is investigated.

- The general aim of this chapter is to test the hypothesis that GDF deposits associated with the same Trough Mouth Fan (TMF) system are homogenous in their biomarker composition and are characterised by a unique biomarker signature different from that of GDF from other locations and from hemipelagic sediments and therefore can be used as a source proxy for IRD in Heinrich layers.

GDF deposited around the continental margins of the Polar North Atlantic and often forming trough mouth fans (TMFs), are recognised as useful indicators of former ice streams (e.g. Dowdeswell & Siegert, 1999). GDF deposits contain terrigenous sediments originated from the outcrops eroded by ice streams. IRD in the Heinrich layers in the deep ocean has the same origin. Sedimentological analysis reveal highly mixed and often homogenous nature of the sediments in GDF deposits (e.g. King *et al.*, 1998; 1996; Vorren & Laberg, 1997). In view of this, GDF sediments may prove useful as a source proxy to characterize IRD in HLs. To our knowledge, such approach has only been considered in one IRD-provenance study: Farmer *et al.* (2003) used isotopic analysis of the lithic fraction of ice proximal sediments including some debris flows to characterise sources of IRD in HLs.

Because of the shared geological history, isotopic signatures of the minerals (igneous and metamorphic from Archaean to Palaeozoic) from different areas surrounding the North Atlantic could be difficult to distinguish from one another (Farmer *et al.*, 2003). Biomarker signatures reflect composition of younger (Palaeozoic onwards) sedimentary minerals and may reflect higher variability between different potential source areas. Biomarker fingerprints may also provide a more detailed description of the sediments. For instance, specific compounds, unique to a particular source, may be identified.

Previous studies show that the IRD in the HLs is mainly derived from northern Canada (e.g. Andrews & Tedesco, 1992; Bond *et al.*, 1992; Hemming *et al.*, 1998). The input of IRD from European sources has also been reported (e.g. Bond & Lotti, 1995; de Abreu *et al.*, 2003; Grousset *et al.*, 2001; Scourse *et al.*, 2000). For this study, sediment samples from several glacigenic debris flow deposits in the Nordic Seas and North America were used (**Fig. 3.1**).

Around the margins of the Nordic Seas, several well-defined greatly varying in size TMFs, each formed at the mouth of a single large ice stream, have been documented (e.g. Vorren & Laberg, 1997 and references therein). Samples from four TMFs representing east Greenland (Scoresby Sund), Fennoscandian ice sheet (North Sea Fan), Barents Sea (Bear Island Fan) and Svalbard (Isfjorden and Bellsund TMFs) were considered. Thus, most potential source areas in this region were considered except for the British Isles and Iceland. IRD input from Iceland in the HLs is usually identified by the presence of volcanic rock particles. Therefore, Icelandic IRD is probably organic poor and its biomarker signature in HLs may be swamped by signals from other locations. However, there is a study using Cretaceous cooccoliths from chalk deposits in Iceland (Rahman, 1995). The Murrey fan (off Iceland (Ruddiman, 1977)) and the two British Isles TMFs, Sula Sgeir (Stoker, 1995) and Barra (Knutz *et al.*, 2001) fans, are significantly smaller than most TMFs in the Nordic Seas (Vorren & Laberg, 1997) and represent relatively small potential source area. Analysis of these TMFs, as well as Storfjorden TMF off east Svalbard and two minor western Svalbard TMFs (Vorren & Laberg, 1997), should be considered in the future to obtain a complete biomarker portrait of the IRD sources from European/Nordic Seas margins. However, probably none of these deposits is likely to represent the predominant source of IRD in the region.

In contrast with the Nordic Seas, glacigenic deposits on the North American and West Greenland margins are characterised by line-source sedimentation from a number of the ice stream outlets and are thought to vary across the Baffin Bay and Labrador Sea basins (e.g. Aksu, 1984; Hesse *et al.*, 1990). In the Labrador Sea, in addition to debris flow process, suspension settling from meltwater and turbidite activity played an important part in glacigenic sediments deposition (Hesse *et al.*, 1997). In this study, North American sources were represented by Baffin Bay and

Labrador Sea sediments since these areas were identified as major outlets for Laurentide Ice sheet ice streams containing Palaeozoic carbonate rich IRD. Samples from other possible Laurentide Ice Sheet outlets (e.g. Newfoundland slope and Laurentian Fan) were not available at the time. This may prove a shortcoming when identifying IRD inputs in Chapter 4 because the Gulf of St Laurence is considered a potential source area (Bond & Lotti, 1995; Grousset *et al.*, 2001). Recently, circum-Arctic areas were shown to have supplied icebergs from Arctic Laurentide and Innuitian ice sheets into the Nordic Seas and possibly North Atlantic via Fram Strait during the last glaciation (Darby *et al.*, 2002). This source area was overlooked in the present study and probably should be considered in the future.

3.2 Background. Debris flows considered in this study

Knowledge on the location and nature of GDF in the North Atlantic has improved considerably since the start of this thesis. The selection of the study sites was based on the state-of-the-art regarding GDF at the beginning of the work, and it is appreciated that a more comprehensive undertaking could now be carried out to characterize the potential sources of IRD than as reported here. The suite of cores selected represent, however, a considerable number and type of GDF present in the northern North Atlantic, deposited during the last glacial period, and known at the time when the study was undertaken.

Samples from Bear Island Fan and Scoresby Sund Fan were collected during ARCICE cruise on board RRS James Clark Ross (British Antarctic Survey) that took place in July - August 2000 (Dowdeswell *et al.*, 2000). Debris flows were identified using GLORIA (Geological Long Range Inclined Asdic) sidescan sonar and 3.5 kHz sub-bottom profiler data obtained during the cruise. Sampling sites were chosen close to those of the cores described in literature in order to compare biomarker data with other proxies records for the same locations. Sampling locations from other GDF deposits were chosen from publications and samples obtained through scientific collaboration. Cores JR51-GC08, 10, 11, 12, 30, 31 and 32 were opened, described and sub-sampled onboard the RRS *James Clark Ross*. All organic geochemical sub-samples were kept either refrigerated or (preferably) frozen at -20°C, between sub-sampling and analytical work-up. Some bulk properties of the sediment cores from JR51 cruise were analysed using split core logging system developed in the BOSCOR facility, Southampton Oceanography Centre. Magnetic susceptibility, bulk density (using gamma-ray attenuation) and compressional (P) wave velocity (500 kHz) were measured (Gunn & Best, 1998).

When possible, each location was represented by several cores in order to evaluate variability within each TMF; several GDF samples from different depths in each core were compared to assess within the core variability. Biomarker signatures of some hemipelagic and glacimarine sediments were compared with those of the GDF. Core locations and collection data are presented in **Table 3. 1**, **Table 3. 2** and

Fig. 3.1. Sediment samples information is listed in **Table 3. 3, Table 3. 4** and **Table 3. 5**. In **Fig. 3.2**, stratigraphic data for the cores from Bear Island Fan and Scoresby Sund Fan are shown in order to demonstrate distinctive sedimentological features of debris flows and to illustrate the sampling strategy. Core descriptions for the other GDF deposits used in this study can be found in the literature cited in the Sections 3.2.1 and 3.2.2.

Table 3. 1 Locations of cores retrieved from debris flows in the Nordic Seas. Mbsf – meters below sea floor.

Location	Core	Position	Water depth, m	Recovery, mbsf	Reference
Bear Island Fan	JR51 GC08	73°10.00'N, 9°40.00'E	2289	3.20	Dowdeswell *et al.*, 2000
	JR51 GC10	74°29.30'N, 10°52.00'E	2409	2.16	
	JR51 GC11	74°28.70'N, 10°44.00'E	2409	2.52	
	JR51 GC12	74°10.98'N, 10°44.09'E	2320	1.96	
Scoresby Sund Fan	JR51 GC30	70°22.01'N, 19°04.36'W	460	0.60	
	JR51 GC31	69°22.47'N, 19°36.90'W	1072	2.14	
	JR51 GC32	69°13.00'N, 19°53.00'W	1220	1.52	
North Sea Fan	HM 8303	62°55.6'N, 00°48.0'W	1615	3.00	King *et al.*, 1998
	HM 8306	64°16.8'N, 02°40.8'W	3002	3.20	
	HM 7908	62°52.4'N, 00°01.8'W	1327	2.70	
Svalbard	ODP 986 A	77°20.438'N, 09°04.661'E	2268	181.30	Jansen *et al.*, 1996
	ODP 986 B	77°20.431'N, 09°04.664'E	2053	15.10	
	ODP 986 C	77°20.431'N, 09°04.664'E	2051	229.78	

Table 3. 2 Locations of cores retrieved from debris flows in the Labrador Sea and Baffin Bay. N.a. – not available.

Location	Core	Position	Water depth, m	Recovery, m	Reference
Labrador Sea	HU87-025-07P	57°04.37'N 50°12.25W	3592	8.40	Hesse *et al.* (1990)
	HU88-024-02P	58°42.40'N 55°07.6'W	3220	7.35	Hesse *et al.* (1990)
Baffin Bay	HU77-027-002	74°30.40'N, 69°45.8'W	1646	5.10	Aksu & Piper (1987)
	HU76-029-036	south of Lancaster sound GDF	n.a.	n.a.	Geological Surway of Canada, personal communication (2000)

Table 3. 3 List of sediment samples. Nordic Seas. Cmbsf – cm below sea floor.

Location	Core	Sample depth, cmbsf	Sediment type
Bear Island Fan	JR51 GC08	0-3	Hemipelagic
		130-133	IRD*
		143-146	Debris Flow
		222-225	Debris Flow
		300-303	Debris Flow
	JR51 GC10	0-3	Hemipelagic
		63-65	IRD
		77-79	Debris Flow
		130-132	Debris Flow
		190-192	Debris Flow
	JR51 GC11	0-2	Hemipelagic
		60-62	IRD
		75-77	Debris Flow
		150-152	Debris Flow
		230-232	Debris Flow
	JR51 GC12	0-2	Hemipelagic
		34-36	IRD
		48-50	Debris Flow
		120-122	Debris Flow
		180-182	Debris Flow
Scoresby Sund Fan	JR51 GC30	0-2	Glacial Till
		18-20	Glacial Till
		30-32	Glacial Till
		50-52	Glacial Till
	JR51 GC31	0-2	Hemipelagic
		40-42	Debris Flow
		55-57	Debris Flow
		130-132	Debris Flow
		210-212	Debris Flow
	JR51 GC32	0-2	Hemipelagic
		74-76	Glacimarine
		90-92	Debris Flow
		120-122	Debris Flow
		140-142	Debris Flow
North Sea Fan	HM 8303	170-174	Debris Flow
		220-224	Debris Flow
	HM 8306	62-64	Glacimarine
		72-74	Debris Flow
		84-86	Debris Flow
		94-96	Debris Flow
		114-116	Debris Flow
		124-126	Debris Flow
	HM 7908	230-234	Debris Flow
		260-264	Debris Flow

*(as interpreted by Laberg & Vorren, 1995; 2000)

Table 3. 4 List of sediment samples. Svalbard

Location	Core	ODP label	Sample depth, cmbsf	Sediment type
Svalbard	ODP 986 A	1H-2W-20	170-172	Debris Flow
		1H-2W-90	240-242	Debris Flow
	ODP 986 B	1H-2W-20	170-172	Debris Flow
		1H-2W-90	240-242	Debris Flow
	ODP 986 C	1H-2W-20	170-172	Debris Flow
		1H-2W-90	240-242	Debris Flow

Table 3. 5 List of sediment samples Labrador Sea and Baffin Bay.

Location	Core	Sample depth, cmbsf	Sediment type
Labrador Sea	HU87-025-07P	5-6	Hemipelagic
		15-16	Debris Flow
		20-21	Debris Flow
		25-26	Debris Flow
		30-31	Debris Flow
		50-51	Debris Flow
		65-66	Debris Flow
	HU88-024-02P	15-16	Hemipelagic +IRD
		20-21	Hemipelagic +IRD
		30-31	Hemipelagic +IRD
		40-41	Hemipelagic +IRD
Baffin Bay	HU76-029-036	102-103	Glacimarine
		103-104	Debris Flow
		108-109	Debris Flow
		113-114	Debris Flow
		118-119	Debris Flow
		123-124	Debris Flow
		133-134	Debris Flow
		143-144	Debris Flow
	HU77-027-002	152-153	Glacimarine
		153-154	Debris Flow
		154-155	Debris Flow
		158-159	Debris Flow
		163-164	Debris Flow
		168-169	Debris Flow
		172-173	Debris Flow

3.2.1 Nordic Seas margins

3.2.1.1 Bear Island Fan

Bear Island Fan (BIF) is situated in front of the Bear Island Trough. It served as a major drainage pathway for the Barents Sea Ice Sheet and occupies an area of 215,000 km^2 (Laberg & Vorren, 2000; O Cofaigh *et al.*, 2003; Vorren & Laberg, 1997). The most recently active (late Quaternary) northern part of the BIF covers an area of 125,000 km^2 with up, middle and lower slope gradients of 0.8°, 0.5° and 0.2°(Laberg & Vorren, 1995; Taylor *et al.*, 2002). A series of stacked debris flow lobes were revealed in the northern part of the fan using GLORIA long-range sidescan sonar and 3.5 kHz sub-bottom profiler data. Individual lobes range from 30 to 200 km in length, 2 to 10 km width and 10 to 50 m in thickness (Dowdeswell *et al.*, 1996). They were deposited during the last glacial maximum (Laberg & Vorren, 1995; 1996). The main depositional processes delivering the sediments in the area south of 72°N were suspension settling from turbid meltwater plumes and contour-current activity (Taylor *et al.*, 2002)

The fan's source area in the Barents Sea is dominated by Early Tertiary and Cretaceous mudstone and sandstone (Laberg & Vorren, 1996; Sigmond, 1992) covered by a massive muddy glacigenic diamicton up to 300 m thick (Vorren *et al.*, 1989). Laberg and Vorren (1995; 2000) studied several cores from the northern BIF (**Table 3. 6**). They described debris flow deposits as massive dark grey (5Y4/1 on Munsell colour chart) diamicton containing clasts of sedimentary and crystalline rocks. Grain size distribution is 1-10% gravel, 10-30% sand, 30-50% silt and 30-55% clay (Laberg & Vorren, 1995). The authors report relatively uniform physical properties and grain size distribution in debris flow sediments from different debris flow lobes with a higher degree of variation in the upper BIF. The relative uniformity of the middle and lower parts is explained by a highly mixed nature of the GDF sediments due to remoulding and deformation during the downslope flow (Laberg & Vorren, 2000). Laberg and Vorren (1995) observed similarity in the grain size distribution and water content with the glacigenic till described by Saettem *et al* (1992). Physical properties of the overlaying hemipelagic mud displayed a much higher variability and differed from those of GDF deposits (Laberg & Vorren, 1995).

For this study, samples from four cores from 3 different debris flow lobes in the lower part of the northern BIF were analysed (**Table 3. 3** and **Figs. 3.1 and 3.2a**). Two cores, JR51-GC10 and JR51-GC11, belong to the same debris flow lobe (Laberg & Vorren, 1995), close to core –6/1 in Laberg & Vorren (Laberg & Vorren, 2000), core JR51-GC12 is from lobe 5 and JR51-GC08 is ~1°south from them. All four cores are dominated by debris flows (dark grey (10YR4/1) diamicton), sharply overlain by massive or weakly stratified (GC08) olive-grey (5Y4/2) silty mud/muddy diamict (O Cofaigh *et al.*, 2002). This facie was interpreted by Laberg and Vorren (1995; 2000) as ice rafted debris. It may also be a GDF deposit given its sharp contact and massive nature. The upper parts of the cores consist mainly of hemipelagic mud.

Wet bulk density, water content and magnetic susceptibility were measured every 2 cm. The results are presented in **Table 3. 6** and **App. 2 a-d**. Similar water content of ~28% (± 4%) to that reported previously was measured (Laberg & Vorren, 2000), whereas values for wet bulk density and TOC are slightly higher (**Table 3. 6**). Magnetic susceptibility is low and averages 16 X 10^{-5} SI. Laberg and Vorren (1995) reported slight decrease in water content of GDF downcore and increase of shear strength. However, in their subsequent publication (Laberg & Vorren, 2000), the authors did not report such a trend. No particular trend was observed in the distribution of bulk properties. Only in core JR51-GC08 there is a shift from 208 to 260 cmbsf towards drier sediments (16 % water) with higher density (2.12 g/cm^3). Overlaying mud/muddy diamict has a higher water content (33-43%) and lower density (1.60-1.78 g/cm^3) with a slightly lower magnetic susceptibility (11 X 10^5 SI). Postglacial hemipelagic sediments are characterised by high variability in their physical properties. They are generally wetter with lower density and higher magnetic susceptibility then GDF.

3.2.1.2 Scoresby Sund Fan.

The Scoresby Sund Fan (SSF) is a relatively small wedge-shaped TMF situated on the East Greenland continental margin between 69°N and 71°N offshore of the mouth of the Scoresby Sund fjord system. It has a steeper (1.8-2°) continental slope

than BIF (Dowdeswell *et al.*, 1997). The drainage basin of SSF comprises mostly igneous Neogene/Palaeogene and Precambrian metamorphic rocks. There is an outcrop of late Palaeozoic and Mesozoic sedimentary rocks, dominantly marine in origin (Linthout *et al.*, 2000).

The most recent sediment delivery {last glaciation, \Dowdeswell, 1997 #171} to the southern part of the fan was in the form of glacigenic debris flows. GDF lobes 1-2 km wide and 5-15 m thick were identified using GLORIA long-range sidescan sonar and 3.5 kHz sub-bottom profiler data. They were deposited when the ice sheet was at or close to the shelfbreak (Dowdeswell *et al.*, 1997). The youngest debris flows on the northern part of the fan were deposited prior to MIS 5 and are overlain by hemipelagic and ice rafted sediments (Dowdeswell *et al.*, 1997; Nam *et al.*, 1995).

For this study, samples from three cores were studied, JR51-GC30 (from the continental slope east of the mouth of the Scorseby Sund fjord), JR5-GC31 and JR51-GC32 from one of the debris flow lobes on the southern part of the fan. Core GC30 contains massive dark grey diamicton of glacial till produced by iceberg rafting and scouring. Core GC31 consist of four units of debris flow deposits, overlain by postglacigenic hemipelagic sediments. It consists of dark grey (7.5YRN4/) muddy diamicton at the bottom of the core, overlain by light grey (10YR5/1-10YR6/1) silty mud, dark grey (7.5YRN4/) diamicton and olive grey (5Y4/2) muddy diamict. These units were interpreted as glacigenic debris flows on the basis of their massive structure, poorly sorted nature, stacked stratigraphic context and geophysical signature (acoustically transparent elongate lenses) (O Cofaigh *et al.*, 2002). Core GC32 contains one GDF unit of dark grey (7.5YRN4/) massive diamicton, overlain by a layer of grey (2.5Y5/2) mud interpreted as ice rafted debris mixed with hemipelagic sediment, and postglacial hemipelagic sediments interrupted by a sandy turbidite (**Table 3. 3** and **Figs. 3.1 and 3.2 b**).

Wet bulk density, water content and magnetic susceptibility were measured every 2 cm. The results are presented in **Table 3. 6** and **App. 2 e-g**. Bulk properties of GDF sediments differ from those of hemipelagic and of glacial till. Water content of GDF deposits averaged 17% (± 3%), which is lower then 24% (± 5%) of the

glacial till (GC30). GDF sediments were also found to have higher density (2.11 vs. 1.96) and magnetic susceptibility (300 10^5 SI vs. 97 10^5 SI) then glacial till. Overlaying hemipelagic sediments are generally wetter, less dense and have lower magnetic susceptibility (**App. 2 e-g**).

3.2.1.3 North Sea Fan

North Sea Fan (NSF) is deposited in front of the Norwegian Channel and extends into the Norwegian Sea. Similar to the BIF, it is a large (108,000 km^2) TMF with a low continental slope gradient (0.6°, 0.3° and 0.2° for upper, middle and low sections) (King *et al.*, 1998; 1996). Norwegian Channel served as an important drainage path of the Fennoscandian ice sheet, depositing Late Cenozoic sediments from Norway, Denmark and part of the North Sea (Dowdeswell & Siegert, 1999; King *et al.*, 1998; 1996).

The younger part of the NSF, deposited since Middle Pleistocene, consists mainly of stacked debris flows (80%) separated by thick hemipelagic sequences. Individual GDF lobes are 2-40 km wide and 15-60m thick (King *et al.*, 1996). The latest GDF on the middle and lower fan were deposited before 16 ka (King *et al.*, 1998).

King *et al.* (1998) reported extreme homogeneity of GDF in terms of lithological composition and their striking similarity to Weichselian IRD till from Norwegian Channel. In contrast, overlaying glacimarine sediments (IRD mixed with hemipelagic) are distinctly different and characterised by high variability. GDF sediments are comprised of structureless poorly sorted grey (5Y4/3 to 5Y4/1) diamicton. Average grain size distribution is 1% Gravel, 29% sand, 36% silt and 34% clay. Water content gradually decreases and ranges from 32 to 24%, wet bulk density and sheer strength increase correspondingly. TOC is low (0.5%). So is it's magnetic susceptibility (34 X 10^{-5}) (**Table 3. 6**).

For this study, sediment samples from three cores described by King *et al.* (1998): glacimarine and GDF sediments from HM 8306 and GDF sediments from HM 8303 and HM 7908 were used (**Table 3. 1** and **Table 3. 3**).

3.2.1.4 ODP site 986: Bellsund and Isfjorden TMFs

Bellsund and Isfjorden are two TMFs along the western shelf margin of Spitsbergen. They are small (6000 and 3700 km^2 respectively), with a relatively steep continental slope of 1.8° and 3.2° (Vorren & Laberg, 1997). The younger GDF sequences are attributed to the time of LGM. They were deposited when Barents Sea ice sheet engulfed the entire Svalbard archipelago and glaciers reached the shelfbreak off the major fjords (Landvik *et al.*, 1998). Individual GDF lobes on the Isfjorden TMF are 1-5 km wide, 20-30 m thick and 10-30 km long (Elverhøi *et al.*, 1997).

ODP site 986 is located between the Bellsund and Isfjorden TMFs. Butt *et al.* (2000) interpreted depositional sequences past 1.3 Ma as stacked debris flows. High carbonate content with the dominance of dolomite and the presence of metamorphic and crystalline clasts indicates provenance of these sediments from the mainland Svalbard (Butt *et al.*, 2000). Isfjorden drainage area includes Late Palaeozoic limestone and dolomite, Mesozoic-Tertiary- sand- and siltstones, quartzite/micashists and igneous rocks (Elverhøi *et al.*, 1995b). Jurassic and Cretaceous strata contain coal seams and black shales (Wagner & Hölemann, 1995).

For this study, sediment samples from the uppermost debris flow deposit from three holes (A, B and C) were used (**Table 3. 4** and **Table 3. 6**). Sediments are comprised of very dark grey (5Y3/1) silty clayey mud with occasional clasts of predominantly sedimentary origin. Particle size distribution is 1% sand, 37% silt and 62% clay (Jansen *et al.*, 1996). These are finer sediments than the ones in the Isfjorden TMF (20-30% sand, 35-40% silt and 35-40% clay) (Elverhøi *et al.*, 1997). Total organic carbon is 1% and magnetic susceptibility is 40 X 10^5 SI (**Table 3. 6**).

Table 3. 6 Representative bulk properties of Glacigenic Debris Flow (GDF) sediments from different TMFs in the Nordic Seas. SSF – Scoresby Sund Fan, BIF – Bear Island Fan, NSF – North Sea Fan. TOC – total organic carbon.

GDF	Sediment	Colour	Water content (%)	Undrained shear strength (kPa)	wet bulk density (g/cm^3)	Particle size mean (Phi)	Magnetic susceptibility (SI)	TOC (%)	Reference
BIF	massive, poorly sorted diamicton, clasts	dark grey 5Y4/1	27.7-29.7 28 (±4)*	83-97	1.18-1.25 1.87(±.09)*	7-9 silty clay	16 X 10^{-5}*	0.7-1.3 1.5*	(Laberg & Vorren, 1995; 1996; 2000)
SSF	massive unsorted diamicton, clasts	dark grey 7.5YRN4/	17 (±3)*		2.11(±.07)*	3-5 coarse silt-fine sand	300 X 10^{-5}*	0.3 0.45*	(Nam et al., 1995)
NSF	massive homogenous diamicton, clast-poor	grey 5Y4/3-5Y4/1	24-32	5-30		4-5 coarse silt-fine sand	34 X 10^{-5}	0.5	(King *et al.*, 1998)
ODP 986	massive homogenous mud, clasts	dark grey 5Y3/1				8-9 silty clay	40 X 10^{-5}	1.0	(Jansen et al., 1996) (Butt et al., 2000)

* This study.

3.2.2 Labrador Sea and Baffin Bay margins

Glacigenic debris flow deposits of North America present a more complicated picture than those in the Nordic Seas. Not one but several ice streams fed both Baffin Bay and Labrador Sea (e.g. Aksu, 1984; Hesse *et al.*, 1990). For this reason and due to the topography of these basins, there are no TMFs in the same sense as in the Nordic Seas but rather a series of GDF deposits, characterised by certain variability in their lithological characteristics (Aksu & Hiscott, 1989; Aksu & Piper, 1987; Hesse *et al.*, 1990; Wang & Hesse, 1996).

3.2.2.1 Labrador Sea

Hudson bay drainage basin (Hudson Bay and the highlands north and south of Hudson Strait) was the largest drainage basin of the Laurentide Ice Sheet (1-2 x 10^6 km^2) (Hesse *et al.*, 1999a). It fed Hudson Strait ice stream during the Quaternary and is thought to have been the principal source of the ice-rafted Heinrich layers in the North Atlantic (Andrews, 1998; Andrews & Tedesco, 1992; Bond *et al.*, 1992; Dowdeswell *et al.*, 1995). There was also a series of lesser ice streams through the deep transverse troughs on the continental shelf south of Hudson Strait (Hesse *et al.*, 1999a).

Northern part of the Labrador Sea (LS), directly offshore from the mouth of Hudson Strait is a relatively low-gradient area dominated by debris flows and turbidites with shallow (<150 m) broad-floored canyons. To the south, lies a major submarine channel system, North Atlantic Mid Ocean Channel (NAMOC), the area of deeply incised narrow canyons (200-500 m deep) (Hesse *et al.*, 1999a). Sediments of terrestrial origin, glacigenic debris from upper continental slope, were resedimented as turbidites and debris flows in the central Labrador Sea (Hesse *et al.*, 1997; Hesse *et al.*, 1999a; Hesse *et al.*, 1990).

There is a marked lithological dissimilarity between the detrital sediments supplied through the Hudson Strait and the smaller outlets to the south. The former contained fine-grained Palaeozoic carbonates from southern Baffin Island, Foxe Basin, Hudson Bay and surroundings, whereas the latter brought coarser igneous and

metamorphic crystalline material derived locally (Hesse *et al.*, 1999a; Wang & Hesse, 1996). Detrital carbonate from northern Greenland and northern Canada was found in the LS IRD deposits constituting up to 35% of the coarse silt and sand fractions (Wang & Hesse, 1996). Up to 80% of detrital carbonate in proximal HLs on the Labrador slope occur in silt- clay fraction (Hesse & Khodabakhsh, 1998).

There have been three recognised types of debris flow deposits in the Labrador Sea varying in grain size, colour and structure: D1 – coarse-grained, thick-bedded clast-bearing deposits characterised by a sharp contact with adjacent facies, D3– coarse-grained thin-bedded facies, both of glacigenic origin, and D2 that formed from hemipelagic sediments (Wang & Hesse, 1996).

Unfortunately, samples of sediments from the GDF deposit at the Hudson Strait outlet were not available. For this study, several samples of debris flows and overlaying hemipelagic sediments from the southern part of the debris flow deposit (facie D1) west of NAMOC (core HU87-025-007p) were analysed (**Table 3. 2** and **Table 3. 5**). These GDF were deposited during early stages of deglaciation (Hesse *et al.*, 1990). GDF sediment consists of dark greyish-brown extremely poorly sorted gravely mud with polymodal grain size distribution displaying a distinct mode in the gravel fraction (<-1.0 phi) and secondary modes in clay and silt fractions (8-10 phi) (Wang & Hesse, 1996). It is appreciated that GDF sediments from this core may only represent sedimentary material from secondary ice streams along the Labrador Sea margin. However, igneous and metamorphic rocks are low in organic content and the biomarker signature of the GDF sediments from this location is likely to be derived mainly from Palaeozoic carbonates. In fact, the carbonate content in these sediments is 25-30% (Wang & Hesse, 1996).

For comparison, samples from core HU88-024-002 containing ice rafted debris with some hemipelagic sediment were also included (facies HI with 10-30% carbonate (Wang & Hesse, 1996)). They contain dark greyish-brown gravely-silty clay (1-3, 8-10 phi) (**Table 3. 2** and **Table 3. 5**).

3.2.2.2 Baffin Bay

Baffin Bay (BB) is a small ocean basin, ~ 1350 km long and from 110 to 650 km wide with 2300-m-deep central abyssal plain (Hiscott & Aksu, 1994). The width of the continental shelf ranges from under 35km in the west (off Baffin Island) to over 150 km off Greenland. Continental slope steepness is 2-3°. In the northern Baffin Bay, a gentle slope of 0.4° leads from the shoreline directly to the abyssal plain without recognisable continental shelf (Aksu & Hiscott, 1989).

The morphology of the continental slope of BB is characterised by the absence of submarine channel- fan systems except for a large sediment apron in the north (Aksu & Piper, 1987). U-shaped transverse troughs extend across the total width of the shelf (Aksu & Hiscott, 1989). This is characteristic of a line-source sedimentation – persistent high-sediment yield from the entire length of the ice front without permanent loci of sediment supply (Aksu & Hiscott, 1992); (Hiscott & Aksu, 1994); (Aksu & Hiscott, 1989); (Aksu & Piper, 1987). That resulted in production of abundant stacked lenses of debris where sediments have not been reworked by powerful channelised turbidity currents. Morphology of the debris flow deposits off the Home Bay has been well documented. Younger debris flows (since 0.4 Ma) reach 180m in thickness on the upper slope and are very thin, ~15m on the lower slope. Larger debris flows occupy areas from 50 to over 1000 km^2 and have volumes from 0.4 to over 7.7 km^3 (Hiscott & Aksu, 1994).

Mineral composition of the outcrops surrounding Baffin Bay varies from north to south (Andrews & Jennings, 1987). Due to the line-source sedimentation, it is feasible to expect variation in sedimentological composition of debris flows between different areas of Baffin Bay. For example, debris flow lenses at the ODP site 645 are comprised of structureless grey (5Y4/1) pebble-bearing silty mud (Aksu & Hiscott, 1989). Sediments from debris flow apron in the north (facies from core HU77-029-002 (Aksu & Piper, 1987)) are massive or graded dark reddish-brown (10YR 3/2) gravely-sandy mud. Particle size distribution in the graded mud is 2-20% gravel, 18-30% sand, 25-30% silt and 25-50% clay. They contain 19% detrital carbonate in sand-clay fraction and 31% in gravel fraction (Aksu & Piper, 1987).

Debris flow sediments in the BB were derived from Lower Palaeozoic carbonates and Cretaceous red sandstones from the areas northwest of the BB and Tertiary rocks on the continental shelf, as indicated by their mineralogical composition and presence of specific palynomorphs (Ordovician-Silurian, Cretaceous and Eocene) (Aksu & Piper, 1987). Precambrian metamorphic detritus from Baffin Island and Greenland is also present and dominates in the southern part of the bay (Aksu & Piper, 1987; Andrews *et al.*, 1989).

For this study, debris flow sediment from two cores, HU77-027-002 and HU76-029-036 were used. The former is situated in the GDF apron off Lancaster Sound in the northern part of Baffin Bay and its sedimentological and mineralogical composition has been described in literature (Aksu & Piper, 1987). The latter was collected from one of the GDF deposits further south and represents a different source area (Rashid, H., personal communication) (**Fig. 3.1** and **Table 3. 2** and **Table 3. 5**).

3.3 Biomarker composition of Debris Flow cores

In this section, the biomarker composition of different samples (debris flow, glacimarine and hemipelagic) from the Nordic Seas and North American debris flow deposits is described. GDF consist of sediments of terrestrial origin delivered to the continental shelf by ice streams during periods of iceberg discharge. They should contain allochthonous biomarkers typical of the ancient sedimentary rocks eroded by the ice streams. On the other hand, in the overlaying hemipelagic sediments, the presence of autochthonous biomarkers was expected (see Section 1.4.2) as well as allochthonous biomarkers delivered by aeolian and/or fluvial mechanisms and sea ice (Wagner & Henrich, 1994). In this study, photosynthetic pigments, n-alkanes, UCM (mixture of highly branched aliphatic compounds unresolved by gas chromatography) and long-chain alkenones were used to identify and characterize the allochthonous and autochthonous signal in different sediments on the Polar North Atlantic continental margins.

Chlorophyll-derived, photosynthetic pigments can be detected and classified using a relatively simple technique such as UV-visible spectrophotometry (Rosell-Melé *et al.*, 1997). Green sedimentary chlorins, products of short-term degradation of chlorophyll a, are usually thought to present an autochthonous signal, whereas red porphyrins, whose formation by diagenesis of chlorins takes millions of years, are representative of an allochthonous signal (e.g. Baker & Lauda, 1986; Callot *et al.*, 1990). The presence of porphyrins in Heinrich Layer sediments of a north Atlantic core BOSF 5K was attributed to ice rafted input (Rosell-Melé *et al.*, 1997). Relative abundance of Ni and VO porphyrins is thought to reflect oxidative conditions in the ancient depositional environment and may be useful in distinguishing between different sediments sources (Lewan, 1984). See also Section 1.4.3.

N-alkanes are usually the most abundant compound class in the sedimentary organic matter and are easily recognised on a gas chromatogram. Here, gas chromatographic fingerprints are used to characterise and compare sediments in GDF deposits in the same way as they are used in petroleum industry (Peters & Moldowan, 1993; Tissot & Welte, 1984). Distribution of n-alkanes reflects both the

depositional environment and the degree of reworking of the organic matter. N-alkane distributions in the samples from glacigenic sediments should reflect the reworked nature of the organic matter from ancient sedimentary rocks. Allochthonous n-alkanes are usually present in hemipelagic sediments, but their origin from aeolian or fluvial input, mainly from eroded soils, should be reflected in different n-alkane fingerprints indicative of younger organic matter sources (Simoneit, 1977; Tissot & Welte, 1984). They could also represent an autochthonous n-alkane signal because low molecular weight n-alkanes (n-C_{15-19}) can be produced by marine algae (Gelpi *et al.*, 1970; Tissot & Welte, 1984). Presence of chromatographic UCM is characteristic of reworked organic matter (Simoneit, 1977; Tissot & Welte, 1984).. Certain amount of reworked terrigenous organic matter is expected in the background sediments from glacial periods due to input from icebergs and sea ice (Wagner & Henrich, 1994). See also Section 1.4.4.

The long-chain C_{37}-C_{39} methyl and ethyl unsaturated ketones (alkenones) are almost ubiquitous in the sediments of the world's oceans. They are known to be synthesized in the water column by a limited number of haptophyte microalgae (the order Isochrysidales) and therefore reflect an autochthonous biomarker signal (e.g. Conte *et al.*, 1994; de Leeuw *et al.*, 1980; Marlowe *et al.*, 1984). However, there is a possibility of allochthonous input of alkenones from ancient sediments: they were identified in Eocene sediments (~45 Ma BP) (de Leeuw *et al.*, 1980; Marlowe, 1984; Volkman *et al.*, 1980) and in two Cretaceous black shales dated at 100 Ma BP (Farrimond et al., 1986). Unusually high SST estimates from alkenone unsaturation indices reported by Rosell-Mele & Comes (1999) for Last glacial maximum in the Nordic Seas may be a result of such input.

A list of variables used for comparison of biomarker signatures of sedimentary organic matter is presented in **Table 1.1** (Section 1.4). The results of biomarker analysis are presented in **Table 3. 7**. Data for individual samples are presented in **App. 3**.

3.3.1 Description of Allochthonous and Autochthonous signals

3.3.1.1 Photosynthetic Pigments

All samples analysed contained photosynthetic pigments. UV-VIS absorbance of the blanks was below the detection limit. *S/I* ratios for all samples were greater than 5 suggesting the presence of porphyrins (**Table 3. 7**), which was later confirmed by more detailed spectrophotometric analysis. Thus, absorption maxima peaks corresponding to nickel (550 nm) and vanadyl porphyrins (570 nm) were present in most debris flow samples, glacial till and glacimarine sediments containing IRD (e.g. GC32-74 cm and HU88), but not detected in the hemipelagic sediments devoid of IRD. This confirms terrestrial origin of materials in the debris flow sediments in this study. The values of *S/I* for hemipelagic sediments were generally lower than for debris flows from the same deposit suggesting the predominant presence of chlorins over porphyrins. On average, the highest *S/I* ratios were calculated for the sediments from the BIF (*S/I*~29.5) and SSF (*S/I*~21). Glacial till sediments from SSF are characterised by the similar *S/I* ratio (18). The lowest *S/I* values were recorded for debris flows from NSF (*S/I*~8) and 4 out of 6 Svalbard samples (*S/I*~7-9). Absorbance spectra of representative extracts of debris flows as well as some hemipelagic and glacimarine samples are presented in **Fig. 3.3**.

Absorption maxima peaks corresponding to chlorins (665 nm) were detected in debris flow samples the North Sea Fan and Svalbard and absent from all other GDF sediments. Distribution of pigments in the sediment samples from three different cores several kilometres apart from the NSF appears very homogenous (relative standard deviation of *S/I* ratio is 14% compared with 30-50% for other TMFs). Sediments from Svalbard can be divided into two groups. Deeper samples (986B-90 cm and 986C-90 cm) are characterised by low abundance of chlorins relative to porphyrins (*S/I*~25), whereas in shallower samples (986B&C-20 cm) and in both samples from 986A, relative abundance of chlorins is higher (*S/I*~5-9) (see also **Fig. 3.3**). Lower abundance of porphyrins in the two deeper samples from the holes B and C coincides with lower concentration of alkenones (see Section 3.3.1.3).

In the samples form the BIF and SSF, Ni and VO porphyrins are present in almost equal amounts with some preference for vanadyl porphyrins in BIF ($VO/((VO+Ni))$ = 0.59±0.17). Glacial till sediments, however, contained relatively

higher relative abundance of VO species compared to debris flows (*VO/(VO+Ni)* = 0.73±0.08 vs. 0.49±0.04 in GDF sediments). Predominantly oxic conditions were present at the time of formation of the source sediments of NSF debris flows as indicated by lower porphyrins ratio (*VO/(VO+Ni)* = 0.34±0.09). Results for Svalbard samples are inconclusive because of high degree of variation in the relative abundance of porphyrins. Two low values (0.18 &0.20) belong to both samples from the hole B. In the rest of the samples porphyrins ratios range from 0.45 to 0.70 with deeper samples showing higher preference for vanadyl porphyrins. This may reflect genuine heterogeneity of the debris flow sediments in this location. However, n-alkane distribution and UCM content of five out of six ODP 986 samples are very similar (See Section 3.3.1.2 and **Table 3. 7**). There is also a possibility that high variation is a result of a flawed HPLC separation. Towards the time of analysis, the elution times of different fractions shifted because of the ageing of the column and vanadyl porphyrins in some samples were partially eluted into the fourth fraction. This complicated quantification and may have resulted in a bias in the results. In the Labrador Sea debris flow sediments and one of the Baffin Bay cores (HU77), VO porphyrins dominate: they comprise 98% and 72% of total VO and Ni species respectively. Absolute abundance of porphyrins is very low in both BB cores and Ni species are absent or scarce in core HU76. The differences between the two cores can be explained by the line-source deposition of GDF (Aksu & Hiscott, 1989).

3.3.1.2 N-alkanes

Gas chromatograms of the saturated hydrocarbon fraction of the sediment extracts of representative samples of debris flows, glacimarine and hemipelagic sediments are presented in **Fig. 3.4**. Linear n-alkanes ranging from 16 to 35 carbon atoms were the dominant compounds in all the samples (>50%). Lighter compounds (Cn<16) could have been lost during evaporation of the extraction solvent. The average concentrations of total n-alkanes (C_{17-33}) per gram dry sediment range from 0.03 to 2.4 μg/g in hemipelagic sediments and from 0.13 to 13.1 μg/g in GDF. Long-chain n-alkanes (Cn > 24), biomarkers for epicuticular waxes of higher terrestrial plants (Eglinton & Hamilton, 1967) were present in all sediment samples indicating their terrestrial origin.

N-alkane distribution in GDF

N-alkane distributions in GDF from NSF, LS and BB show unimodal chromatographic envelopes with maxima at n-C_{27} or n-C_{29} alkane typical of terrestrial organic matter (**Fig. 3.4 c, e &f**). In BIF and SSF, n-alkanes show bimodal distribution with maxima at n-C_{25} and n-C_{19} or n-C_{22} (**Fig. 3.4a & b**). Displacement of n-alkane envelope towards lower carbon number values is indicative of reworked (mature and biodegraded) organic matter (Tissot & Welte, 1984). High relative abundance of the short-chain n-alkanes may also be indicative of lacustrine algal and bacterial inputs (Peters & Moldowan, 1993). Glacial till sediments from the continental shelf off Greenland (core GC30) display similar n-alkane distribution to GDF deposits in the SSF (**Table 3. 7** and **Fig. 3.4b).** With one exception, n-alkanes from Svalbard are characterised by a unimodal distribution with maximum at n-C_{23} alkane. One sample (ODP 986C-90cm) differs considerably, showing unimodal distribution with a maximum at n-C_{31} (**Fig. 3.4d**). Other parameters for this sample are markedly different from those for other samples from this location displaying a signature of a less reworked organic matter (**App. 3**).

Carbon preference indices were calculated for the long-chain n-alkanes (n-$C_{24\text{-}31}$) and short-chain n-alkanes (n-$C_{17\text{-}23}$) (**Table 3. 7**). High CPI values (>3) are associated with younger organic matter (Fahl & Stein, 1999). CPI <3 is attributed to the fossil sources. With maturity, CPI tends to approach 1 (Peters & Moldowan, 1993). NSF n-alkanes display the highest CPI that ranges from 3.8 to 4.1. Samples from core HU77 in the BB are characterised by higher CPI values than those from HU76 (2.7-4.0 vs. 1.9-2.4). CPI for the LS samples was in the range of 2.0-2.5. Lower values were obtained for Svalbard (1.7-2.3), BIF (1.5-2.0) and SSF (1.3-1.6).

Average chain length (ACL) values for the GDF range from 27.9 (Svalbard) to 28.8 (LS) with standard deviations of ~0.2 (**Table 3. 7**). This parameter is determined by the depositional environment and post-depositional transformation of the sedimentary organic matter of the rocks which gave rise to the GDF (Madureira *et al.*, 1995; Peters & Moldowan, 1993; Poynter *et al.*, 1989). (See also Section 1.3.4.4).

All debris flow samples contained mixtures of highly branched aliphatic molecules which are not resolved by gas chromatography and can be seen in the gas chromatogram as unresolved complex mixture (UCM) that rises as a hump above the baseline of the chromatographic trace (**Fig. 3.4**). Such mixtures are the result of the biodegradation of organic matter in the sedimentary rocks eroded by ice streams (Peters & Moldowan, 1993). In this study, GDF sediments containing the most biodegraded organic matter (as exemplified by the highest UCM values) are characterised by the highest degree of maturation as reflected in the n-alkane envelope and CPI values. The UCM values are quite low (UCM to total n-alkanes ratio <4) for NSF, LS and BB (**Table 3. 7**). It has a maximum at the GC retention time of the n-C_{31} alkane. The highest UCM amounts (*UCM/TNA* range from 8 to 13) are calculated for SSF with one extreme value of 57 (core GC32 140 cm). BIF samples also contains high amounts of branched aliphatic compounds (*UCM/TNA* range from 6to11) in the wide range of molecular weights with the highest abundance of molecules with GC retention time close to n-C_{29} alkane (**Table 3. 7** and **Fig. 3.4a**). In the Svalbard samples, theUCM hump is higher at the retention times of the short chain n-alkanes (n-C_{14-24}) and *UCM/TNA* averages ~7. There is one exception: sample 986C-90cm is characterised by a low degree of biodegradation (*UCM/TNA* = 0.98).

Quantification of pristane and phytane in most of the samples from the LS and BB proved impossible due to very low abundances and coelution in the gas chromatogram with some unidentified compounds (possibly contaminants). For the rest of the debris flows, the *Pr/Ph* ratios are low (<2) (see **Table 3. 7**), with higher values for BIF (1.6 – 2.0) and Svalbard (1.3 - 2.0). One sample, 986C-90 cm, is characterised by a lower *Pr/Ph* ratio (0.6). *Pr/Ph* ratios of SSF debris flows, however, are close to those of NSF (0.71 and 0.73) (**Table 3. 7**). *Pr/Ph* ratio is thought to reflect Redox conditions during the deposition of organic matter in the sedimentary rock (Peters & Moldowan, 1993) but can also indicate maturity of organic matter (Ten Haven et al., 1987 in Peters & Moldowan, 1993). Higher Pr/C_{17} and Ph/C_{18} ratios were found in BIF and most of the Svalbard samples. It is probably due to biodegradation rather than maturation because the isoprenoid/n-alkane ratios are substantially higher for the 986C-90 cm sample containing less mature organic

matter (see this Section) than other samples from this location (Pr/C_{17} =3.9 and Ph/C_{18}=0.6 compared with 1.1 and 0.4).

N-alkane distributions in hemipelagic and glacimarine sediments

A number of samples of hemipelagic sediments from BIF (4), SSF (2) and LS (1) were analysed. A unimodal envelope with high abundance of the long-chain n-alkanes in these samples (**Fig. 3.4**) indicates their terrestrial origin (Eglinton & Hamilton, 1967). Distribution of n-alkanes in hemipelagic sediments from BIF and SSF is markedly different from that of GDF sediments from the same locations. Their n-alkane envelope has maxima at n-C_{29} or n-C_{31} alkane. N-alkanes in these samples are characterised by higher CPI and ACL than in GDF (**Table 3. 7**). Low abundances of short-chain n-alkanes and absence of UCM point at low maturity and low degree of biodegradation in hemipelagic sediments (Peters & Moldowan, 1993 and references therein). N-alkanes in hemipelagic sample from LS core HU87-025-07P show similar characteristics.

Glacimarine sediments present a mixture of hemipelagic and ice rafted matter. N-alkane distribution in those samples often resembles that of GDF from the same location (e.g. **Fig. 3.4c,f**) and often shows similar characteristics presumably when IRD content is high (e.g. glacimarine samples above BB debris flows **Table 3. 7**). However, higher inputs from hemipelagic sediments result in higher variability between GDF and glacimarine deposits (e.g. SSF and LS **Table 3. 7**).

Table 3. 7 Mean values and standard deviation (in brackets) of variables used for comparison of sediment samples. N – number of observations. HP –hemipelagic, GDF – debris flow, GM – glacimarine, GT – glacial till. HI – hemipelagic +ice rafted debris.

TMF (type of sediment)	N	*TNA (μg/g)*	$CPI_{17\text{-}23}$	$CPI_{24\text{-}31}$	C_{27}/C_{29}	C_{29}/C_{31}	$\frac{\sum C_{29\text{-}31}}{\sum C_{29\text{-}31}+\sum C_{17\text{-}19}}$	*ACL*
BIF (HP)	4	1.5 (0.6)	1.29 (0.06)	2.77 (0.25)	0.94 (0.17)	0.97 (0.20)	0.86 (0.02)	28.7 (0.5)
BIF (GDF)	**16**	**8.4 (2.9)**	**1.16 (0.06)**	**1.67 (0.21)**	**1.23 (0.08)**	**1.65 (0.17)**	**0.43 (0.10)**	**28.0 (0.1)**
SSF (HP)	2	2.4 (0.7)	1.48 (0.05)	3.20 (1.27)	0.83 (0.12)	1.06 (0.17)	0.94 (0.01)	28.8 (0.3)
SSF (GM)	1	3.0	1.44	3.52	0.94	1.07	0.87	28.6
SSF (GT)	**4**	**2.2 (0.5)**	**1.06 (0.04)**	**1.38 (0.17)**	**1.19 (0.14)**	**1.40 (0.09)**	**0.50 (0.15)**	**28.2 (0.1)**
SSF (GDF)	**7**	**2.0 (1.2)**	**1.01 (0.09)**	**1.40 (0.09)**	**1.20 (0.20)**	**1.49 (0.29)**	**0.44 (0.13))**	**28.1 (0.3)**
NSF (GM)	1	2.6	1.37	3.65	1.01	1.06	0.92	28.6
NSF (GDF)	**9**	**7.2 (1.6)**	**1.67 (0.11)**	**3.89 (0.12)**	**1.33 (0.12)**	**1.15 (0.06)**	**0.92 (0.04)**	**28.4 (0.15)**
SVAL (GDF)	**5**	**13.1 (3.6)**	**0.88 (0.07)**	**1.93 (0.20)**	**1.30 (0.11)**	**1.28 (0.08)**	**0.45 (0.06)**	**27.9 (0.1)**
SVAL 986C1H2-90 (GDF)	**1**	**2.9**	**1.03**	**2.44**	**0.87**	**0.95**	**0.87**	**28.7**
LS (HP)	1	0.014	1.47	1.91	0.89	1.02	0.87	28.6
LS (HI)	4	0.13 (0.06)	1.30 (0.14)	1.79 (0.20)	1.01 (0.04)	1.51 (0.27)	0.80 (0.02)	28.3 (0.4)
LS (GDF)	**6**	**0.13 (0.1)**	**1.41 (0.16)**	**2.31 (0.19)**	**0.89 (0.05)**	**0.98 (0.13)**	**0.89 (0.04)**	**28.8 (0.2)**
BB (GM)	2	2.5 (1.6)	1.99 (0.15)	2.94 (1.11)	1.06 (0.12)	2.02 (0.59)	0.87 (0.03)	28.3 (0.1)
BB (GDF)	**11**	**2.5 (1.2)**	**2.15 (0.35)**	**2.83 (0.82)**	**1.00 (0.10)**	**1.94 (0.29)**	**0.92 (0.05)**	**28.3 (0.2)**

Table 3.7 continued. Mean values and standard deviation (in brackets) of variables used for comparison of sediment samples. N – number of observations. HP –hemipelagic, DF – debris flow, GM – glacimarine, GT – glacial till. HI – hemipelagic +ice rafted debris.

TMF	N	*S/I*	$\frac{VO}{VO+Ni}$	*UCM/g(μg/g)*	*UCM/TNA*	*Pr/Ph*	Pr/C_{17}	Ph/C_{18}
BIF (HP)	4	14.8 (4.9)	0	0	0	1.21 (0.72)	0.47 (0.22)	0.59 (0.59)
BIF (GDF)	**16**	**29.5 (10.0)**	**0.59 (0.17)**	**76.2 (27.5)**	**9.31 (1.33)**	**1.23 (0.33)**	**1.80 (0.28)**	**0.99 (0.15)**
SSF (HP)	2	11.38 (0.69)	0	0	0	-	-	-
SSF (GM)	1	23.00	0.63	8.8	2.96	1.10	0.40	0.35
SSF (GT)	**4**	**18.1 (4.8)**	**0.73 (0.08)**	**28.8 (12.0)**	**12.72 (3.52)**	**0.72 (0.37)**	**0.92 (0.30)**	**0.65 (0.07)**
SSF (GDF)	**7**	**21.2 (9.5)**	**0.49 (0.04)**	**40.5 (59.5)**	**17.3 (17.57)**	**0.71 (0.31)**	**0.97 (0.38)**	**0.72 (0.15)**
NSF (GM)	1	10.7	0	7.95	3.04	0.35	0.55	0.63
NSF (GDF)	**9**	**7.9 (1.1)**	**0.34 (0.09)**	**19.5 (5.7)**	**2.67 (0.30)**	**0.76 (0.09)**	**0.76 (0.07)**	**0.77 (0.16)**
SVAL (GDF)	**5**	**11.3 (9.2)**	**0.41 (0.19)**	**71.9 (25.3)**	**7.31 (3.85)**	**1.61 (0.32)**	**1.07 (0.14)**	**0.37 (0.06)**
SVAL 986C1H2-90 (GDF)	**1**	**22.8**	**0.70**	**9.01**	**0.98**	**0.61**	**3.94**	**0.60**
LS (HP)	1	4.6	0	0	0	-	-	-
LS (HI)	4	6.4 (1.4)	0.98 (0.03)	1.2 (0.5)	9.24 (3.37)	-	-	-
LS (GDF)	**6**	**12.2 (0.9)**	**0.98 (0.04)**	**0.4 (0.3)**	**2.91 (0.65)**	-	-	-
BB (GM)	2	13.8 (1.4)	[a]0.22/[b]0	18.9 (15.7)	6.90 (1.85)	-	-	-
BB (GDF)	**11**	**16.4 (3.0)**	**[a]0.72 (0.14) / [b]0 – 0.19**	**8.8 (3.3)**	**3.86 (1.74)**	-	-	-

[a]Core HU77. [b]Core HU76. Relative abundance of Ni porphyrins in core HU76 - 0.81 – 1.

3.3.1.3 Long-chain alkenones

Hemipelagic and glacimarine samples from the considered locations typically contained traces or significant amounts of long-chain alkenones. These were absent from GDF samples from Bear Island Fan, Scoresby Sund Fan, Baffin Bay and Labrador Sea (HU87-025). This was expected because GDF contain ancient terrestrial sedimentary material not known to contain alkenones, biomarkers produced in the water column by photosynthetic algae. However, and surprisingly, alkenones were found in debris flows from North Sea Fan and Svalbard margin (Bellsund/Isfjorden Fans (ODP 986)) (**Figs. 3.5** and **3.6** and **Table 3. 8**). This indicates a possible input from the ancient outcrops of marine origin. Occurrence of alkenones in Eocene and Cretaceous sedimentary rocks has been reported previously (de Leeuw *et al.*, 1980; Farrimond *et al.*, 1986; Marlowe, 1984; Volkman *et al.*, 1980).

The U^K_{37} indices were calculated as (Brassell *et al.*, 1986b); (Prahl & Wakeham, 1987)

$$U^K_{37} = \frac{37{:}2 - 37{:}4}{37{:}2 + 37{:}3 + 37{:}4} \text{ and } U^K_{37}{}' = \frac{37{:}2}{37{:}2 + 37{:}3},$$

where U^K_{37} stands for relative abundance of unsaturated ketones with 37 carbon atoms and 2, 3or 4 double bonds. SSTs for core top samples were calculated from U^K_{37} index using equation by Rosell-Melé *et al.* (1995): SST=(U^K_{37} -0.043)/0.033. For the calculation of sea surface temperature estimates based on U^K_{37}', the calibration equation of Prahl *et al.* (1988), following Rosell-Melé & Comes (1999): SST=(U^K_{37}'-0.039)/0.034 were used.

The values of sea surface temperature (SST) in hemipelagic sediments from the BIF are consistent with those reported for core tops in the Nordic Seas by Rosell-Melé & Comes (1999). Relatively high SSTs were calculated for the Labrador Sea (~10°C). For the core top sample from Greenland, high SST (12.1°C) was calculated. This may be a result of bias due to the low concentration of alkenones in this sample (53 ng/g) (Rosell-Mele & Comes, 1999). Such low concentration can be attributed to dilution of autochthonous signal by input of terrestrial organic matter of

aeolian or fluvial origin. GDF alkenone signals are different from those of hemipelagic and glacimarine. SST values for debris flows from NSF are ~ 9°C, and those from Svalbard range from 8.4 to 11.2°C (**Figs. 3.5** & **3.6** and **Table 3. 8**). Most samples contained $C_{37:4}$ alkenone. Its concentration is relatively high in the debris flows (7-11% in NSF and up to 24 % on the Svalbard margin).

Table 3. 8 Alkenones in HP – hemipelagic, GM – glacimarine, GDF – debris flow. TOC – total organic carbon, SST – sea surface temperature estimate using U^{K}_{37}', ΣC_{37} – concentration of total triunsaturated and diunsaturated alkenones, % C37:4 – relative abundance of the tetraunsaturated alkenone. * U^{K}_{37} and equation by Rosell-Melé *et al.* (1995) was used for core top samples and U^{K}_{37}' and equation by Prahl *et al.* (1988) for debris flow samples. SST standard deviation $\delta < 0.5$°C.

Location		Core	Sample, cmbsf	TOC (%)	*U^{K}_{37}/ U^{K}_{37}'	SST (°C)	ΣC_{37} (ng/g)	% $C_{37:4}$	Gas Chromatogram
Bear Island Fan	HP (Holocene)	JR51GC08	0-3	1.00	*0.32	8.5	157	1.8	
		JR51GC10	0-3	1.03	*0.31	8.1	164	2.0	
Scoresby Sund Fan	HP (Holocene)	JR51GC31	0-2	0.61	*0.47	12.8	53	-	
North Sea Fan	GDF	HM 8303	170-174	0.41	0.35	9.4	166	7.3	
			220-224	0.48	0.35	9.3	128	6.7	
			270-274	0.50	0.35	9.3	117	7.8	
		HM 7908	230-234	0.50	0.35	9.2	165	7.4	
			260-264	0.60	0.35	9.3	127	7.9	
Svalbard	GDF	ODP 986A	1H 20-22		0.34	9.0	116	20.3	20-22 cm
			1H 90-92		0.38	10.1	138	21.3	
		ODP 986B	1H 20-22		0.36	9.6	566	18.4	
			1H 90-92		0.42	11.4	66	24.2	90-92 cm
		ODP 986C	1H 20-22		0.33	8.6	223	14.8	
			1H 90-92		0.40	10.7	56	20.8	
Labrador Sea	HP	HU88-025-02P	15-16 cm		0.43	11.7			
	GM		20-21cm		0.40	10.8			

3.3.2 Origin of biomarkers signatures in GDF deposits

The presence of reworked allochthonous organic matter in deep sea sediments from Nordic Seas has been described by Hölemann & Henrich (1994), Wagner & Henrich (1994) and Wagner & Hölemann (1995). The authors linked its origin to the erosion of continental outcrops in nearby land masses or the surrounding continental shelf. The authors described bulk properties of organic matter associated with different lithofacies deposited during glacial and interglacial periods in several cores from the Nordic Seas. Layers of dark diamicton which were formed under maximum glacial and early deglacial conditions as a result of iceberg transport and meltwater plumes were characterised by very low carbonate content (0-0.5 %), absence of foraminifera, elevated TOC levels (0.5 – 1.5 %) and a high amount of a coarse terrigenous fraction (20-40 %). These diamictons contained mature and overmature organic matter of terrestrial origin characterised by low hydrogen indexes (~50mgHC/gTOC), high T_{max} (420°-440°C), C/N >> 10 and $\delta^{13}C_{org}$ <-24‰ PDB) (Wagner & Henrich, 1994). The presence of fossil phytoclasts (coal, black shale and organic-rich siltstone clasts) and detrital vitrinites pointed at Mesozoic sediments from Scandinavian and Western Barents Sea shelves as a source area (Hölemann & Henrich, 1994; Wagner & Hölemann, 1995). There was also evidence for inputs from the northern North Sea and the Baltic Sea as indicated by the presence of Cretaceous nannofossils (Hölemann & Henrich, 1994).

In addition to these layers of diamicton, allochthonous organic matter was also present in sediments deposited during seasonally variable ice cover and iceberg drift as well as interglacial periods (Wagner & Henrich, 1994). In some of those sediments, the autochthonous signal is very weak possibly because of the early degradation of labile (marine) organic matter and dilution by allochthonous inputs. Unlike coarse-grained, mature and overmature organic matter in the diamictons, most organic matter in interglacial and glacial background deposits is finer-grained (10-20 % terrigenous coarse fraction), has lower TOC content (0.4 – 0.2 %) and shows lower thermal maturity (T_{max} <400°C) (Wagner & Henrich, 1994).

Similar to IRD, composition of different GDF deposits should reflect that of the outcrops eroded by the glaciers. It was also expected to differ from that in overlaying hemipelagic sediments. Biomarker signatures of organic matter from different sedimentary outcrops in the North Atlantic must reflect the differences in the depositional environments and post depositional transformation of the organic matter in these outcrops.

3.3.2.1 Description of continental outcrops

A simplified map of the main sedimentary outcrops along the North Atlantic margin is presented in **Fig. 3.8**. North American source areas are dominated by Palaeozoic carbonates. In addition to that, there are some Mesozoic sedimentary strata (Choubert *et al.*, 1987). Source areas along the Nordic Seas margin are characterised by high variability containing sedimentary rocks from Lower Palaeozoic to Late Cenozoic.

The drainage area of BB comprises Lower Palaeozoic dolomite and limestone from Ellesmere and Devon Islands, northwest Greenland and the Brodeur and Borden peninsulas. There is an outcrop of Mesozoic sediments in the north and Tertiary and Cretaceous sediments on the continental shelf of Baffin Island and Greenland (Aksu & Piper, 1987; Andrews *et al.*, 1989). GDF sediments in the LS supplied through the Hudson Strait, were derived from Palaeozoic carbonates from Hudson Bay, Baffin Island and Foxe Basin (Hesse & Klaucke, 1995). Secondary outlets along the eastern LS mostly delivered igneous and metamorphic material.

BIF drainage basin in the Barents Sea is dominated by Cretaceous and Early Tertiary mudstone and sandstone covered with muddy glacigenic diamicton up to 300 m thick (Elverhøi *et al.*, 1995a; Laberg & Vorren, 1996; Sigmond, 1992). Palaeozoic carbonates are present but they are largely overlaid by Mesozoic strata (Butt *et al.*, 2000).

The sedimentary succession of Svalbard comprises carbonates of Carboniferous age with a transition into silicaclasts from Permian onwards (Butt *et al.*, 2000; Elverhøi *et al.*, 1995a). Late Palaeozoic carbonate outcrops (limestone and

dolomite) are present in western Svalbard and northern and northeastern parts of Isfjorden (Butt *et al.*, 2000; Elverhøi *et al.*, 1995b). Tertiary sand- and siltstones are found south of Isfjorden. Jurassic and Cretaceous strata from the southeastern part Of Svalbard contain coal seams and black shales (Elverhøi *et al.*, 1995b; Wagner & Hölemann, 1995). A contribution from these outcrops in the GDF was confirmed by rock fragment and palynological analyses (Butt *et al.*, 2000; Elverhøi *et al.*, 1995a).

NSF source area contains deposits of Mesozoic-Tertiary sediments (sand- and siltstones, chert, coal and chalk) from Norway, Denmark, Skagerrak and the North Sea (Dowdeswell & Siegert, 1999; King *et al.*, 1998; 1996).

Sedimentary rocks from Carboniferous to early Tertiary period crop out in Jemesson Land north of Scoresby Sund (Krabbe, 1996; Linthout *et al.*, 2000). Surrounding areas west and south are dominated by igneous and metamorphic rocks that are of little interest for biomarker studies.

3.3.3 Palaeoceanographic significance of the presence of different biomarkers in GDF deposits

3.3.3.1 Terrestrial carbon in GDF and hemipelagic sediments

Terrestrial organic matter was present in all the sediment samples analysed, GDF, glacimarine and hemipelagic as indicated by high abundance of long-chain n-alkanes (Cn > 24). However, hemipelagic sediments contain younger, less reworked organic matter lacking such indicators of maturity and biodegradation as porphyrins and chromatographic UCM (Peters & Moldowan, 1993 and references therein) (**Figs. 3.3a,b&f** and **3.4a,b &f** and **Table 3. 7**). Distribution of n-alkanes in these sediments (chromatographic traces with unimodal envelope, maxima at n-C_{27-31} alkanes and high CPI) is consistent with a terrestrial origin of these components from higher plants (Eglinton & Hamilton, 1967). Deposition of these sediments probably resulted from aeolian input of dust (Poynter *et al.*, 1989), fluvial contribution of eroded soils (Prahl & Carpenter, 1984) or sea ice (Fahl & Stein, 1999). Very low relative abundance of short-chain n-alkanes indicates microbial degradation of marine organic matter (Peters & Moldowan, 1993). Low preservation of autochthonous organic matter in the North Atlantic waters during Cenozoic has been

reported by Hölemann & Henrich (1994). In this thesis, the presence of an autochthonous signal in the hemipelagic sediments has been identified by the presence of alkenones and chlorins.

Allochthonous organic matter is also predominant in GDF sediments, however, its biomarker composition is different from that of hemipelagic sediments. For instance, all GDF analysed contained porphyrins. These biomarkers form as a result of long-term (~10^6 years) transformation of chlorophyll in sediments (e.g. Baker & Lauda, 1986; Callot *et al.*, 1990). Porphyrins are commonly present in ancient sedimentary rocks (Eglinton *et al.*, 1985) and therefore their discovery in GDF sediments was expected. Vanadyl porphyrins were found in HLs 2 and 4 from core BOSF 5K from East Thulean Rise and Norwegian Sea core M23260 (Rosell-Melé & Koç, 1997; Rosell-Melé *et al.*, 1997). Absence of nickel porphyrins from these cores is surprising because they were present in all GDF sediments, but this could be due to the detection limit of the methods employed to measure them. Another indicator of the reworked nature of the GDF sediments is the presence of a mixture of highly branched aliphatic compounds that appear as a UCM hump in gas chromatograms of all GDF samples. These mixtures are not present in the hemipelagic sediments.

To conclude, biomarker signatures of GDF indicate terrestrial origin of sedimentary organic matter that resulted from glacial erosion of ancient sedimentary rocks. These biomarker signatures are sufficiently distinct from autochthonous signals and other allochthonous inputs during glacial stages. Allochthonous input in hemipelagic sediments was from younger, less reworked sedimentary organic matter and can clearly be distinguished from that in GDF.

3.3.3.2 Chlorins – autochthonous or allochthonous signal?

The presence of chlorins and alkenones in deep-sea sediments is usually attributed to autochthonous inputs, i.e. is thought to have been produced by photosynthetic microorganisms in the water column. Therefore, the discovery of these compounds in the debris GDF from the North Sea Fan and Svalbard was unexpected. The presence of such compounds in these sediments may be explained by admixture of

the pelagic sediments to the glacigenic ones prior to GDF deposition or presence of younger, less reworked, organic matter in the outcrops eroded by the ice streams. NSF contains relatively young (Cenozoic) sediments (Section 3.2.1.3). It may be suggested that chlorins here were not formed *in situ* but most likely belong to the sedimentary rocks eroded by the ice streams. King *et al.* (1998), for instance, demonstrated derivation of GDF sediments in the NSF from the mainland and offshore outcrops from Norway, Denmark, Skagerrak and the North Sea..

GDF sediments from Svalbard, on the other hand, differ from the other GDF analysed here in that they were collected outside any of the TMFs, between two fans. Because of such location, GDF here may contain considerable amounts of hemipelagic sediments. This view is supported by the fact that GDF sediments from this location are fine-grained in contrast with coarse-grained GDF sediments reported for the Isfjorden TMF (Elverhøi *et al.*, 1995b). This may indicate incorporation of a large proportion of hemipelagic sediments into the ODP 986 debris flow (similar to Wang & Hesse, 1996). However, results of mineralogical and palynological analyses strongly suggest terrestrial origin of these sediments (Butt *et al.*, 2000; Smelror, 1999). They contain abundant detrital carbonate (>15%) from Palaeozoic outcrops on the mainland Svalbard, numerous clasts of various ages and Mesozoic dinoflagellate cysts. Wide age distribution of the sedimentary sources contributing to the GDF sediments from the ODP986 (from Permian onward, Section 3.2.1.4) may explain the presence of chlorins from younger sedimentary sources together with porphyrins and reworked hydrocarbons from the more mature ones as a result of GDF formation.

Rosell-Melé *et al* (1997) attributed elevated amounts of chlorins in HLs to enhanced preservation of organic matter during HEs. The presence of these compounds in the sediments from some of the potential sources of IRD indicates a possibility of allochthonous input of chlorins in addition to autochthonous. The age of chlorins could be determined using isotopic analysis in order to confirm or reject the likelihood of such input.

3.3.3.3 Presence of Alkenones

The presence of alkenones in some of the GDF indicates that during glacial times, deposition of alkenones in the deep sea could be a product of allochthonous as well as autochthonous and input. This poses some questions for the use of these biomarkers to reconstruct palaeoceanographic conditions (e.g. SST) in the environments where IRD inputs were significant. For instance, Rosell-Melé & Comes (1999) reported unusually high (warmer than at present) sea surface temperature estimates derived from alkenone indices (U^K_{37} and U^K_{37}') for the LGM in the Nordic seas (**Fig. 3.5**). As one of the possible explanations for the bias in SST estimates, the authors suggest the admixture of allochthonous alkenones into the sediments as a result of ice rafting. Input of terrestrial sediments containing alkenones from warmer, pre-Quaternary, climates could bias U^K_{37} estimates towards warmer values.

SST values calculated for the GDF from NSF and Svalbard (**Table 3. 8**) are significantly lower then the speculated ~30°C for source sediments representing pre-Quaternary environments (Rosell-Melé & Comes, 1999). They are in fact lower then those obtained for the LGM samples by Rosell-Melé & Comes (1999). Even an input of the equivalent amount of allochthonous alkenones with U^K_{37}'=0.4 (~11°C) (as observed for some of the samples from Svalbard) would only increase the presumed U^K_{37}' autochthonous signal of U^K_{37}'=0.2 (~5°C) to 0.3 (7.7°C), still lower than 12.0-16.8 °C reported by Rosell-Melé & Comes (1999). Moreover, such high input from Svalbard seems unlikely since Bellsund and Isfjorden Fans are several orders of magnitude smaller then other major TMFs. Although the size of the TMF is not directly proportionate to the sedimentary output of the ice stream (O Cofaigh *et al.*, 2003), such vast difference in size of the TMFs is likely to reflect the difference in the amount of sediments passed through each glacier outlet. Therefore, the alkenone signal from Svalbard would probably be diluted to a large extent by that from other source areas and could not be responsible for such elevated values for SST.

The presence of the $C_{37:4}$ alkenone in some of the debris flows (**Table 3. 8** and **Fig. 3.7**) suggests that $C_{37:4}$ content of LGM sediments is also of mixed origin and therefore the tetraunsaturated component cannot be considered as a better

representative of autochthonous signal then di- and triunsaturated ones. High concentration of $C_{37:4}$ alkenone in the debris flows (7-11% in NSF and up to 24 % on the Svalbard margin) allows us to speculate that the autochthonous concentration of this component in LGM sediments was probably lower then calculated by Rosell-Melé & Comes (1999). For example, to result in the mixed $\%C_{37:4}$ =5%, with an input of equal amount of total allochthonous alkenones with $\%C_{37:4}$ =8%, autochthonous $\%C_{37:4}$ would have to be only 3%. That would make the suggestion by Rosell-Melé & Comes (1999) that SST during LGM was not higher then 6°C less certain.

3.4 Comparison of biomarker signals in debris flow deposits from the North Atlantic

In order to use GDF sediments as a source proxy for IRD in the deep ocean, it is of course necessary to prove that biomarker composition of these sediments is equivalent to that of the IRD. In this Section it will be shown whether the composition of biomarkers in GDF

1. differs significantly from that of overlying hemipelagic sediments

2. is homogenous within each source area. The latter is understood to be the drainage area of the ice-stream that gave rise to the formation of a TMF and the associated GDF.

3. is significantly different between potential source areas.

The comparison of the distribution of biomarkers from different locations is based on visual and statistical comparison of gas chromatograms and UV-VIS absorbance spectra results. The statistical methods employed are based on a similar approach used in oil exploration and geochemical research (e.g. Peters *et al.*, 2000). Biomarker composition of glacigenic and hemipelagic sediments from debris flow deposits from the Nordic Seas and North America was compared based on the distributions of

- photosynthetic pigments
- saturated hydrocarbons
- unresolved complex mixture (UCM).

Biomarker composition of the sedimentary organic matter in the samples analysed was expressed in a number of variables representing absolute and relative abundances of different components (See Sections 1.4.3 and 1.4.4). The list of variables used for comparison and mean values for different sediments are presented in **Table 3. 7**. For the full list of values, see **App.3**.

3.4.1 Principal component analysis

Eleven variables were used for comparison of GDF biomarker data. Variables used for principal component analysis (PCA) and their mean values are listed in **Table 3. 7**. Pristane/phytane and isoprenoids/n-alkane ratios were not included because they were missing from most of the North American samples due to low abundances and coelution (see Section 3.3.1.2). Eleven principal components (PC) were created. First three PCs have eigenvalues greater then one. They are responsible for 76 % of variance (**Table 3. 9**).

Table 3. 9 Results of principal component analysis of debris flow sediments. Eigenvalue – proportion of variability represented by each component. Difference in eigenvalues between the components PC_i and PC_{i+1}; Proportion - proportion of variability represented by each component normalised to 1; Cumulative – cumulative proportion of variability represented by components PC_1- PC_i.

Component	Eigenvalue	Difference	Proportion	Cumulative
1	**4.29098**	2.20993	0.3901	0.3901
2	**2.08105**	0.12191	0.1892	0.5793
3	**1.95914**	1.05856	0.1781	0.7574
4	0.90058	0.16924	0.0819	0.8393
5	0.73134	0.19770	0.0665	0.9057
6	0.53363	0.28841	0.0485	0.9542
7	0.24523	0.10692	0.0223	0.9765
8	0.13831	0.08263	0.0126	0.9891
9	0.05568	0.01502	0.0051	0.9942
10	0.04066	0.01726	0.0037	0.9979
11	0.02340		0.0021	1.0000

Table 3. 10 Eigenvectors (coefficients reflecting varying contributions of the variables).

Variable	PC1	PC2	PC3
TNA	0.26550	-0.08380	**0.44124**
CPI_{17-23}	**-0.31999**	**0.38144**	0.24206
CPI_{24-31}	**-0.32618**	0.00149	**0.40171**
C_{27}/ C_{29}	**0.29225**	-0.19646	**0.43813**
C_{29}/ C_{31}	0.08689	**0.66417**	-0.02546
ACL_{25-33}	-0.22169	**-0.55552**	-0.16552
$\frac{\sum C_{29-31}}{\sum C_{29-31}+\sum C_{17-19}}$	**-0.45623**	0.03850	0.13541
S/I	**0.28179**	0.23375	-0.18357
$\frac{VO}{VO+Ni}$	-0.05890	0.01956	**-0.51678**
UCM/g	**0.42935**	-0.02744	0.14589
UCM/TNA	**0.32133**	-0.04363	-0.15798

Most of the variables are strongly represented in PC1 (**Table 3. 9** and **Table 3. 10**), which accounts for 39% of variance. In this component, UCM correlates with ratio of n-C_{27} to n-C_{29} and abundance of porphyrins represented by *S/I* ratio. These variables are opposed by Carbon preference indexes and relative abundance of long-chain n-alkanes (n-C_{29-31}). UCM is a result of biodegradation and amount of UCM reflects the degree of biodegradation. Predominance of long-chained n-alkanes decreases with maturity and biodegradation as a result of reworking of the organic matter (e.g. Tissot & Welte, 1984). Relative abundances of different long-chain n-alkanes (e.g. n-C_{27} to n-C_{29}) are characteristic of specific environments in which organic matter was formed. Thus, in PC1, higher values are favoured by higher degree of biodegradation and maturity, higher relative abundance of porphyrins and predominance of n-C_{27}, over n-C_{29} alkane.

The second component (**Table 3. 9** and **Table 3. 10**) represents 19% of variance. In this component, CPI of short-chained n-alkanes correlates with ratio of n-C_{29} alkane to n-C_{31} and contrasts with average chain length (ACL). PC2 accounts for specific characteristics of each sediment source related to their depositional environments and degree of maturity.

PC3 accounts for 18% of variance (**Table 3. 9**). Here, CPI of long-chained n-alkanes, ratio of n-C_{27} to n-C_{29} alkane and amount of total n-alkanes are opposed to relative abundance of vanadyl porphyrins (**Table 3. 10**). Abundance of vanadyl porphyrins indicates predominance of anoxic conditions in the ancient depositional environment (Lewan, 1984). In this component, predominance of n-C_{27} alkane over n-C_{29} is associated with more organic-rich younger sediments deposited in the environments with higher Redox potential..

To illustrate variability in biomarker composition within and between GDF sediments from different locations, principal components 1, 2 and 3 are plotted against each other (**Fig. 3.9**). Pristane/phytane and isoprenoid ratios for GDF from the Nordic Seas are plotted in **Fig. 3.11**.

3.4.2 Variability within each GDF deposit

3.4.2.1 Homogeneity of GDF sediments within each TMF

Debris flows from the Nordic Seas show largely homogenous n-alkane, pigment and alkenone distribution within each TMF. This is consistent with the character of GDF formation in this area: each TMF formed at the mouth of a single large ice stream (e.g. Vorren & Laberg, 1997 and references therein).

Sediment samples from NSF show little variability within this TMF. They form a tight group on PCA plots (**Fig. 3.9**). NSF samples belong to three cores from different debris flow lobes. The homogeneity of n-alkane and pigment content is in agreement with homogeneity in other properties reported by King *et al.*, (1998). It may be concluded that sediments from the NSF are highly homogenous in their biomarker composition.

One out of six debris flow samples from ODP 986 (C-90cm) is markedly different from the rest of the samples. It displays lower concentration of n-alkanes and porphyrins, lower maturity and lower degree of biodegradation and low abundance of porphyrins. There is also variation in *TNA* content between deeper (90cm) samples and the shallower ones (20 cm) with shallower samples being more *TNA* rich. However, the variability between the five typical samples from Svalbard (excluding C-90) is lower than that between Svalbard and other GDF deposits (**Figs 3.9 and 3.10**).

Most samples from SSF display low degree of scatter **Fig. 3.9**. Sample GC32-140 cm is characterised by very high UCM (*UCM/TNA*=57). This explains its very high PC1 score. Two samples from the upper part of the thick debris flow in cores GC31 and GC32 (55 and 90 cm respectively) are characterised by higher $CPI_{24\text{-}31}$ and n-C_{29} to n-C_{31} ratio (reflected in PC3 and PC2 respectively) than other samples from SSF. They plot closer to BIF samples. Sample GC31-55 cm cannot be distinguished from BIF sediments. There is higher variability in GC32 debris flow sediments.

Only one core containing GDF from LS was analysed, and the samples from that core show high homogeneity in their biomarker composition. Due to the existence of several sources of GDF sedimentation along the LS margin (Hesse *et al.*, 1990; Wang & Hesse, 1996), analysis of samples from other locations in the LS is needed to present a clear picture of biomarker distribution in this area.

N-alkane distributions from the two BB cores display unimodal envelope with maximum at n-C_{29} and low abundance of short-chain components but differ from one another in some of the parameters. HU77 samples have higher *CPI*, lower C_{27}/C_{29} and higher C_{29}/C_{31} ratios (App. 3). In both cores, porphyrins are in low abundance but in HU76 VO species are absent or have much lower abundance than Ni (Table 3.7). This explains high variability in PC2 and PC3. However, BB sediments are different from the rest of the samples in this study and form a group, albeit a loose one. Difference between the two cores from different locations in BB is expected because of the line-source character of sedimentation in this area (Aksu & Hiscott, 1989; Aksu & Piper, 1987).

So, to conclude, GDF sediments are largely homogenous in their biomarker composition, which indicates a highly mixed nature of these sediments. Therefore the biomarker fingerprints of the organic matter in each GDF can be considered as a combined signature of a variety of outcrops eroded by a particular ice stream.

3.4.2.2 Comparison of GDF and other types of sediments

As it could be expected, biomarker composition of debris flows differs markedly from those of hemipelagic sediments (**Figs. 3.3a,b&f** and **3.4a,b &f** and **Table 3. 7**). Hemipelagic sediments are characterised by lower abundance of n-alkanes, higher CPI and ACL, absence of UCM and porphyrins and well defined predominance of the long-chain n-alkanes over the short-chain ones than GDF sediments. This indicates the presence of the less reworked organic matter in hemipelagic sediments than in the GDF. In order to support discussion based on visual comparison of gas chromatograms and UV-VIS absorbance spectra, analysis of variance (ANOVA) was used in order to consider variability in individual parameters. In **Table 3. 11**, the results of comparison of GDF and hemipelagic sediments from BIF are presented. All parameters show significantly higher variability between the two types of sediments than within each type. Only *Pr/Ph* ratios are not significantly different due to the high variability of this variable in hemipelagic sediments. This may be due to the reduced accuracy in measurement of pristane and phytane abundances in the hemipelagic sediments because of their very low concentration (<10 ng/g dry sediment).

As was mentioned above, glacial till sediments from the continental shelf off Scoresby Sund show similar n-alkane distribution to those from GDF despite the difference in some of the bulk properties (see Section 3.2.1.2). This similarity is confirmed by the analysis of variance (**Table 3. 11**). However, relative abundances of Ni and VO porphyrins in the two types of sediments are significantly different, i.e. substantially higher for the glacial till sediments ($VO/(VO+Ni)$ = 0.72 vs. 0.49). This may indicate variability in the sedimentary input between the two types of sediments. In the study of BIF, Laberg and Vorren (1995) observed similarity in the grain size distribution and water content of GDF sediments with those from the glacigenic till.

King *et al.* (1998), although emphasised the similarities between the two types of sediments from NSF, report gradual increase in mainland-derived rock fragments relative to offshore Mesozoic-Tertiary strata in sediments in NSF GDF compared to Glacial till from the same location. The variability in porphyrin ratios in SSF sediments could be a result of similar variability between GDF and glacial till sediments. If the mainland sediments from East Greenland contain lower proportion of Ni porphyrins than the offshore strata, this would be reflected in the porphyrins ratio. However, these two types of sediments are indistinguishable using all other variables and are more similar to each other than to any other GDF analysed. That allowed including glacial till sediments in the principal components analysis together with the GDF samples. We propose that GDF may be more accurate in representing sources of IRD transported by icebergs into the ocean than glacial tills because they contain higher amounts of the mainland derived sediments. However, not all ice streams resulted in GDF formation. Development of GDF is determined by several factors including steepness of continental slope, availability of erodible sediments and width of continental shelf (O Cofaigh *et al.*, 2003). In locations where ice streams did not result in GDF formation, glacial till sediments from continental shelf can probably be used as a source proxies largely to the same effect. Continental shelf sediments were used by Grousset et al. (2001) as source proxies of IRD in HLs in core SU90-09.

It was initially intended to use ice rafted debris mixed with hemipelagic sediments from core HU88 (HI facies from Wang & Hesse, 1996) because of the similarity in the general appearance of their n-alkane envelope and absorbance spectra (**Figs. 3.3f** and **3.4f**). Analysis of variance, however, shows significant difference in most variables between the two types of sediment (**Table 3. 11**).

So, to conclude, biomarker composition of GDF sediments is significantly different from that in the overlaying hemipelagic sediments that indicates different origin of these two types of sediments (glacial erosion vs. aeolian/fluvial weathering). On the other hand, glacial erosion is responsible for the formation of both glacial till and GDF sediments and variability in their composition is probably due to variability in the relative representation of the mainland and offshore outcrops.

Table 3. 11 Comparison of different types of sediments within GDF deposits. Statistical significance (p) of variability between glacigenic debris flows and hemipelagic sediments from Bear Island Fan, glacial till (GC30) and GDF sediments (GC31,32) from Scoresby Sund Fan and glacimarine (HI) (HU88) and GDF sediments (HU87) from the Labrador Sea. $P<0.05$ – variability statistically significant with 95% confidence.

Groups compared	BIF(GDF) vs. BIF(HP)	SSF(GDF) vs. SSF(GT)	LS(GDF) vs. LS(HI)
TNA (ng/g)	0.0002	**0.9255**	**0.6470**
$CPI_{17\text{-}23}$	0.0007	**0.9355**	**0.5693**
$CPI_{24\text{-}31}$	0.0000	**0.4728**	0.0020
C_{27}/C_{29}	0.0000	**0.8671**	0.0384
C_{29}/C_{31}	0.0000	**0.8084**	0.0232
$ACL_{25\text{-}33}$	0.0000	**0.9536**	0.0208
$\frac{\sum C_{29-31}}{\sum C_{29-31}+\sum C_{17-19}}$	0.0000	**0.9370**	0.0021
S/I	0.0111	**0.5071**	0.0000
$\frac{VO}{VO+Ni}$	0.0000	0.0002	**0.8611**
UCM/g	0.0000	**0.7959**	0.0217
UCM/TNA	0.0000	**0.7578**	0.0048
Pr/Ph	**0.9436**	**0.8507**	
Pr/C_{17}	0.0000	**0.9371**	
Ph/C_{18}	0.0178	**0.8354**	
PC1	0.0000	**0.7849**	0.0181
PC2	0.0000	**0.8376**	0.0385
PC3	0.0000	**0.6905**	0.0063

3.4.3 Variability between GDF deposits

3.4.3.1 Nordic seas

GDF can be used as proxies for IRD sources in the North Atlantic Heinrich Layers if their biomarker signatures are different from one another. In the Nordic Seas, four GDF deposits analysed show such dissimilarities in their biomarker content and composition. For example, concentration of n-alkanes in the SSF GDF is ~ 4 times lower than in the BIF and 6 times lower than in the Svalbard GDF. This is explained by predominance of organic-poor igneous and metamorphic outcrops in the SSF drainage basin. NSF sediments differ from those in the other TMFs from this area in that they contain less reworked organic matter as indicated by the presence of chlorins, unimodal n-alkane envelope with high CPI and low abundance of short-chain n-alkanes and low chromatographic UCM (**Figs. 3.3c, 3.4c, 3.10** and **Table 3. 7**). Five out of six samples from Svalbard present a mixture of thermally mature, biodegraded organic matter as indicated by low CPI, high relative abundance of short-chain n-alkanes and the presence of UCM in the chromatographic trace, as well as relatively young, unoxidised organic matter represented by chlorins and alkenones (**Figs. 3.3d, 3.4d** and **Table 3. 7**).

With maturation, original n-alkane distributions from different sources become more and more similar as a result of input of reworked n-alkanes (Peters & Moldowan, 1993). However, differences can be seen in the n-alkanes fingerprints of GDF from BIF, SSF and Svalbard (**Figs. 3.4** and **3.10**). The most abundant n-alkane in the BIF, SSF and Svalbard GDF are n-C_{19}, n-C_{22} and n-C_{23} alkanes respectively. There is slight odd over even preference in the low molecular weight n-alkanes from BIF ($CPI_{17\text{-}23}$= 1.2) whereas there is no such preference in the samples from SSF($CPI_{17\text{-}23}$= 1.0) and even n-alkanes predominate in the samples from Svalbard ($CPI_{17\text{-}23}$= 0.88). Distribution of the long-chain n-alkanes shows different degrees of maturation which is the highest in SSF (lowest $CPI_{24\text{-}31}$ =1.4) and the lowest for Svalbard ($CPI_{24\text{-}31}$= 1.9). Mixtures of the highly branched aliphatic compounds from SSF and BIF form similar UCM humps in the chromatograms. They are large and have maximum at the retention time of the n-C_{29} alkane, whereas UCM from

Svalbard is lower in high-molecular weight components and has a maximum at the retention time of the nC_{20-23} n-alkanes.

Nordic Seas GDF can also be distinguished from one another based on their *Pr/Ph* and isoprenoid/n-alkane ratios (**Fig. 3.11**). There is an overlap between SSF and NSF samples. These TMFs, however, are well separated by other variables.

3.4.3.2 Labrador sea/Baffin Bay

GDF sediments from BB and LS contain lower amounts of n-alkanes than the Nordic Seas sediments. This can be explained by lower organic content in the ancient carbonates compared to shale and also an admixture of sediments from igneous and metamorphic sources along the LS eastern margin (Wang & Hesse, 1996). Concentration of n-alkanes in the LS GDF is an order of magnitude lower than in the BB GDF. GDF from the two locations differ from each other in their n-alkane distributions (**Figs. 3.4e, f and 3.10**). BB n-alkanes are characterised by lower maturity as exemplified by higher CPI. Relative abundance of $n\text{-}C_{31}$ is substantially lower in BB GDF. This is reflected in lower ACL and higher C_{29}/C_{31} ratio for the BB samples.

3.4.3.3 Overall comparison of the North Atlantic GDF signatures

Debris flows were compared using results of the PCA analysis. The results are presented in **Fig. 3.9.** Debris flow sediments containing organic matter of lower maturity and biodegradation (NSF, LS and BB) are separated from those with more mature, biodegraded and more porphyrin rich organic matter (BIF, SSF and most Svalbard) by PC1 (**Fig. 3.9a** and **Table 3. 7**). PC2 separates BB GDF from the LS and NSF. LS samples have the lowest values because of their lowest CPI and highest abundance of $n\text{-}C_{31}$ alkane. In contrast, BB CPI_{17-23} is the highest and abundance of $n\text{-}C_{29}$ alkane nearly twice that of $n\text{-}C_{31}$. PC3 is the highest for NSF sediments with high abundance of total n-alkanes, high CPI_{24-31} and C_{27}/C_{29} ratio and predominance of Ni porphyrins. The lowest values are obtained for LS samples

because of low concentration of total n-alkanes, C_{27}/C_{29} ratio <1 and VO porphyrins predominance (**Table 3. 7**).

Debris flows containing more reworked organic matter are less well separated by PC2: there is an overlap between BIF and SSF on the PC1/PC2 plot **Fig. 3.9a**). This is because sediments from these TMFs are close in degree of maturity and biodegradation. There is also high deviation in C_{29}/C_{31} ratio for SSF samples that causes high variability in PC2 for this TMF. BIF and SSF are separated on a PC3/PC2 plot with only one sample (GC31-55 cm) plotting with BIF samples (**Fig. 3.9b**). NSF and LS, although slightly overlap on PC1/PC2 plot, are well separated by PC3 due to their contrast in total n-alkane concentration, C_{27}/C_{29} ratios and relative abundance of porphyrins (**Table 3. 7**). Svalbard debris flows form a discrete group on PC1/PC2 plot except for one outlier (ODP 986C-90cm).

To conclude, GDF sediments analysed in this study are characterised by specific biomarker signatures unique to each TMF deposit. This makes it possible in principle to use biomarker composition of GDF as a proxy for the source of IRD in the North Atlantic.

3.4.4 Use of biomarker composition of GDF to constrain sources of IRD in the North Atlantic

In the provenance studies to date, mostly continental outcrops are considered as proxies to characterise the composition of the sources of IRD. These studies have concentrated on the bulk properties of sediments from potential sources (see Section 1.2) and, to our knowledge, biomarker composition of potential sources of IRD has not been considered previously. Because of the heterogeneity of the continental outcrops eroded by glaciers (see Section 3.3.2), GDF composition is more likely to represent that of IRD in the deep ocean than composition of individual outcrops. For instance, sediments from Svalbard were shown to contain a mixture of reworked organic matter with that from a younger source (or sources) (see Section 3.4.3.1). Biomarker fingerprinting presents a more detailed and a more specific approach than analysis of bulk properties of the sediments from potential sources. Sediments characterised by similar mineralogical composition may differ in their biomarker

content, which preserves information about depositional environments and post depositional diagenesis of organic matter.

The results or this study show that debris flows from different locations in the North Atlantic can be distinguished from one another based on biomarker fingerprints using GC traces alone (**Figs. 3.4** and **3.10** and **Table 3. 7**). UV-VIS analysis provided additional information (**Fig. 3.3** and **Table 3. 7**). Use of biomarkers allows distinguishing not only between American and European sources but also between different locations in the Nordic Seas and the North America. GC and UV-VIS spectrophotometry are robust and the least specific methods of describing biomarker composition of potential IRD sources. Great potential lies in using Gas Chromatography linked to Mass Spectrometry, which will allow identification of other hydrocarbons, such as for instance aromatic compounds, steranes and hopanes. These biomarkers are commonly used in petroleum industry in correlation studies. They are more resistant to reworking through geological time and better reflect the depositional environments of the original sediment sources (Peters & Moldowan, 1993). Broadening the spectre of biomarkers used to describe potential sources of IRD would allow clearer separation between them, especially between the GDF containing highly reworked organic matter. Use of Liquid Chromatography coupled to Mass Spectrometry would allow not only differentiation between different types of tetrapyrrolic pigments but also identification of the molecular structure of individual pigments. Relative abundances of porphyrins in different GDF may be similar reflecting Redox conditions at the time of formation. However, other factors such as temperature, salinity and availability of nutrients may have resulted in different microbial assemblages and consequently different diagenetic pathways of chlorophyll degradation. That should be reflected in the structure of the porphyrins formed in different locations. Potentially, compounds unique to a specific source may be identified.

It is important, however, to bear in mind that different potential sources of IRD differ not only in their biomarker composition but also in biomarker concentrations. For instance, GDF from BB and LS analysed here are low in organic carbon and contain low absolute abundances of n-alkanes. Because sedimentary rocks are much higher in TOC than igneous and metamorphic and shales are more

organic-rich than carbonates, contribution of biomarkers from each source is not proportionate to the relative input of the IRD from that source. That is why it would be difficult to use biomarker approach to quantify contribution from different potential sources since a relatively insignificant source characterised by high organic matter content may be stronger represented in the HL sediments than a more important but TOC-poor source. Biomarker analysis should be used in combination with methods that take into account all other contributions (i.e. igneous and metamorphic).

With regards to the identification of potential sources, probably more samples need to be studied from the Baffin Bay and Labrador Seas because of the heterogeneity of the GDF input in these areas. It is possible that because of the line-source sedimentation in the LS and BB, the samples analysed in this study may not be representative of the main drainage area. For instance, the presence of undegraded organic matter of low maturity in the GDF sediments from North America was unexpected. Palaeozoic carbonates from the drainage areas of these GDF should contain organic matter of marine origin with high relative abundance of shorter-chain n-alkanes and no odd over even carbon numbers predominance (Peters & Moldowan, 1993). Given the old age of these rocks, high degree of reworking of organic matter was expected. However, biomarker composition of the sample from HL2 from core HU87-025-07P shows similar organic matter composition to that from GDF from the same core and probably reflects genuine composition of the IRD input from a number of sources in the northern Canada. In support of this view, GDF from both locations are high in their detrital carbonate content (see Section 3.2.2). It is possible that biomarker signature of the organic-poor carbonates in GDF is swamped by that of the younger outcrops containing large amounts of n-alkanes (**Fig. 3.8**).

Timing of the GDF deposition is also important. The composition of the IRD and GDF from the same location may differ through time. This may be due to complete erosion of particular geological strata or a change in the pathway of the ice streams. For example, such change of the ice stream trajectory was proposed to explain the variability between HL3 and HLs 2 and 4 (Andrews & MacLean, 2003; Kirby & Andrews, 1999) Such occurrences may result in glacial erosion of different

outcrops and different composition of IRD from the same location but from different time periods. Thus variability in composition of IRD observed between and within different HLs (Grousset *et al.*, 2001; e.g. Huon *et al.*, 2002) may not only be a result of different sources of IRD but also of the change in composition of IRD from the same source. Analysis of GDF deposited during different episodes of ice rafting may provide more accurate information on the changes in IRD composition through time.

There is a possibility that GDF do not accurately represent composition of IRD in the deep ocean. Different outcrops eroded by icebergs contribute to different size fractions depending on the type of rock, e.g. shale is most likely to be predominant in the fine fraction. Particle size distributions in the deep-ocean sediments may differ from those forming GDF. For instance, <63 μm fraction in the deep-ocean sediments can be transported by means other than ice rafting (e.g. Andrews, 2000) and contain different biomarker signatures than those in GDF. In addition to that, scouring by bottom currents can modify the grain size distributions in the ocean sediments by removing the fine fraction (e.g. McCave, 1995). However, analysis of the coarse fraction (>150 μm) alone will result in bias towards the rock types that tend to break into larger particles (Hemming, 2004). Thus, different grain size fractions should probably be studied in both sources and sinks of IRD.

3.5 Conclusions

- GDF deposits in the North Atlantic margins are rich in organic matter. GDF sediments are largely homogenous in their biomarker composition, and the biomarker fingerprints of the organic matter in each GDF can be considered as a combined signature of a variety of organic-rich outcrops eroded by a particular ice stream. GDF contain biomarker distributions that are characteristic and unique to each TMF deposit.

- The biomarker composition of GDF is thus significantly different from that of the overlaying hemipelagic sediments. GDF sediments contain generally a very high proportion of biodegraded and thermally mature organic matter originating from ancient outcrops eroded by former ice streams. Hemipelagic sediments overlying GDF or in deep sea cores contain a less reworked organic matter signature, both autochthonous and allochthonous.

- In consequence and in principle, biomarker composition of GDF could be used to constrain the sources of IRD in the North Atlantic during the last glacial

- Because the biomarker composition of glacial till deposits is similar to that of GDF, it can also be used as a proxy to infer the organic composition of IRD in deep ocean.

- Given the complexity of biomarker distributions in GDF, biomarker analyses of potential IRD sources presents a potentially more detailed and more specific approach than analysis of bulk properties of the sediments to characterise sources of IRD present in deep sea sediment cores of the glacial North Atlantic. This will be investigated further in Chapter 4.

- Some GDF contain biomarkers that are also found in "contemporary" glacial hemipelagic sediments, namely alkenones and chlorins. It is to be expected that IRD originating from the TMF where these deposits are located also contained alkenone and chlorin signatures that were indistinguishable from

autochthonous inputs in the areas where the IRD finally sedimented in the deep sea. In consequence, interpretation of the distributions of these biomarkers in deep sea cores during the last glacial is constrained by the uncertainties regarding the predominantly autochthonous or allochthonous origin of such biomarkers signatures. In other words, the use of these biomarkers to reconstruct palaeoceanographic conditions (i.e. SST and primary productivity) during glacial times in the North Atlantic may be incorrect because of the potential bias caused by the possible existence of allochthonous contributions of these biomarkers.

4. Sources of Organic matter In North Atlantic Heinrich Layers

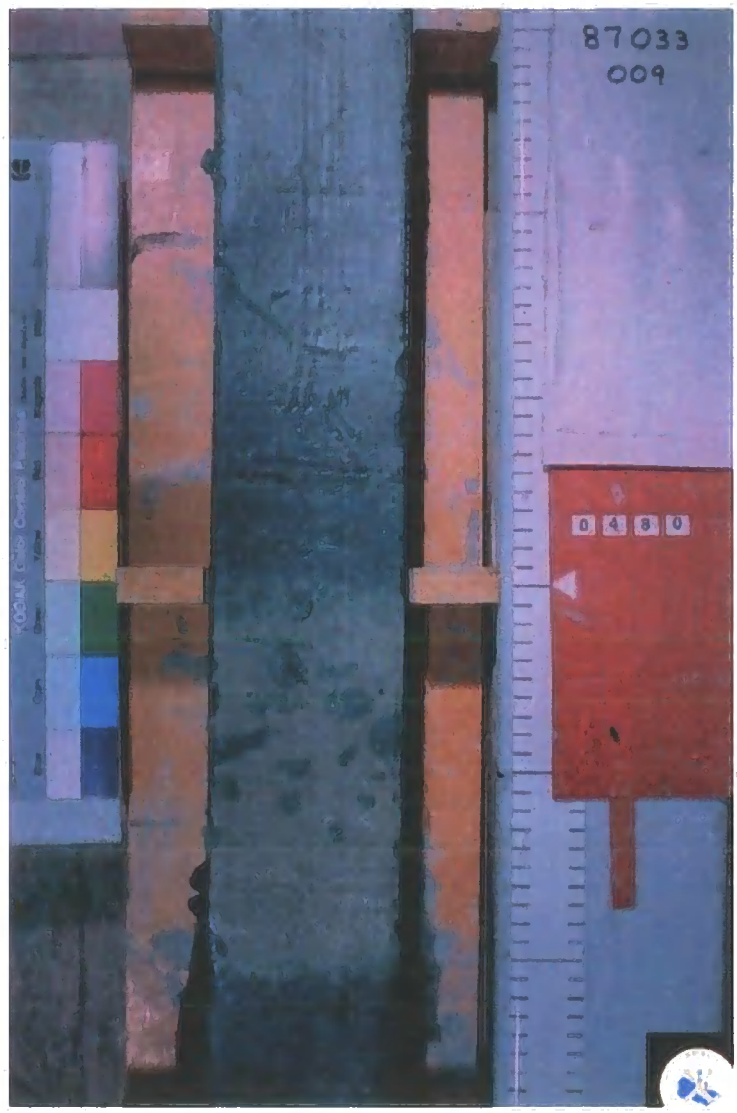

Cover image: Deep-sea sediment core with Heinrich event 1 represented by the light-coloured sediment in the bottom half of the image. Photo: Bedford Institute of Oceanography

CONTENTS

TABLES

(See volume II for figures).

4.1 Introduction

In this chapter, the use of biomarkers to investigate the provenance of ice rafted debris (IRD) in deep-sea sediments during the ~60-10.5 kyr BP interval is investigated.

- The general aim of this chapter is to test a hypothesis that the IRD deposited in HLs carry biomarker signatures analogous to those from potential sources, and therefore sources and sinks of IRD can be correlated based on their biomarker signatures or fingerprints.

In order to understand the causes and mechanisms of climatic change during the last glacial period, some questions on provenance of ice rafted debris in the North Atlantic still need to be clarified. While the Hudson Strait outlet of the Laurentide Ice Sheet has been established as the main source of IRD in the North Atlantic Heinrich layers (HLs) 1, 2, 4 & 5 (e.g. Andrews & Tedesco, 1992; Bond *et al.*, 1992; Gwiazda *et al.*, 1996b; Hemming *et al.*, 1998), the significance of European input of IRD has been questioned (Farmer *et al.*, 2003). According to most studies, the sources of sediments in the "untypical" HLs 3 and 6 appear to differ from those in the "typical" HLs 1, 2, 4 and 5 (e.g. Andrews & MacLean, 2003; Grousset *et al.*, 1993; Gwiazda *et al.*, 1996a; Kirby & Andrews, 1999). However, some authors contest these findings (Hillaire-Marcel *et al.*, 1994; Rashid *et al.*, 2003a; Stoner *et al.*, 1996).

In addition to the "untypical" character of HLs 3 and 6, there is indication of variability between prominent HLs 1, 2, 4 and 5 (e.g. de Abreu *et al.*, 2003; Hemming & Hajdas, 2003; Huon *et al.*, 2002) that needs further investigation.

High-resolution study of core SU90-09 showed that deposition of each HL occurred in a series of pulses lasting 2-5 centuries and may indicate intermittent iceberg release from the Laurentide or latitudinal oscillations in the pathway of the icebergs (Grousset *et al.*, 2001).

The main focus of provenance studies so far has been on investigation of mineralogical and isotopic composition of lithic fraction of the HLs (e.g. Bond & Lotti, 1995; Grousset *et al.*, 2000; Hemming *et al.*, 1998) and bulk properties of organic matter (Huon *et al.*, 2002). As an alternative proxy for IRD in the North Atlantic, Rosell-Melé *et al* (1997) proposed using ancient biomarkers. The presence of porphyrins (Rosell-Melé & Koç, 1997; Rosell-Melé *et al.*, 1997) and reworked n-alkanes (Villanueva *et al.*, 1997) in Heinrich layers has been attributed to input from ice rafting. Villanueva *et al.* (1997) suggested that variability in n-alkane distributions between two North Atlantic cores (SU90-39 and SU90-08) reflects different origin of IRD in the two locations. In this chapter, the use of biomarkers (porphyrins and n-alkanes) to address some of the questions on provenance of IRD in HLs is investigated.

4.2 Background. Cores used in this study

Samples from 4 locations in the North Atlantic were analysed (**Fig. 4.1**). They are expected to represent sinks of ice rafted material potentially originating from different areas in the North Atlantic. All cores had been extensively studied previously using a diversity of methods, dated by accelerator mass spectrometry (AMS) ^{14}C dates and placed on a common timescale using their geomagnetic palaeointensity records (Grousset *et al.*, 2001; Stoner *et al.*, 1996; 1998). Core locations and collection data are presented in **Table 4. 1**.

In order to investigate biomarker evidence for down core variability in composition of organic matter in North Atlantic Quaternary sediments, core SU90-09 was chosen. This core had previously been exhaustively studied using a number of parameters (Grousset *et al.*, 2001; Huon *et al.*, 2002; Tamburini *et al.*, 2002) (See Section 4.2.1). Following the strategy of Grousset *et al.* (2001), SU90-09 was analysed at high resolution: samples from Heinrich layers (HLs 1-5) and sediments just below and above them were subsampled every 0.5-1 cm to investigate variability within HLs as reported by Grousset *et al.* (2001). Hemipelagic sediments were sampled every 5cm to obtain a biomarker signature for ambient glacial sediments deposited between HLs. To investigate variability in HL biomarker composition between different HEs and different locations in the North Atlantic, several samples from cores ODP 609 and MD95-2024 were analysed. From one to four samples from each HL (HLs 1-6) were analysed in cores ODP609 and MD95-2024. The number of samples from some of the HLs was limited due to their availability. Several samples of ambient hemipelagic sediments from ODP 609 were obtained to compare HE signal to that of ambient glacial sediments. One sample from HL2 in the western Labrador Sea (HU87-025-07P) was also included for comparison. A list of samples except for core SU90-09 is presented in **Table 4. 2**. For the list of samples from core SU90-09 see **App. 3**.

Table 4. 1 Core locations and collection data for North Atlantic cores used in this study. HL – Heinrich Layer, DC – high detrital carbonate layer, LDC – low detrital carbonate layer.

Core name	Position	Water depth, m	Number of samples analysed	Core sections analysed	Reference
SU90-09	43°05N, 31°05W	3375	134	HLs 1-5 + hemipelagic	Grousset *et al.* (2001)
ODP-609	49°52 N, 24°14 W	3884	17	HLs 1-6+ hemipelagic	Bond *et al.* (1992)
MD95-2024	50°12.26N, 45°41.14W	3448	14	DC 1-5 (HLs 1-5) +LDC 5-6 (HL6)	Stoner *et al.* (2000)
HU87-025-07P	57°04.37'N 50°12.25W	3592	1	HL2	Hesse *et al.* (1990)

Table 4. 2 List of samples. DC- high detrital carbonate layer, LDC – low detrital carbonate layer (Stoner *et al.*, 1998)

Core	Sample depth, cmbsf	
ODP-609	**84-86**	HL1
	95-97	hemipelagic
	116-118	HL2
	137-138	hemipelagic
	144-146	HL3
	152-156	
	159-162	
	185-187	hemipelagic
	225-228*	HL4
	277-278	
	295-297*	HL5
	304-305	
	350-352	hemipelagic
	385-387	HL6
	393-395	
	403-495	
	415-417	
MD95-2024	**485-486**	DC1 (HL1)
	490-491	
	495-496	
	515-516	
	745-746	DC2 (HL2)
	910-911	DC3 (HL3)
	920-921	
	1075-1076+1085-1086	DC4 (HL4)
	1105-1106	
	1285-6+1291-2+1295-6	
	1305-1306	DC5 (HL5)
	1325-1326	
	1515-1516	LDC5
	1555-1556	LDC6 (HL6)
HU87-025-07P	**241-242**	H2

* samples from the carbonate-rich layers (Bond *et al.*, 1992)

4.2.1 SU90-09

Core SU90-09 is located on the southern border of the "IRD belt" in the Atlantic Ocean (Ruddiman, 1977). High-resolution record (1-2 centuries) of foraminifera abundance and $\delta^{18}O$ composition, isotopic composition of bulk organic matter, petrological, geochemical and elemental composition of sediments are published for this core (Grousset *et al.*, 2001; Huon *et al.*, 2002; Tamburini *et al.*, 2002). HLs 1-6 were identified by Grousset *et al.* (2001) by correlating the reflectance (grey scale) record of bulk sediment with the magnetic susceptibility record and comparison with the same records of the well-studied neighbouring core SU90-08 (Grousset *et al.*, 1993).

HL sediments of core SU90-09 were shown to differ from the ambient glacial sediments in their petrological, geochemical and isotopic composition, reflecting enhanced detrital supply from terrestrial sources and higher rates of preservation of organic matter during HEs (Grousset *et al.*, 2001; Huon *et al.*, 2002; Tamburini *et al.*, 2002). It is well established that "typical" HLs 1, 2, 4 & 5 differ from the "untypical" HLs 3 and 6 in their sedimentary characteristics and spatial distribution in the North Atlantic (e.g. Grousset *et al.*, 1993). HLs 3 and 6 are poorly represented in the SU90-09 and only HL3 has been studied in detail (Grousset *et al.*, 2001; Huon *et al.*, 2002). This HL is hardly distinguishable in the magnetic susceptibility record and shows no internal structure in contrast to HL1 and HL2 which display a three-step sequential deposition of IRD as reflected in their lithological and isotopic composition (Grousset *et al.*, 2001; Huon *et al.*, 2002). Huon *et al.* (2002) also reported significant differences in the $\delta^{15}N$ and organic carbon to total nitrogen ratio composition between earlier (HLs 4 and 5) and later (HLs 1 and 2) HLs trends. HLs4 and 5 also differ from each other in their detrital phosphorous and carbonate minerals content of the fine-size organic matter (Tamburini *et al.*, 2002).

The age and duration of HEs 1 and 2 were calculated in core SU9009 using AMS ^{14}C dates. High sedimentation rates allowed collection of samples of HLs with very high resolution (Huon *et al.*, 2002). For HL1, sediment accumulation rate ranges from 8.4 to 14.6 cm ka^{-1} and every 5 mm of the core represent 27 to 75 years of sediment deposition. The authors assume similar sampling resolution for the rest of HLs. Sampling at high resolution permitted distinction of fine structure within

HLs. Based on analyses of lithology and Sr and Nd isotopic composition, Grousset *et al.* (2001) distinguished three periods in the deposition of HLs 1 and 2 attributed to the contributions of different sources of IRD: European, Laurentide (Gulf of St. Lawrence) and other Canadian sources (Hudson Strait & Baffin Bay). Sequential deposition of phosphorous is reported in HL4 possibly representing change of the fine organic matter source from European (low detrital P) to Canadian (high detrital P) and European again (Tamburini *et al.*, 2002).

Abrupt oscillations of shorter periods (~ 2-5 centuries) within HLs1 and 2 are reflected in the amount of coarse grains, Sr-Nd composition and $\delta^{13}C$ and $\delta^{15}N$ composition of organic matter (Grousset *et al.*, 2001). These pulses may be a result of changes in location of the "IRD belt" boundary or intermittent iceberg release during HEs.

4.2.2 ODP609

North Atlantic core ODP609 is one of the most analyzed cores in HE provenance studies. It is situated in the northeastern part of the "IRD belt". Heinrich layers in this core were identified on the basis of increased amount of ice rafted lithic fragments and decreased foraminifera shell abundance in comparison with ambient glacial sediments (Bond *et al.*, 1992; Broecker *et al.*, 1992). HLs 1-3 were dated using ^{14}C accelerator mass spectrometry (AMS) on foraminifera shells and the ages for the rest three HEs were calculated by extrapolation of ^{14}C-based sedimentation rates (Bond *et al.*, 1992).

HLs 3 and 6 in this core are different from the "typical" HLs 1, 2, 4 and 5. The lithic composition of HLs 3 and 6 resembles that of the ambient glacial sediments (Bond *et al.*, 1992). In HL3, there is no increase in the total abundance of lithic grains compared with ambient glacial sediments (Broecker *et al.*, 1992). HLs 1, 2, 4 & 5 were found to contain deposits of detrital limestone and dolomite (Bond *et al.*, 1992). A narrow carbonate peak was later reported for HL3 (Bond & Lotti, 1995). HL6 did not contain carbonate.

Detrital carbonate deposits range from 1 cm (in HL1) to 10 cm (in HLs 4 and 5) in thickness but do not extend through the entire depth of each HL (as defined by increased amount of IRD and drop in foraminifera abundance). Bond *et al.* (1992) suggested that the carbonate-rich layers (20-25% of IRD) within low foraminifera zones were deposited by icebergs originating in eastern Canada. Results of isotopic analysis of the samples from the carbonate-bearing layers from the nearby core VM28-82 (49°27'N, 22°16'W) confirm that view (Hemming *et al.*, 1998). Hemming *et al.* (1998) attributed the source of IRD in the Churchill province of the North American shield (north of Hudson Bay and Baffin Island). Pb isotope composition of feldspar grains from HLs 1, 2, 4 & 5 in this core matched that of the glacial till samples from Baffin Island (Hemming *et al.*, 2000). HL1 in this core appears different from other "typical" HLs in its lower carbonate content and younger ε_{Nd} signature (Hemming *et al.*, 1998).

The high IRD to planktonic foraminifera ratio above and below carbonate-rich layers and in HL3 was originally thought to be a result of reduction in the planktonic foraminifera in response to decreased SST and salinity (Bond *et al.*, 1992). Grousset *et al.* (1993; 2000) proposed multiple sources for IRD in HLs with discharge from the European ice sheets responsible for the deposition of the carbonate-poor parts of HLs. Analysis of isotopic composition of HL3 sediments of core VM28-82 led Gwiazda *et al* (1996a) to a conclusion that there is no evidence for ice rafting origin for that layer in the North-eastern Atlantic since HL3 sediments did not display an increase in IRD and their isotopic signature was similar to that of ambient glacial sediments. The mineralogical record of core ODP609, however, points at the ice rafted origin of the HLs. There is an increase in % of basaltic glass (Icelandic origin) and hematite-coated grains (Gulf of St. Lawrence) preceding a carbonate peak in HL3 as well as in the other HLs (Bond & Lotti, 1995) although the lithic grains content in HL3 is low compared with other HLs.

In this study, biomarker composition of samples from both carbonate-rich and carbonate-poor HL sediments from the "typical" HLs 1, 2, 4 &5 as well as sediments from the "untypical" HLs 3 & 6 was analysed **Table 4. 2**.

4.2.3 MD95-2024

Labrador Sea core MD95-2024 was collected by the R.V. Marion Dufresne II from the Labrador Rise in a small channel east of Orphan Knoll from the same location as the extensively studied core HU91-045-094P (Stoner *et al.*, 2000). This core is situated on the path of the icebergs and detrital carbonate meltwater pulses released from the Northern Canadian margins (Andrews *et al.*, 1995; Andrews *et al.*, 1994). According to Stoner *et al.* (1996) spillover turbidites from the Northwest Atlantic Mid-Ocean Channel (NAMOC) were the main mechanism of transporting detrital sediments from Hudson Strait, Davis Strait and the western Irminger basin. The site is located below the WBUC (Western Boundary Undercurrent) and therefore is not subjected to direct erosion by this current but is influenced by its sedimentary supply (Fagel *et al.*, 1997). As a result, the most complete record for reconstruction of the Laurentide ice dynamics is preserved in the cores from this location (Veiga-Pires & Hillaire-Marcel, 1999).

HLs in MD95-2024 were identified by correlating common lithological features and magnetic parameters of this core with those of core HU91-045-094P (Stoner *et al.*, 2000). Several rapidly deposited layers are recorded in this core, at least 8 layers high in detrital carbonate content (DC) and 6 low in detrital carbonate content (LDC) (Hillaire-Marcel *et al.*, 1994; Stoner *et al.*, 1996). The DC layers are composed of grayish-brown (2.5Y 5/1) silty mud, some containing gravel. They show sharp contact with gray to dark gray mud of the ambient hemipelagic sediments. LDC layers were also deposited over a sharp contact but show no change in colour. Based on ^{14}C AMS dates and geomagnetic palaeostratigraphy record, DC 1-5 were correlated with HLs 1-5 in the Northern Atlantic core ODP 609 and LDC6 with HL6 (Stoner *et al.*, 1998). Veiga-Pires & Hillaire-Marcel (1999) reported that carbonate-rich layers DC1-4 were deposited as subunits of HLs as marked by the increase in the grain size fraction >125 μm. HL1 and to a lesser degree HL4 contain two peaks of coarse fraction (at the beginning and at the end) in contrast with HL2 & HL3. HL3 is less pronounced on the magnetic palaeointensity, % detrital carbonate and isotopic records of core HU91-045-094P (Stoner *et al.*, 1998; Veiga-Pires & Hillaire-Marcel, 1999). However, its correlation with HL3 in the North Atlantic (ODP 609) led Stoner *et al.* (1998) to assign North American origin to HL3 in the

North Atlantic. In support of this view, Veiga-Pires & Hillaire-Marcel (1999) propose similar mechanisms of deposition for this layer and HLs 1, 2 and 4 based on U-Th isotopic analysis. Variability between HL3 and HLs 1, 2, 4 & 5 in this core may be explained by a different Laurentide source of carbonate-rich sediments – ice advancing across (from Ungava Bay) rather than down the Hudson Strait similar to Younger Dryas episode deposition proposed by Andrews *et al.* (1995). Hemming *et al.* (2000) attributed HL3 origin from core GGC29 on Orphan Knoll to Ungava Bay based on Ar and Pb isotopic composition of hornblende and feldspar grains. Different mineralogy of the HL6 probably indicates another source region of iceberg discharge such as Davis Strait or Irminger basin (Hillaire-Marcel *et al.*, 1994; Stoner *et al.*, 1998).

Stoner *et al.* (1996) name turbidite activity in the NAMOC as the predominant source for HL formation in this location. However, increase in coarse fraction and very high sedimentation rates (Veiga-Pires & Hillaire-Marcel, 1999) point at enhanced IRD supply in addition to that. SST and $\delta^{18}O$ records of the nearby core MD95-2025 (49°47'N, 46°41'W) correlate with that of ice rafting for HE3 - HE5 although with leads and lags of ~500-1000 years (Hiscott *et al.*, 2001). The authors speculate that oceanic and climatic warming that led to increased glacial melting triggered iceberg discharge from the carbonate-rich sources in Northern Canada. Such a course of events is inconsistent with an internal mechanism of Laurentide collapse (MacAyeal, 1993). There is a possibility, however, that millennial-scale climate changes might influence hydrological conditions at the base of the ice sheet and thus trigger the iceberg release (Marshall & Clarke, 1997). For the rest of the Heinrich events in this location, IRD deposition is decoupled from SST and $\delta^{18}O$ changes (Hiscott *et al.*, 2001).

For this study, samples from five HLs containing high detrital carbonate deposits (HLs 1-5) and 2 layers low in detrital carbonate (HL6 and LDC5) were analysed (See **Table 4. 2**).

4.3 Biomarker evidence for Heinrich Events in a North Atlantic core SU90-09

4.3.1 Biomarker composition of HLs and ambient glacial sediments

4.3.1.1 Photosynthetic Pigments

The relative abundance of the total content of porphyrins was estimated using the ratio of absorbance bands of tetrapyrrolic pigments at 406 nm (Soret band) and 665 nm (satellite band I) (Baker & Lauda, 1986), herewith referred to as the *S/I* ratio. This measurement provides a quick insight into the relative presence of chlorophyll derivatives in a core, namely the relative proportion of chlorins vs. porphyrins. As described in Chapter 3, when *S/I* ratio is greater than 5 it is taken to indicate reduced concentration of chlorin derivatives and enhanced presence of porphyrins in sediments. Values of the *S/I* ratio for all samples in core SU90-09 are greater than 5, being higher in most of the HL samples than in the ambient glacial sediments. The increase in the *S/I* ratio is more pronounced in HLs 2, 4 & 5 and at the bottom part of HL1 and samples immediately before it (precursor event in Grousset *et al.*, 2001). HL3 is practically indistinguishable on the *S/I* plot from the background signal (**Fig. 4.2**). This is interpreted that HLs, except HL3, are characterised by an increased input of porphyrins. Given that porphyrins cannot be from an autochthonous source, their enhanced presence in some intervals shows that transport of organic carbon to the deep sea from allochthonous sources was more intense during some of the HEs.

The presence of porphyrins was also confirmed by the identification of some of their absorbance spectral features in the organic extracts from samples. The porphyrins identified in the samples form complexes with Ni and VO. These are the most common chelates of porphyrins in organic rich source rocks of pre-Quaternary age. A plot showing variations in Ni and VO porphyrins largely correlates with the *S/I* ratio plot (**Fig. 4.2**). Absorption maxima peaks corresponding to VO porphyrins (570 nm) were present in most samples in HLs 2, 4 & 5 and in a few samples from HL1 and HL3 (**Fig. 4.2**). Ni porphyrins (550 nm) were detected in some of the samples containing VO porphyrins but at lower concentration. On average, their abundance is 5 times lower than that of the VO species. In HL1, porphyrins were detected only in the bottom part attributed by Farmer *et al.* (2003) to the Gulf of St. Lawrence source. They are also present in some samples from the interval in the

core interpreted by Grousset *et al.* (2001) as a European precursor to HEs. Only VO porphyrins were present in the precursor to HE2. Their concentration, however, is about an order of magnitude lower than in HL2 itself. Most samples from HL2 contain both porphyrin species with VO dominating (58-90% of the total Ni and VO species). Ni porphyrins were not detected above 84 cm. They were also absent from the precursor to HL2. HE3 is poorly represented in magnetic susceptibility and IRD records of this core (Grousset *et al.*, 2001). Only one sample in this interval (112 cm) was found to contain porphyrins (VO). Four periods may be distinguished within HL4: i) VO species only (144-147 cm), ii) VO and Ni (147.5-148 cm), iii) low or absent porphyrins (148.5-150 cm) and iv) (150.5-153)– both species again. All HL5 samples contain VO porphyrins. Ni species are only present in four samples from this layer. Unusually, in the sample at 189 cmbsf, Ni are the dominant species comprising 90% of the total Ni and VO porphyrins.

Small amounts of mostly vanadyl porphyrins were detected in the ambient glacial sediments above and below HLs 4 and 5. Pigment concentration in these sediments, however, is about an order of magnitude lower than in the HL samples. HLs are also marked by an increase in total tetrapyrrolic pigments concentration. That includes chlorins. Chlorins are autochthonous biomarkers but their elevated amounts are connected with ice rafting: Rosell-Melé *et al.* (1997) attributed high concentration of chlorins to enhanced preservation of organic matter during HEs as a result of reducing conditions created by diminished thermohaline circulation.

4.3.1.2 Aliphatic hydrocarbons: n-alkanes

Linear n-alkanes with a number of carbon atoms ranging from 17 to 35 were the dominant compounds in all the samples (**Fig. 4.3**). The average concentrations of total n-alkanes (C_{17-33}) per gram dry sediment range from 1 to 6 μg/g and are usually higher for HL sediments than for adjacent ambient glacial sediments **Table 4.3**. Lighter compounds (C_n<16) could have been lost during evaporation of the extraction solvent. Long-chain n-alkanes (C_n > 24), biomarkers for epicuticular waxes of higher terrestrial plants (Eglinton & Hamilton, 1967), were present in all sediment samples indicating their terrestrial origin. The absence of alkenones in the

amounts detectible by GC-FID further confirms predominance of terrestrial organic matter in the HL samples. Madureira *et al* (1997) attributed the presence of n-alkanes in a core T88-9P (48°23'N, 25°05'W) to mostly aeolian dust input or transport of wind-eroded sediments by sea ice. Villanueva *et al.* (1997) came to contrasting conclusions. They studied n-alkane distribution in cores SU90-08 (43°30'N, 30°24'W) and SU90-39 (52°34'N, 21°06'W). Due to the reworked nature of the n-alkanes and correlation of n-alkanes concentration with magnetic susceptibility records, the presence of these compounds in the HL sediments from these cores was attributed to ice-rafted rather than aeolian input (Villanueva *et al.*, 1997).

Most of the HL samples in our study contained high amounts of cyclic and branched alkanes especially in the region of the short-chain n-alkanes (**Fig. 4.3a**). These compounds may be of ice rafted origin since they were absent from the ambient glacial sediments (**Fig. 4.3a**). For instance, branched n-alkanes were present in Neoproterozoic carbonates of Spitsbergen, East Greenland and Baffin Island (Greenwood *et al.*, 2004). There is a possibility of autochthonous origin for these compounds as they can be produced by certain algae and bacteria (e.g. Derenne *et al.*, 1996; Kenig *et al.*, 1995) and their absence from the ambient glacial sediments could be a result of higher preservation of organic matter during HEs. The source of the short-chain n-alkanes is probably a mixture of the autochthonous, i.e. produced by marine algae (Tissot & Welte, 1984), and allochthonous, formed at the source as a result of maturation of organic matter (Peters & Moldowan, 1993). Short-chain n-alkanes were abundant in debris flow sediments from Svalbard, Bear Island Fan and Scoresby Sund Fan (See Chapter 3). In addition to that, the marine signal is likely to be overcome by the terrestrial input. Huon *et al.* (Huon *et al.*, 2002) attributed 80-100% of the fine-sized organic matter deposited during HEs to terrestrial input in core SU90-09 based on organic carbon to total nitrogen molar ratios, $\delta^{13}C$ and $\delta^{15}N$ content. A study of the n-alkane distribution, TOC and alkenone concentration in cores SU90-08 and SU90-39 suggested that terrigenous organic matter accounts for up to 90% of the organic matter in the glacial sediments (Villanueva *et al.* (1997).

Distributions of n-alkanes were described using various indices that reflect the relative abundances of these components in the sediments. These are the carbon

preference index (CPI_{23-31}) (Bray & Evans, 1961), the average chain length (*ACL*) (Poynter & Eglinton, 1990; Ternois *et al.*, 2001), the relative proportions of n-C_{27}, n-C_{29} and n-C_{31} long-chain alkanes, and the relative amount of unresolved complex mixture (*UCM*) (Simoneit & Mazurek, 1982; Volkman *et al.*, 1992). The significance of these parameters is discussed in Chapter 1. The relative abundance of high molecular weight n-alkanes (% n-C_{29-31}) was not used here because a significant part of the short-chain n-alkanes (n-C_{17-19}) may be of marine origin (Gelpi *et al.*, 1970; Tissot & Welte, 1984). This chapter concentrates mostly on n-alkanes of undoubtedly terrestrial origin (nC_{21-33}). The data is listed in the **Table 4.3** and **App.3**.

Distribution of n-alkanes in the Heinrich Layers

In most HL samples from SU90-09 n-alkanes show chain-length distributions with odd-over-even predominance and maxima at n-C_{25}, n-C_{27} or n-C_{29} (**Fig. 4.3**). On average, the carbon preference indices (CPI) of most of HL samples are much lower than 3 (**Table 4.3**). Values close to 1 are typical of mature, highly reworked organic matter. CPI values are the lowest for HLs 1 and 2 (1.59 and 1.50 respectively) and highest for HL5 (2.59). CPI for the rest of the HLs is around 2. Precursor events (Grousset *et al.*, 2001) are characterised by higher values of CPI (2.27 and 1.97) than the corresponding HLs 1 and 2. There is high variability of this parameter within HL4 (**Table 4.3** and **App.3**). Variability between and within HLs is further discussed in Section 4.4.

n-C_{29} n-alkane is more abundant than n-C_{31} alkane in HL1 and HL2 (C_{29}/C_{31}=1.43) (**Table 4.3**). Samples corresponding to the precursor events of Grousset *et al.* (2001) are characterised by a lower C_{29}/C_{31} ratio (1.26). Dominance of the n-C_{29} n-alkane is even less pronounced in HLs 4 and 5 (C_{29}/C_{31} ratios are 1.21 and 1.22 respectively). There is no clear predominance of n-C_{29} in HL3 (1.10 ±0.19). n-C_{27} and n-C_{29} alkanes are present in more or less equal amounts in most HL samples (**Table 4.3**). In the precursor to HL1 and, to a lesser degree, to HL2, n-C_{29} specie is more abundant than n-C_{27} (C_{27}/C_{29} ratios are 0.80 and 0.92 respectively). Average chain length (ACL) values range from 28.2 (HL2) to 28.6

(HL3), with standard deviation of ~0.2 (**Table 4.3**). Variability in these parameters reflects that of the depositional environments and post-depositional transformation of organic matter in the outcrops that served as sources of sediments in HLs analysed here (Madureira *et al.*, 1995; Peters & Moldowan, 1993; Poynter *et al.*, 1989).

Most of the HL samples contained a mixture of highly branched aliphatic compounds that could not be separated by gas chromatography (GC). They appear in a chromatogram as a hump of unresolved complex mixture (UCM). The chromatographic UCM in the HL samples from core SU90-09 is generally higher in the low molecular weight region (maximum at the retention time of n-C_{21} n-alkane). Some of the samples are characterised by a second maximum at the retention time of n-C_{33} n-alkane (**Fig. 4.3**). The ratio of the UCM amount to that of total n-alkanes (TNA) for all HLs samples is greater than 4 indicating highly biodegraded character of organic matter in the HLs (Volkman, 1992). The average ratio of UCM to TNA ranges from 10 (HL4) to 17 (HL3) (**Table 4.3**). UCM to TNA ratios are higher for the precursor events than for the corresponding HLs although there is a significant overlap.

Quantification of pristane (Pr) and phytane (Ph) was only possible for HL4 & HL5 samples. In most of the other samples, low abundances of these compounds and coelution in the chromatographic trace made quantification unreliable. The values of the ratio (*Pr/Ph*) of these components for HL4 and HL5 are in the range of 0.3-0.5. This may indicate anoxic conditions during the formation of the IRD source sediment (Peters & Moldowan, 1993). This is in agreement with the photosynthetic pigments data where VO species predominance indicates anoxic depositional conditions for the ancient sedimentary organic matter (e.g. Baker & Lauda, 1986). Pristane/C_{17} and phytane/C_{18} ratios, which are also used in correlation studies, were calculated 0.3-0.9 and 0.9-1.8 for HL4 and HL5 respectively.

Table 4.3 Mean values and standard deviation (in brackets) of total n-alkane concentration (TNA), relative abundances of long-chain n-alkanes, carbon preference index (CPI), average chain length (ACL), relative abundance and concentration of unresolved complex mixture (UCM), relative abundance of porphyrins (*S/I*) and relative concentration of VO porphyrins. N – number of observations. HP – hemipelagic sediments, HL1pr and HL2pr – precursor events, AU – absorption units.

	N	*TNA*, μg/g	C_{29}/C_{31}	C_{27}/C_{29}	$CPI_{24\text{-}31}$	$ACL_{25\text{-}33}$	*UCM/ TNA*	UCM/g, μg/g	*S/I*	VO, AU/g
HP1	12	2.1 (1.9)	1.23 (0.15)	0.84 (0.07)	1.90 (0.30)	28.6 (0.2)	1.5 (2.0)	3.0 (4.3)	31.2 (31.5)	0.01
HL1	**23**	**2.6 (1.3)**	**1.43 (0.34)**	**1.01 (0.24)**	**1.59 (0.16)**	**28.4 (0.4)**	**10.9 (5.6)**	**28.2 (20.3)**	**22.2 (8.8)**	**0.01**
HL1 pr	5	1.6 (0.6)	1.26 (0.31)	0.80 (0.04)	2.27 (0.45)	28.6 (0.25)	16.2 (4.0)	25.5 (13.2)	65.3 (33.8)	0.03
HP2	7	3.8 (1.1)	1.28 (0.49)	1.29 (0.52)	1.66 (0.38)	28.1 (0.4)	17.6 (9.2)	69.7 (46.9)	26.2 (11.4)	0.01
HL2	**14**	**3.3 (1.5)**	**1.43 (0.20)**	**1.12 (0.14)**	**1.50 (0.19)**	**28.2 (0.2)**	**15.9 (7.8)**	**51.0 (35.4)**	**37.2 (28.9)**	**0.23**
HL2 pr	5	3.5 (1.7)	1.26 (0.10)	0.92 (0.12)	1.97 (0.54)	28.4 (0.18)	17.3 (3.6)	65.1 (41.4)	27.9 (12.1)	0.01
HP3	8	5.9 (1.6)	1.19 (0.22)	1.04 (0.38)	1.69 (0.39)	28.4 (0.4)	16.6 (4.3)	101.9 (48.1)	24.7 (8.3)	0
HL3	**5**	**5.9 (1.4)**	**1.10 (0.19)**	**0.97 (0.11)**	**2.28 (0.18)**	**28.6 (0.3)**	**17.4 (2.0)**	**99.5 (29.9)**	**37.4 (11.4)**	**0.00**
HP4	9	1.8 (0.4)	0.96 (0.16)	0.79 (0.12)	3.14 (0.80)	28.8 (0.3)	3.9 (3.7)	7.5 (7.1)	73.4 (37.4)	0.03
HL4	**17**	**2.0 (0.5)**	**1.21 (0.10)**	**1.12 (0.12)**	**1.99 (0.39)**	**28.3 (0.2)**	**10.1 (2.5)**	**19.4 (4.6)**	**111.2 (48.1)**	**0.17**
HP5	11	1.6 (0.6)	1.07 (0.11)	0.79 (0.05)	3.13 (0.47)	28.7 (0.2)	2.9 (3.5)	3.9 (2.9)	57.2 (22.5)	0.02
HL5	**13**	**1.9 (0.7)**	**1.22 (0.12)**	**1.03 (0.15)**	**2.59 (0.47)**	**28.3 (0.2)**	**11.0 (2.7)**	**21.0 (6.7)**	**81.9 (32.9)**	**0.04**
HP6	5	1.3 (0.2)	1.10 (0.09)	0.88 (0.07)	3.01 (0.22)	28.5 (0.2)	5.9 (5.3)	8.5 (8.4)	76.1 (26.2)	0.02

N-alkane distribution in ambient glacial sediments

The distribution of n-alkanes in ambient glacial sediments varies within the core. Three periods can be distinguished: prior to HL3 (HP4-HP6), between HL3 and HL1 (HP2-HP3) and after HL1 (HP1). Hemipelagic sediments prior to HE3 tend to contain lower amounts of n-alkanes (<2μg/g) probably originating from sources with younger organic matter that is characterised by higher CPI (>3), ACL (>28.5) and lower UCM (<10μg/g, UCM/TNA<6). N-C_{29} alkane is predominant over nC_{31} but to a lesser degree than on in HLs samples. In contrast with HLs, n-C_{29} alkane shows strong predominance over n-C_{27} specie (**Table 4.3** and **Fig. 4.3**). Sediments deposited after HL1 show similar distributions. Such values are consistent with aeolian inputs of dust (e.g. Poynter *et al.*, 1989; Villanueva *et al.*, 1997).

Between HL3 and HL1, hemipelagic sediments contain amounts of n-alkanes comparable to those in HLs and are characterised by lower CPI (1.7±0.4) and ACL (<28.5), and high UCM (>70μg/g, UCM/TNA~17). In fact, n-alkane distributions in the ambient glacial sediments of this period are characteristic of highly reworked organic matter similar to sediments deposited during Heinrich events (**Table 4.3** and **Fig. 4.3**). Ice rafting must also have played an important part in the deposition of n-alkanes in the ambient glacial sediments between HL3 and HL1 in the North Atlantic.

4.3.2 Comparison between HLs and ambient glacial sediments

The biomarker composition of HL and ambient glacial sediments was compared on the basis of the distribution of saturated hydrocarbons and photosynthetic pigments and the amount of UCM in the chromatographic traces. The mean values of the variables are presented in **Table 4.3**. For the full list of values see **App.3**.

4.3.2.1 Principal component analysis

Variables used for principal component analysis (PCA) are listed in **Table 4. 5**. Eight principal components (PC) were created. The first three PCs have eigenvalues greater then one. They are responsible for 75 % of variance (**Table 4. 4**).

All variables that represent n-alkane distribution as well as UCM abundance are strongly represented in PC1 (**Table 4. 4** and **Table 4. 5**), which accounts for 39% of variance. In this component, the abundance of total n-alkanes correlates with UCM and ratios of n-C_{27} to n-C_{29} and n-C_{29} to n-C_{31}. These variables are contrasted with the Carbon preference index and average chain length (ACL). N-alkanes are the most abundant class of compounds in the analysed samples therefore their concentration probably reflects the abundance of organic matter in each sample. The amount of UCM indicates the degree of biodegradation. The predominance of odd-numbered n-alkanes decreases with maturity and biodegradation as a result of reworking of the organic matter (e.g. Tissot & Welte, 1984). So does the abundance of long-chain n-alkanes and therefore average chain length (Peters & Moldowan, 1993). Relative abundances of different long-chain n-alkanes (e.g. C_{27}/ C_{29} ratios) are characteristic of specific environments in which organic matter was formed (Brault et al., 1988; Brincat et al., 2000; Cranwell, 1973; McCaffrey et al., 1991). Thus, in this component, higher values are assigned to samples with more organic-rich, biodegraded and mature organic matter, whose n-alkane distribution shows a predominance of n-C_{27} alkane over n-C_{29} and n-C_{31}.

The second component (**Table 4. 4** and **Table 4. 5**), representing 20% of variance, combines pigment data and n-alkane distribution. Here, the relative abundance of porphyrins (*S/I*) correlates with the relative abundance of vanadyl species to total Ni and VO porphyrins and the C_{27}/C_{29} ratio. They are contrasted to ACL. Thus, PC2 values are higher for porphyrin-rich samples, whose organic matter was formed under predominantly anoxic conditions (Lewan, 1984) with the chromatographic n-alkane envelope displaced towards lower molecular weight n-alkanes.

PC3 accounts for 14% of variance (**Table 4. 4**). Here, CPI of long-chained n-alkanes and amount of UCM correlate with relative abundance of porphyrins and are opposed to the ratio of n-C_{29} alkane to n-C_{31}. In PC3, the maturity of organic matter (as represented by CPI) is contrasted to the degree of biodegradation (UCM) and abundance of porphyrins (*S/I*). The value of this component is higher for samples with less mature and more biodegraded organic matter, higher porphyrin content and a predominance of n-C_{29} over n-C_{31} alkane.

Table 4. 4 Results of principal component analysis of Heinrich layers sediments. Eigenvalue – proportion of variability represented by each component. Difference in eigenvalues between the components PC_i and PC_{i+1}; Proportion - proportion of variability represented by each component normalised to 1; Cumulative – cumulative proportion of variability represented by components PC_1- PC_i.

Component	Eigenvalue	Difference	Proportion	Cumulative
1	**3.50830**	1.52565	0.3898	0.3898
2	**1.98265**	0.71074	0.2203	0.6101
3	**1.27191**	0.56382	0.1413	0.7514
4	0.70809	0.21883	0.0787	0.8301
5	0.48926	0.03859	0.0544	0.8845
6	0.45067	0.03830	0.0501	0.9345
7	0.41237	0.28107	0.0458	0.9804
8	0.13130	0.08583	0.0146	0.9949
9	0.04547		0.0051	1.0000

Table 4. 5 Eigenvectors (coefficients reflecting varying contributions of the variables).

Variable	PC1	PC2	PC3
TNA	**0.36675**	-0.33636	0.15816
$CPI_{24\text{-}31}$	**-0.36953**	-0.03627	**0.40216**
UCM/TNA	**0.34202**	-0.07218	**0.45002**
UCM/g	**0.41274**	-0.28249	**0.40019**
C_{29}/C_{31}	**0.32708**	0.23856	**-0.42317**
C_{27}/C_{29}	**0.36760**	**0.35593**	0.00306
ACL	**-0.41517**	**-0.37556**	0.03521
S/I	-0.10166	**0.44542**	**0.46998**
$\frac{VO}{VO+Ni}$	-0.12961	**0.52677**	0.22223

4.3.2.2 Comparison between HLs and ambient sediment

In order to use biomarker fingerprints of the HL sediments as a source proxy, it is important to prove that they differ significantly from those in non-ice-rafted sediments. Plots of down-core variations in PC1, PC2 and PC3 for SU90-09 are presented in **Fig. 4.4**.

Samples from core SU90-09 were divided into 13 groups corresponding to five different HLs, two precursor events (Grousset *et al.*, 2001) and six groups of hemipelagic sediments between HLs. MANOVA of 13 groups containing 135 samples indicated one or more differences among the two-dimensional mean vectors for the 13 groups (**App.3**). Individual groups were compared in subsequent tests and results are presented in **Table 4. 6**.

The biomarker composition of hemipelagic sediments deposited before HL3 and after HL1 is significantly different from that of adjoining HLs and "precursor events" with 95% or higher confidence interval ($P<0.05$) (**Table 4. 6** and **Fig. 4.4**). Most HL sediments are characterised by presence of porphyrins, highly degraded n-alkanes and high amounts of UCM whereas hemipelagic sediments contain no or very low amounts of porphyrins and UCM and less mature n-alkanes signatures. Difference is less pronounced for HL5 and hemipelagic sediments preceding it (HP6) ($P=0.09$). However, the n-alkane distribution (as reflected in PC1) is significantly different for these two periods. Comparison of PC1 using ANOVA indicates significant difference in n-alkane distribution between HL5 and HP6 with 99% confidence interval.

Difference between HL2 and hemipelagic sediments deposited after it (HP2) is less certain ($P=0.08$). Variability in n-alkane distribution within the hemipelagic sediments interval is greater than between HL2 and HP2. However, these sediments can be distinguished on the basis of their pigment concentrations (**Fig. 4.2**). Except for one sample (80cm, **Fig. 4.4**) abundance of porphyrins in the hemipelagic sediments (HP2) is lower than in HL2. It is reflected in lower values of PC2 calculated for HP2 sediments. There is no significant difference between HL3 and HP3 sediments ($P=0.3$).

Table 4. 6 Comparison of hemipelagic sediments (HP) with HL and "precursor event" sediments from SU90-09. Results of MANOVA of PC1-PC3. P - probability of one or more differences between the two-dimensional mean vectors for different groups of sediment samples.

Groups compared			Probability>F
HP1-HP6		HLs1-6 +HL1pr+HL2pr	0.0000
HP1		HL1	0.0165
HP2		HL1+HL1pr	0.0007
HP2		HL1pr	0.0027
HP2		HL2	**0.0847**
HP3		HL2+HL2pr	0.0001
HP3		HL2pr	0.0429
HP3		HL3	**0.3190**
HP4		HL3	0.0000
HP4		HL4	0.0000
HP5		HL4	0.0000
HP5		HL5	0.0000
HP6		HL5	**0.0889**
HP2+HP3		HP4+HP5+HP6	0.0000
HP1		HP2+HP3	0.0000
HP2		HP3	0.0164
HP4	HP5	HP6	**0.3339**

4.3.2.3 Sources and transport mechanisms of terrestrial organic matter in the North Atlantic HLs and ambient glacial sediments.

The presence of ancient photosynthetic pigments (porphyrins), highly degraded n-alkanes and high amounts of UCM in marine sediments deposited during Heinrich events in the North Atlantic core SU90-09 indicates input of ancient sedimentary material of terrestrial origin. Madureira *et al.* (1997) proposed aeolian input as a main source of terrestrial organic matter in the HLs. The core used in that study (T88-09P) is located north from SU90-09 and the n–alkane distributions in HLs

(expressed as ACL) did not differ significantly from those in hemipelagic sediments. There was, however an increase in concentrations of n-alkanes and other terrestrial biomarkers (long-chain alcohols and fatty acids) during HEs that was attributed to a more efficient atmospheric transport (Madureira *et al.*, 1997). If this were the case, biomarker composition of the hemipelagic sediments would be similar to that of HLs. In addition, aeolian input is usually associated with younger organic matter with higher CPI and ACL and low or no UCM (e.g. Poynter *et al.*, 1989). Hemipelagic sediments deposited prior to HL3 and after HL1 in core SU90-09 show such signatures. Thus a predominantly aeolian origin for the organic matter in those sediments is proposed. In contrast, the presence of organic matter in HL sediments is most likely to be a result of ice rafting. Analysis of n-alkanes in the nearby core SU90-08 led Villanueva *et al.* (1997) to the same conclusion. N-alkane distributions in that core are characteristic of reworked organic matter and peaks in n-alkanes concentrations largely coincided with magnetic susceptibility increases in that core. Other indications of the refractory nature of the organic matter in the HLs from core SU90-09 are Rock-Eval pyrolysis indices (Tamburini *et al.*, 2002). Lower oxygen and higher hydrogen indices than in ambient glacial sediments characterise HLs 4 and 5 sediments.

Madureira *et al.* (1997) argued that the IRD (grain size >125 μm) core record did not match that of terrigenous biomarker concentrations. The highest abundance of terrigenous biomarkers was recorded for HL3 characterised by only a moderate increase in IRD. What is more, elevated biomarker concentrations were recorded throughout MIS 2 to 4. This can be explained by the position of the polar front. In core SU90-09, hemipelagic sediments deposited between HLs 3 and 1 contain highly reworked organic matter similar to that in the HLs. This shift in the hemipelagic sediment composition probably reflects the change in the position of the polar front. When polar waters reached the location of core SU90-09, the ice rafting became the predominant source of organic matter in the hemipelagic sediments. The situation reversed again in the Holocene. Calvo *et al.* (2001) came to a similar conclusion comparing cores SU90-08 and MD95-2037 (37°05'N, 32°02'W). Concentrations of n-alkanes in core SU90-08 during MIS2-3 were one or two orders of magnitude higher than in MD95-2037, and that coincided with 6-7°C difference in SST. Increased n-alkane input in SU90-08 was therefore attributed to ice rafting. The

polar front was located south of the core studied by Madureira *et al.* (1997) during MIS2-4 and therefore all hemipelagic sediments from that period probably contain IRD.

Interestingly, and similar to Madureira *et al.* (1997), an increase in n-alkanes concentrations during MIS2-3 does not match that in IRD. Highest amounts of n-alkanes were recorded for HL3 and HP3 that are characterised by relatively low IRD (>150 μm) concentration. Terrestrial organic matter is usually associated with coarse fraction (>63 μm) and TOC in the fine fraction is attributed to marine input (Manighetti & McCave, 1995). The amounts of TOC associated with fine particles were similar for glacial and Holocene sediments in several northeastern Atlantic cores (50-60°N). However, the flux of fine particles in those cores during glacial period was about an order of magnitude higher than during the Holocene. According to Huon *et al.* (2001) fine-sized organic matter in ambient glacial sediments in SU90-09 from MIS2 contains up to 50% of terrestrial material. However, OC/TN, $\delta^{13}C$ and $\delta^{15}N$ records for ambient glacial sediments and HL3 are different from those in HL1 and HL2. This probably indicates different source regions of organic matter in these sediments. Absence of porphyrins in hemipelagic sediments and most samples from HL3 also points at a different source at least from HL2. High abundance of n-alkanes and UCM in these sediments is probably associated with the fraction >63 and <150 μm. For instance, transport by nepheloid layer or sea ice was proposed by Madureira *et al.* (1997) as an explanation of discrepancy between IRD and n-alkane concentration record in core T88-09P. The nepheloid layer is usually associated with clay particles (<2 μm). Although it has been named as an important mechanism in sediment transport in the North Atlantic during the Quaternary, Bout-Roumazeiles *et al.* (1999) demonstrated that it did not reach the location of cores SU90-08 and SU90-38 (close to T88-09P). Sedimentary strata containing highly degraded organic matter could have been subject to wind erosion. Incorporated in sea ice, fine particles containing this extensively reworked organic matter would have been transported far south during MIS2-3 and deposited during HE3 and after. High variability in the biomarker signatures of hemipelagic sediments from this period probably indicates a combination of sources and mechanisms of sediment transport. They may include minor IRD events, transport by sea ice and wind.

4.3.3 Conclusions

Sediments deposited during Heinrich events in core SU90-09 contain highly reworked organic matter characterised by the presence of porphyrins (predominantly vanadyl chelates), n-alkanes with low CPI and ACL indices and high amounts of UCM in the gas chromatographic traces. In contrast, hemipelagic sediments deposited prior to HL3 and during the Holocene contain younger organic matter, with higher CPI and ACL values and lack UCM in the chromatograms and porphyrins.

Ice rafting is thought to be the main source of organic matter in HLs, and aeolian transport is most likely responsible for deposition of ambient glacial sediments prior to HL3 and overlaying HL4 and HL5 and then during Holocene.

A southward shift in the polar front location during MIS3 resulted in deposition of highly degraded organic matter in the ambient glacial sediments in MIS2-3. However, it is probably associated with <150 μm grain size fraction. These sediments are characterised by high variability in their biomarker composition and may contain material from multiple sources.

There is significant difference between biomarker composition of organic matter in HLs 1, 2, 4 and 5 and overlying ambient glacial sediments. No such difference was observed between overlying ambient sediments and HL3. That implies different source of organic matter in the ambient glacial sediments from that in HLs 1 2, 4 and 5.

To conclude, prominent Heinrich events (HE1, HE2, HE4 & HE5) can be identified on the basis of the biomarker composition of their sedimentary organic matter. Identification is more straightforward in locations where hemipelagic sedimentation was not influenced by glacial conditions.

4.4 High-resolution biomarker record of Heinrich Events in North Atlantic core SU90-09: Implication for sources of IRD

Heinrich events are usually divided into two groups – "typical" or prominent HE1, HE2, HE4 & HE5 and "untypical" HE3 and HE6. The main source of IRD in the "typical" HLs is thought to be the Northeastern Canada (e.g. Bond *et al.*, 1992). A mostly European origin has been proposed for HE3 and HE6 (e.g. Grousset *et al.*, 1993). However, detailed studies of HLs from different areas of the North Atlantic show variability within these two groups as well as within each layer. For instance, HL1 in core V28-82 in the eastern part of the "IRD belt" contains sediments with younger Sr-Nd signatures then the rest of the prominent HLs indicating an additional (younger) source of IRD for this layer (Hemming *et al.*, 1998). A European origin was proposed for HL2 in the Eastern Atlantic core KS79-29 (46°18'N, 15°04'W) on the basis of Sr-Nd isotopic analysis (Revel *et al.*, 1996). HL5 in core MD95-2040 from the Iberian Margin did not contain carbonate (de Abreu *et al.*, 2003). According to Kirkby & Andrews (1999), sedimentological record suggests that HE4 in the Labrador Sea was more significant than HE1 and HE2 and had direct influence on HE3. Huon *et al.* (2002) report contrasting $\delta^{13}C$ and $\delta^{15}N$ records for older (HLs 4 and 5) and younger (HLs 1, 2) in core SU90-09. HL3 in the Northeastern Labrador Sea (HU91-045-094P) was rich in detrital carbonate in contrast with HL6 (Stoner *et al.*, 1996).

At the same time, variability within HLs has been reported. Results of mineralogical and isotopic analysis suggest sequential deposition of IRD from Europe, Gulf of St. Lawrence and Northeastern Canada (Bond & Lotti, 1995; Bond *et al.*, 1999; Grousset *et al.*, 2001; 2000; Snoechx *et al.*, 1999). The abundance of IRD (>150 μm), Sr-Nd composition and $\delta^{13}C$ and $\delta^{15}N$ composition of organic matter in core SU90-09 also show high frequency oscillations (~ 2-5 centuries) within HL1 and HL2 (Grousset *et al.*, 2001). Here, variability of biomarker composition between and within different HLs in core SU90-09 was investigated.

4.4.1 Variability between different HLs

In core SU90-09, there is significant variability between HLs. The source of organic matter in HL3 appears to be different from the other HLs in this core. IRD concentration in this layer is close to that in ambient glacial sediments, in contrast with the prominent HLs (**Fig. 4.2**). Porphyrins are absent from most of the samples in HL3 (**Fig. 4.2**). At the same time, the concentration of n-alkanes in HL3 is about twice that of the other HLs (**Table 4.3**). This layer contains highly biodegraded organic matter characterised by large amounts of UCM: UCM content per gram dry sediment is 2-5 times higher than in the other HLs. The maturity of organic matter in this layer appears to be slightly lower than in HLs 1 and 2, comparable with most samples from HL4 and higher than in HE5 as reflected in the CPI values (**Table 4.3** and **App. 3**). There is no clear predominance of n-C_{27}, n-C_{29} or n-C_{31} alkanes, whereas most samples from HLs 1 and 2 and to a lesser degree HLs 4 and 5 have a maximum at n-C_{29}. What is more, the biomarker composition of HL3 sediments does not appear to be significantly different from that in the overlaying ambient glacial sediments (see Section 4.3.2.2). This layer is poorly represented in the magnetic susceptibility record and has low IRD content (Grousset *et al.*, 2001). However, the reworked nature of organic matter in HL3 indicates a terrestrial origin of its sediments (Villanueva *et al.*, 1997). Similarity with the overlaying hemipelagic sediments is explained by the position of the polar front during MIS3 south of the SU90-09 location (Calvo *et al.*, 2001).

Younger HLs 1 and 2 differ from the older HLs 4 and 5 by higher n-alkane concentrations, higher amounts of UCM, lower CPI values (**Table 4.3**) and a more pronounced predominance of n-C_{29} alkane over n-C_{31}. In addition, HL1 differs from the other prominent HLs by its highly variable IRD content (**Fig. 4.2**): the concentration of lithic fragments >150μm oscillates between 1000 and 120000 per gram (Huon *et al.*, 2002). The coarse fraction concentration is in the region of 2000-5000 per gram in HLs 2 and 4, and below 4000 in HL5. Most samples from HLs 1 did not contain porphyrins, in contrast to HLs 2, 4 and 5. Concentration of photosynthetic pigments in HLs 2 and 4 is ~5 times higher than in HL 5 (**Fig. 4.2** and **App.3**). HL 2 is higher in UCM than the other prominent HLs. HL5 n-alkanes are characterised by the highest CPI (**Table 4.3**).

HL and "precursor event" samples from core SU90-09 were first compared using the results of PCA. The results are presented in **Fig. 4.5**. Although there is considerable variability within each HL, they are largely separated from one another on the PCA plots except for HL4 and HL5: these overlap considerably with one another but are for the most part separated from the other HLs. Highest values of PC1 were calculated for HL2. This layer contains the most mature and biodegraded organic matter characterised by the lowest CPI and high UCM. It also has the lowest ACL and a strong n-C_{29} predominance (**Table 4.3**). PC1 values are the lowest for HL5 because it contains less biodegraded (low UCM) and less mature (high CPI) organic matter. PC2 is highest for HL4 and HL5 due to the highest relative abundance of porphyrins, a more pronounced predominance of the vanadyl species (*VO/(VO+Ni)* >0.8) than in the other HLs and the lowest ACL. PC2 is the lowest for HL3 sediments because they are low in porphyrins and have the highest ACL. Samples corresponding to the precursor events (HL1pr and HL2pr) do not form distinct groups on PC1/PC2 plot (**Fig. 4.5**) and tend to cluster with HL1 samples. They show a tendency towards separation from the other HL samples on the PC2/PC3 plot (**Fig. 4.5**) but could not be distinguished from one another.

4.4.1.1 Comparison between HLs using MANOVA

Analysis of variance confirms that variability between most HLs in SU90-09 is greater than variability within each layer with 95% confidence (**Table 4. 7**). The difference is not significant between the two precursor events probably indicating the same source of IRD in both layers, as suggested by Grousset *et al.* (2001). These precursor events were proposed to have originated from Europe. There is a considerable body of evidence for the European provenance of HL3. However, the biomarker composition of the HL3 sediments differs significantly from that from the precursor events (**Table 4.3** and **Fig. 4.4**). The provenance of terrigenous organic matter in HL3 is discussed in Section 4.5.2.

Considerable overlap of HLs 4 and 5 (**Fig. 4.5** and **Table 4.3**) suggests a contribution from a common source of IRD in most of the HLs 4 and 5 samples. However, biomarker compositions of the sediments in these HLs are not identical.

For instance, there is a difference in the *Pr/Ph* and isoprenoid ratios (**Fig. 4.6**). On these plots, HL4 and HL5 are largely separated. This suggests at least partial contribution of organic matter from different sources.

Table 4. 7 Results of MANOVA of PC1-PC3. Probability of one or more differences between the two-dimentional mean vectors for HL and "precursor event"(pr) sediments from SU90-09.

	HL1	HL1pr	HL2	HL2pr	HL3	HL4
HL1pr	0.0001					
HL2	0.0000	0.0067				
HL2pr	0.0003	**0.1908**	0.0334			
HL3	0.0000	0.0011	0.0000	0.0000		
HL4	0.0000	0.0019	0.0000	0.0000	0.0000	
HL5	0.0000	0.0000	0.0370	0.0001	0.0000	**0.5361**

4.4.1.2 Contribution of individual variables

In order to test the contribution of the individual variables towards the variability between the HLs in SU90-09, multinomial logistic regression was used. The results are presented in **Table 4. 8**. Five variables were chosen that account for most of the variability between HL sediments as was determined using ANOVA. CPI, ACL and C_{29}/C_{31} ratio representing the variability in n-alkane distribution, relative amount of UCM and relative abundance of porphyrins come into play in different combinations to account for differences in the biomarker composition of IRD layers.

It is important to note that $P<0.05$ in this exercise does not necessarily mean that a particular variable does vary significantly between two groups of samples and vice-versa. For instance, CPI and C_{29}/C_{31} do not appear to be significantly important in distinguishing between HL2 and HL4 when in fact the two layers are largely separated by these variables plotted against each other (**Fig. 4.7a**). Higher p values for CPI and C_{29}/C_{31} than for UCM/TNA and *S/I* indicate that the amount of UCM and porphyrin abundance are more important in distinguishing between HL2 and HL4 than is n-alkane distribution. At the same time, low probability (P) values for C_{29}/C_{31} and ACL in the comparison of the precursor events indicate that there is less

similarity between HL1pr and HL2pr in these two variables than in CPI and UCM. However, these two layers could not be distinguished on the C_{29}/C_{31} - ACL plot (**Fig. 4.7b**).

Table 4. 8 Results of mlogit analysis of HL and "precursor event" sediments from core SU90-09. Probability>F values for selected variables.

Groups compared		CPI_{24-31}	C_{29}/C_{31}	ACL_{25-33}	UCM/TNA	*S/I*
HLL1	HL1pr	0.111	0.099	0.056	0.082	**0.002**
HLL1	HL2	0.684	0.105	0.053	**0.028**	**0.013**
HLL1	HL2pr	**0.027**	0.112	0.530	**0.021**	0.456
HLL1	HL3	**0.014**	**0.045**	0.981	**0.009**	0.312
HLL1	HL4	0.327	0.068	0.083	**0.038**	**0.001**
HLL1	HL5	**0.003**	**0.034**	**0.009**	0.121	0.104
HL2	HL1pr	**0.053**	**0.022**	**0.013**	0.418	0.102
HL2	HL2pr	**0.010**	0.578	0.492	0.323	0.161
HL2	HL3	**0.005**	0.260	0.207	0.098	0.278
HL2	HL4	0.196	0.229	0.525	**0.006**	**0.026**
HL2	HL5	**0.001**	0.136	0.067	**0.016**	0.411
HL3	HL1pr	0.278	**0.009**	**0.052**	0.633	**0.02**
HL3	HL2pr	0.437	0.594	0.094	0.310	0.895
HL3	HL4	0.100	0.565	0.176	**0.001**	**0.027**
HL3	HL5	0.434	0.399	**0.018**	**0.004**	0.605
HL4	HL1pr	0.475	**0.018**	**0.010**	**0.008**	0.938
HL4	HL2pr	0.200	0.388	0.322	**0.003**	**0.016**
HL4	HL5	**0.003**	0.876	0.162	0.533	**0.013**
HL5	HL1pr	**0.050**	**0.010**	**0.003**	**0.020**	**0.044**
HL5	HL2pr	0.203	0.241	**0.041**	**0.006**	0.413
HL1pr	HL2pr	0.499	**0.019**	**0.029**	0.809	**0.023**

CPI is important in separating HE5 from all of the layers with 95% confidence with the exception of HL3 and HL2pr. It is also significantly different

for HL3 compared with HL1 and HL2 and separates HL2 from its precursor event with 99% confidence.

C_{29}/C_{31} ratios come into play in separating HL1pr from the rest of the IRD sediments. This variable distinguishes HL1 from HL3 and HL5. This ratio is also important in separation of the two precursor events.

ACL separates HL5 from the rest of the IRD layers with at least 93% confidence. The exception is HL4. HL1 and HL2 can also be better distinguished from one another by ACL, as can their two precursor events.

Older HLs (4 & 5) are separated from the younger IRD events by the amount of UCM. The UCM/TNA ratio plays important part in separating HL1 from that of all the other IRD layers with 95% confidence except HL1 precursor and HL5.

The *S/I* ratio separates HL4 from the other HLs with 97% confidence. This variable also varies significantly between HL1 and HL2 and between their precursor events. HL1 precursor can be distinguished from HL1, HL3 & HL5.

It is unlikely that IRD in all five HLs in this core come from different sources. It may be suggested that biomarker composition of sediments in each HL reflects a combined input from several source areas but their representation varies between HLs. For instance, several ice streams existed on the continental margins of Baffin Bay and Labrador Sea and the relative intensity of iceberg discharge from these ice streams may have varied through time. This is further discussed in Section 4.4.3

4.4.2 Variability within prominent HLs

On the basis of a detailed mineralogical study of coarse detrital grains in HLs 1 and 2 from core SU90-09, Grousset *et al.* (2001) proposed 3 periods of IRD deposition – precursor event originating from Europe (sediments rich in volcanic glass), Laurentide-derived step characterised by elevated quartz content and the third period rich in carbonate from Northern Canadian provinces. In agreement with these

findings, analysis of the biomarker composition also indicates variability within each HL. Downcore variation in the biomarker makeup is summarised by PC1, PC2 and PC3 and presented in **Fig. 4.4**. On the basis of variation in the principal components values, a division of prominent HLs into sublayers is proposed. The biomarker composition of the sublayers was compared using MANOVA: the results are presented in **Table 4. 9**

The HL1 precursor can be distinguished by lower PC1 and PC2 and higher PC3 values than the following samples of the HL1. Two periods defined by Grousset *et al.* (2001) can be recognised within HL1 – HL1_1 (56.5-61.5 cm) with higher PC1 and PC2 and HL1_2 (50-56 cm) characterised by a slight drop in PC1 and PC2. Analysis of variance shows significant variability between these three sublayers (**Table 4. 9**).

Similar picture is observed for HL2 – a rise in PC1 and PC2 and a drop in PC3 from precursor event (92-97cm) to HL2_1(86.5-91.5 cm). The third period (HL2_2) is represented by just 4 samples (81-84) but a drop in PC1 and a rise in PC3 are noticeable. However, only the difference between HL2pr and HL2_1 appears to be statistically significant (**Table 4. 9**). This may be due to the small number of observations for HL2_2 and high variability within it. The variability between the two precursors is not significant (P>>0.05) supporting the suggestion of a common source of sediments in these layers.

Three periods can be distinguished within HL4. The first and the third are very similar (**Fig. 4.4** and **Table 4. 9**). There is a drop in PC2 and PC3 in the middle of HL4. This is due to lower CPI and UCM & and *S/I* ratio for samples 148.5 & 150 cm. This middle period (HL4_2) differs significantly from the sediments above and below it. It is not significantly different from the HL1 sediments. A very similar trend appears within HL5: three periods are recognisable with the middle one (189.5-191 cm) characterised by lower CPI, UCM and *S/I* ratio than the sediments above and below it. However, this middle period in HL5 is not as well pronounced as the one in the HL4 (**Fig. 4.4** and **Table 4. 9**). It shows similarity to HL1_1. There appears to be no significant difference between HL4_1, HL4_3, HL5_1 and HL5_3 probably indicating a shared source of IRD. The middle parts of the two HLs show significant variability and probably cannot be attributed to the same source.

Table 4. 9 Comparison of sub layers in prominent HL and "precursor event"(pr) sediments from SU90-09. Results of MANOVA of PC1-PC3. Probability >F.

	HL1_2	HL1_1	HL1pr	HL2_2	HL2_1	HL2pr	HL4_3	HL4_2	HL4_1	HL5_3	HL5_2
HL1_1	0.0023										
HL1pr	0.0000	0.0000									
HL2_2	0.0001	**0.1105**	**0.1256**								
HL2_1	0.0000	0.0239	0.0002	**0.0810**							
HL2pr	0.0004	0.0000	**0.1292**	**0.4107**	0.0022						
HL4_3	0.0000	0.0000	0.0004	0.0002	0.0000	0.0000					
HL4_2	**0.2873**	**0.4956**	0.0031	0.0066	0.0188	0.0035	0.0001				
HL4_1	0.0000	0.0000	0.0000	0.0020	0.0000	0.0000	**0.8773**	0.0003			
HL5_3	0.0000	0.0000	0.0010	0.0382	0.0001	0.0007	**0.1300**	0.0002	**0.1087**		
HL5_2	0.0023	**0.0586**	0.0382	**0.2974**	**0.3416**	0.0130	**0.0814**	0.0244	**0.2635**	**0.0735**	
HL5_1	0.0000	0.0000	0.0022	0.0007	0.0000	0.0000	**0.4575**	0.0000	**0.3216**	**0.4206**	0.0325

4.4.3 Older (HE4 &5) and younger (HE1 &2) events

The prominent HLs in core SU90-09 differ from each other in their biomarker composition. These findings are in agreement with those of previous workers: there is variability in the bulk properties of fine-sized organic matter and IRD content (Huon *et al.*, 2002). Huon *et al.* (2002) linked a change in the isotopic signature of the continental organic matter source of HL4 and especially HL5 compared with HLs1 and 2 to warmer climatic conditions and lower erosion levels during HEs 4 and 5. That may explain lower concentrations of n-alkanes and lower UCM/g content in HLs 4 and 5 than in HLs 1 and 2. Previous research shows that the main source area for IRD in the prominent HLs is in northern Canada dominated by Churchill province base rocks and Palaeozoic carbonates. Several major ice streams (Hudson Strait, Gulf of Boothia-Lancaster Sound, Cumberland Sound) and a number of smaller ice streams along the eastern Canadian margin have been identified (e.g. Andrews & MacLean, 2003; Hulbe *et al.*, 2004). Sediments delivered into the ocean by these ice streams originated from soils and organic-bearing rocks of the underlying geological basement (Huon *et al.*, 2002).

The biomarker composition of sediments is likely to vary from one ice stream to another. Relative input from different source areas within the Laurentide Ice Sheet may have varied during different HEs for example in response to different climatic conditions, resulting in variability in the biomarker composition of IRD in HLs. Kirby & Andrews (1999) suggested that HE4 triggered significant climatic reorganisations and may have influenced subsequent HEs. Input from the Gulf of St. Lawrence and European sources also have to be taken into account. Younger HLs 1 and 2 contain more reworked organic matter than the older HLs 4 and 5: they are characterised by lower CPI, higher UCM and a shift in the n–alkane envelope towards lower molecular weight compounds (**Table 4.3**). This may indicate a different combination of the North American sources of IRD. This may also be a result of enhanced contribution of IRD from Europe in HLs 1 and 2 as a result of the shift in the position of the polar front.

Internal structure of the older HLs also appears different from that of younger ones. Precursor events identified by Grousset *et al.* (2001) from isotopic and mineralogical composition, differ in their biomarker composition from HL and HL2.

A European precursor event was reported for HL4 from core SU92-28 on the southern Portuguese slope based on the isotopic signature of the non-carbonate fraction (Grousset *et al.*, 2000; Snoechx *et al.*, 1999). Such precursor events have not been recognised in the HE4 and HE5 biomarker record of core SU90-09. Further two periods were recognised in HLs 1 and 2, according to Grousset *et al.* (2001) reflecting input from the Gulf of St. Lawrence and northeastern Canada respectively. HLs 4 and 5 can be divided into 3 periods on the basis of their biomarker composition. The first and the third appear similar in both HLs (**Fig. 4.4** and **Table 4. 9**). During the middle period in HL4, organic matter similar to that from HL1 was deposited. The middle period in HL5 is less pronounced and is similar to HL2. While HL4 and HL5 are largely similar; HL1 is different from HL2 (**Fig. 4.5** and **Table 4.3**). It contains lower UCM and for the most part lacks porphyrins.

High frequency pulses observed by Grousset *et al.* (2001) in the coarse fraction content, isotopic composition of organic matter and Sr-Nd isotopic composition of HLs 1 and 2, are also reflected in their biomarker composition record. Grousset *et al.* (2001) proposes two possible causes: a stepwise collapse of the Laurentide Ice Sheet or latitudinal oscillation in the "IRD belt" as a result of the changes in the oceanic current pattern. Step by step breakdown of the Labrador ice sheet is supported by the ice shelf disintegration hypothesis proposed by Hulbe *et al.* (2004).

4.4.4 Conclusions

The biomarker composition of HL sediments from core SU90-09 varies between and within HLs. All five HLs analysed can be distinguished from one another on the basis of the biomarker composition of their sediments. "European" precursor events are recognised in the sedimentary record of HL1 and HL2 but not HL4 and HL5. For the most part, the biomarker composition of the sediments in the older HLs (HL4 and HL5) is similar to one another and differ from the younger HLs 1 and 2. HL1 and HL2 are similar in their n-alkane distribution but differ in their UCM and pigment content. Three steps can be recognised in HLs 4 and 5 with the narrow middle step different from the periods above and below it, and two steps in HL1 and possibly in HL2. The variability between and within HLs may be explained by variability in relative contribution from several IRD sources (American or European) or different ice streams within the same source (e.g. Laurentide Ice Sheet).

4.5 Multiple sources of IRD in the North Atlantic Heinrich Layers

In this section, biomarker composition of HL sediments from four different locations in the Atlantic Ocean is compared: central Atlantic core SU90-09 from the southern part of the "IRD belt", ODP 609 from the northeastern part of the "IRD belt", MD95-2024 from the southwestern Labrador Sea and HU87-025-07P from the western Labrador Sea. The biomarker composition of core SU90-09 was described in Section 4.3.1.

4.5.1 Biomarker composition of HLs in cores MD95-2024, ODP609 & HU87-025-07P

4.5.1.1 Photosynthetic pigments

S/I ratios of most of the HL samples from ODP 609, MD95-2024 and HU87-025-07P are greater than 5, and that suggests the presence of porphyrins (**Figs. 4.8 and 4.9**). Peaks corresponding to both Ni and VO porphyrins are visible on the absorbance spectra of most HL samples. VO are predominant species in most samples probably indicating anoxic conditions at the time of deposition of the allochthonous sediment.

VO species constitute 90% of total Ni and VO porphyrins in HL2 from HU87-025-07P. A similar *VO/(VO+Ni)* ratio was calculated for the uppermost sample of the glacigenic debris flow (GDF) from the same core while the rest of the GDF samples did not contain Ni porphyrins in amounts detectible on the absorbance spectra.

Relative abundances of VO porphyrins in core MD95-2024 show little variation between and within HLs 2-6 (0.79 ± 0.08). HL3 and HL6 in this core appear very similar in their pigment concentrations to the rest of the HLs in that core. Relative abundance of total porphyrins and absolute abundances of Ni and VO species tend to increase downcore in HL4 and HL5 (**Fig. 4.8**). The exceptions are three samples at the top of HL1: no peaks corresponding to porphyrins were detected on the absorption spectra at 495 cm, while the uppermost sample (485 cm) only contains Ni, and 490 cm only VO but both in much lower concentrations than in

other HL samples. HL1 in this core is poorly represented in the magnetic susceptibility record (Stoner *et al.*, 2000).

In core ODP 609, the relative abundance of VO and Ni porphyrins in prominent HLs is quite similar in all the samples and averages 0.87 (± 0.05). However, the amounts of VO and Ni porphyrins calculated for most of the HL3 and 6 samples from ODP 609 are about an order of magnitude lower than those for HLs 1, 2, 4 and 5 (**Fig. 4.9**) from that core. There is a downcore increase in porphyrin concentrations in HL5 (**Fig. 4.9**). One sample from HL3 (159 cm) is characterised by relatively high amounts of Ni porphyrins and absence of VO species. In spite of the downcore increase in both porphyrin concentrations, the relative abundance of VO porphyrins in HL3 and HL6 decreases downcore, except for the 393 cm sample (HL6) where no porphyrin peaks were detected on absorbance spectra. This variability in relative abundance of Ni and VO porphyrins in HL3 and HL6 may indicate change in the source of the IRD with Ni rich sediments deposited at the beginning of the layer gradually giving way to VO rich material. However, sampling at higher resolution is necessary to confirm or disprove this suggestion. High *S/I* ratios at the end of HE6 may be explained by low amounts of chlorins in those samples.

Ambient glacial sediments after HL2 (97 and 50 cmbsf) do not appear to contain porphyrins (*S/I*=3.21 and 2.45). In contrast, these ratios for the earlier ambient sediments are similar to those of HLs (**Fig. 4.9** and **App. 3**). However, the absorbance spectra of those sample extracts do not show peaks corresponding to Ni and VO porphyrin satellite (I) bands (extinction maximum at 570 nm) except for the samples at 137 cm (just after HL3) and between HL5 and HL6 (350 cm). However, the abundances of VO porphyrins in these two samples are at least ten times lower than in prominent HLs.

4.5.1.2 N-alkanes

Gas chromatograms of the saturated hydrocarbon fraction of the sediment extracts of representative samples of Heinrich Layer sediments are presented in **Fig. 4.10** and chain-length distributions in **Fig. 4.11**. The average concentrations of total n-alkanes

(nC_{17-33}) per gram dry sediment in the HLs from cores ODP 609, MD95-2024 and HU87-025-07P range from 0.5 to 6 μg/g **Table 4. 10**. Branched and cyclic hydrocarbons are present in the region of the short-chain n-alkanes similarly to HLs from SU90-09 (See Section 4.3.1.2). The variables used for comparison of the HL sediments from ODP 609, MD95-2024 and HU87-025-07P, and their values are listed in the **Table 4. 10** and **App.3**.

Samples from HLs in cores HU87, MD95-2024 and from the "typical" HLs (HLs 1, 2, 4 & 5) at ODP site 609, show chain-length distributions of n-alkanes similar to HLs from SU90-09 with maxima at n-C_{27} or n-C_{29} (**Fig. 4.11**). Such similarity in n-alkane distribution probably indicates a common source of the terrigenous organic matter (e.g. Cranwell, 1973; McCaffrey *et al.*, 1991). GC fingerprints of HL3 and HL6 at ODP 609 show a maximum at nC_{31}, with a sharp increase in relative abundance from n-C_{27} to n-C_{29} to n-C_{31} (**Figs. 4.10 and 4.11**) indicating a different source of n-alkanes from that in the "typical" HL sediments from this and other locations. The abundance of n-C_{29} is slightly higher than n-C_{31} in HLs from MD95 (1.20) and "typical" HLs from ODP 609 (1.15). The predominance of n-C_{29} is more pronounced in HL2 from the Labrador Sea core HU87 (n-C_{29} to n-C_{31} ratio 1.45) (**Table 4. 10**). In contrast, in HLs 3 and 6 from ODP 609 n-C31 dominates (the C_{29}/C_{31} ratio is 0.77). n-C_{27} and n-C_{29} are present in more or less equal amounts in most HL samples except for the "untypical" HL3 and HL6 from the ODP 609 where the increase in abundance from n-C_{27} to n-C_{29} is well pronounced (C_{27}/C_{29} ratio 0.68) (**Table 4. 10**).

The "untypical" HLs 3 and 6 from ODP 609 are characterised by higher CPI values (CPI~3) then the other HLs (CPI~2) **Table 4. 10**. There is, however, high variability in this parameter within cores (standard deviation =0.57 from MD95-2024 and 0.41 and 0.71 for "typical" and "untypical" HLs from ODP609). Similar to SU90-09, the CPI values in the "typical" HLs are lowest for HLs 1 and 2 (1.04-2.23) and highest for HL5 (2.22-3.46) (**App. 3**). ACL values for the HLs from MD95-2024 and the "typical" HLs from ODP609 range from 28.1 (HLs MD95-2024) to 28.8 (HL5 ODP) **Table 4. 10**. ACL for the "untypical" HL3 and 6 from ODP609 is much higher (29.0-29.7) (**App. 3**) and, similarly to other variables, indicates a

different source of IRD in these samples containing younger, less reworked organic matter.

All HL samples from core MD95-2024 contain a hump of unresolved complex mixture (UCM). This is a further indication of the reworked character of organic matter in HL sediments (Peters & Moldowan, 1993). UCM in that core is mostly confined to the range of low molecular weight (**Fig. 4.10**). UCM appears in the "typical" HL samples from ODP 609 but the "hump" in the low molecular weight region is less prominent and there is a secondary maximum at nC_{31}. UCM is relatively low in the HL2 sample from the Labrador Sea (HU87) and "untypical" ODP HLs (**Fig. 4.10** & **Table 4. 10**). The ratio of the UCM amount to that of total n-alkanes for most HL samples is greater than 4 indicating the highly biodegraded character of organic matter in HLs. The amount of UCM is lower for the North American HLs (cores HU87 and MD95) and "untypical" ODP HLs (**Table 4. 10**) than for the "typical" ODP HLs.

Table 4. 10 Mean values and standard deviation (in brackets) of carbon preference index (CPI), relative abundance of UCM, relative abundances of long-chain n-alkanes and average chain length (ACL). N – number of observations. HP – hemipelagic sediments. AU – absorbance units.

Variable	N	TNA, µg/g	C_{29}/C_{31}	C_{27}/C_{29}	CPI_{24-31}	ACL	*UCM/ TNA*	UCM/g, µg/g	*S/I*	VO, AU/g
HU 87 HL2	**1**	**0.5**	**1.45**	**0.93**	**2.05**	**28.4**	**4.85**	**2.5**	**5.5**	
MD95-2024 HLs 1-6	**14**	**2.0 (1.2)**	**1.20 (0.17)**	**1.04 (0.12)**	**2.28 (0.57)**	**28.4 (0.2)**	**5.6 (4.4)**	**7.4 (3.7)**	**11.7 (3.5)**	**0.85**
ODP 609 HLs1, 2, 4, 5	**5**	**2.6 (2.3)**	**1.15 (0.11)**	**0.93 (0.07)**	**1.88 (0.41)**	**28.5 (0.2)**	**7.9 (2.5)**	**23.7 (27.3)**	**10.2 (3.4)**	**0.78**
ODP 609 HLs 3, 6	**7**	**1.9 (1.3)**	**0.77 (0.10)**	**0.68 (0.09)**	**3.04 (0.71)**	**29.3 (0.2)**	**4.5 (2.2)**	**10.36 (11.42)**	**13.4 (10.6)**	**0.03**
ODP 609 HP	6	1.8 (1.3)	0.86 (0.22)	0.81 (0.17)	2.94 (1.34)	29.1 (0.44)	7.10 (4.69)	16.1 (1.4)	10 (5.9)	0.01

Several samples of the ambient glacial sediments (one sample between each pare of HLs) were analysed for ODP 609. Hemipelagic sediments from ODP 609 show unimodal distributions with a maximum at n C_{31} and a sharp increase in abundance from n-C_{27} to n-C_{29} to n-C_{31} (**Table 4. 10**). They are characterised by higher CPI (2.4-4.9) and ACL (29.0-29.7) and lower abundance of n-alkanes and UCM per gram dry sediment than the adjacent HL sediments (**Table 4. 10** and **App. 3**). High values of UCM/TNA calculated for some of the ambient glacial sediment samples indicate input of ice rafted organic matter in those sediments.

4.5.2 Is there a different source of IRD in HL3 and HL6? Evidence from different locations in the NA

As was discussed previously (Section 4.4.1), HL3 in core SU90-09 differs form the prominent HLs in biomarker composition of its sediments and is similar to the overlaying hemipelagic sediments (see Sections 4.3.2 and 4.4.1). This is in agreement with previous work on this core: HE3 is poorly represented in magnetic susceptibility record and its coarse fraction content and composition of fine-sized organic matter (OC/TN, $\delta^{13}C$ and $\delta^{15}N$) is similar to that of the ambient glacial sediments (Grousset *et al.*, 2001; Huon *et al.*, 2002). Relatively high CPI and ACL and lack of Ni and VO porphyrins indicate the presence of less reworked organic matter in this layer that may be associated with aeolian input (**Table 4.3**). On the other hand, HL3 contains much higher amounts of UCM than the prominent HLs, and that is a feature of heavily biodegraded organic matter usually found in older, ice rafted sediments. Biomarker composition of HL3 sediments is similar to that of the ambient glacial sediments above and below this layer (Section 4.3.2). It has been suggested that during HE3, the icebergs from the Laurentide Ice Sheet did not reach the eastern parts of North Atlantic and HL3 there may be a result of low productivity or dissolution of foraminifera (Bond *et al.*, 1992; Gwiazda *et al.*, 1996a). However, high abundance of terrestrial organic matter and its reworked character in HL3 indicates ice rafting as an important sediment transport mechanism. The similarity of HL3 composition with that of ambient glacial sediments is due to the presence of the reworked organic matter in the ambient glacial sediments from MIS2-3 as a result of the polar waters extending south of SU90-09 location (Section 4.3.2).

Biomarker fingerprints of organic matter in HLs 3 & 6 from ODP 609 also appear different from those in HLs 1, 2, 4 & 5 in their n-alkane distribution, pigments content and amount of UCM. The "untypical" HLs 3 and 6 from this location contain organic matter of relatively low maturity and degree of biodegradation characterised by high CPI and ACL, low abundance of porphyrins and UCM in contrast with more reworked organic matter in the "typical" HLs (**Figs. 4.10 and 4.11** and **Table 4. 10**). These observations are confirmed statistically (**Table 4. 11**) indicating difference in the sediment source for the two groups of HL samples and similarity between HLs 3 and 6. Similar to the lithic composition (Bond *et al.*, 1992; Broecker *et al.*, 1992), biomarker signature of HL3 and HL6 is closer to that of the hemipelagic sediments than of the prominent HLs (**Table 4. 10 & Table 4. 11**). Unusual character of HL3 was reported for the nearby core T88-9P (48°23'N, 25°05'W) (Madureira *et al.*, 1997). Its sediments contained high terrigenous biomarker amounts compared with other HLs (6 (HL3) vs. 0.95 (HL1) – 3.16 (HL5)) probably indicating a different source of organic matter in that layer. HLs 3 and 6 in that core also contained n-alkanes with higher ACL than the "typical" HLs (Madureira *et al.*, 1997).

Table 4. 11 Comparison of "typical" and "untypical" HLs from cores MD95 and ODP 609. Results of MANOVA of PC1-PC3. Probability of one or more differences between the two-dimensional mean vectors.

Groups compared		Probability>F
ODP 609 HLs 1,2,4,5	ODP 609 HLs 3,6	0.0000
ODP 609 HP	ODP 609 HLs 3,6	**0.7355**
ODP 609 HL3	ODP 609 HL6	**0.4884**
MD95 HLs 1,2,4,5	MD95 HL 3,6	**0.8559**

Similarity between HLs 3 and 6 and hemipelagic sediments from ODP 609 may be considered as confirmation of diminished IRD input during HE3 and HE6 compared with the prominent HEs. Since HLs 3 and 6 from the Labrador Sea do not differ from the other HLs, ice rafting from that location took place but icebergs may have not reached the location of core ODP609 (Bond *et al.*, 1992). Such interpretation was given by Gwiazda *et al.* (1996a) on the basis of the isotopic

analysis of the lithic fraction of the nearby core V28-82 (49°27'N, 22°16'W). Sediments from HLs 3 and 6 are low in Ni and VO porphyrins and are characterised by high CPI and ACL values indicative of a less reworked organic matter that may be associated with aeolian input rather than ice rafting. However, a thin detrital carbonate layer was found in HL3 from core ODP 609 (Bond & Lotti, 1995). The presence of IRD is also confirmed by an increase in the sediments accumulation rates albeit modest in comparison with the "typical" HLs in the nearby core V28-82 (McManus *et al.*, 1998) and increase in the non-carbonate fraction in the glacial sediments in core T88-9P (Madureira *et al.*, 1997). Because the peaks in biomarker concentration in core T88-9P did not correlate well with IRD ratio record but showed good correlation with the dust record of the GRIP Summit ice core, the authors suggested aeolian input as a prevailing mechanism in terrigenous biomarker input in that core. Similarly, there may be a substantial proportion of the aeolian sediments in the HLs 3 and 6 from ODP 609. Increased aeolian input may hold an explanation for the low abundance of the coarse fraction in HL3. High CPI and ACL are consistent with biomarker composition of a less mature organic matter originating from weathered soils. However, younger n-alkane fingerprints may also be associated with IRD. For instance, debris flow sediments from the North Sea Fan are characterised by high CPI (>3) (see Section 3.3.1.2).

Similarity of biomarker composition of sediments from HLs3 and 6 with those from the hemipelagic sediments can be explained by the location of the polar front south of the site of the core that resulted in ice rafting during the periods between HEs (Villanueva *et al.*, 1997). This view is confirmed by the change in biomarker composition of the hemipelagic sediments in core SU90-09 with the shift in the location of the polar front (see Section 4.3.2).

In contrast, there is no significant difference between HLs 1, 2, 4 &5 and HLs3 & 6 samples from core MD95 (**Table 4. 11**). They appear to have originated from the same source. There is no difference between biomarker composition of high carbonate (HLs 1-5) and low carbonate layers (HL6 and LDC5) from core MD95-2024. This may indicate that biomarker signal of relatively organic-poor carbonate rocks is overcome by that of other outcrops (e.g. shales) form the same source area. The LDC layer above HL6 is slightly higher in relative abundance of

VO porphyrins and UCM/g. There is no evidence for different source of IRD in HL3 suggested by Andrews & MacLean (2003).

"Typical" and "untypical" Heinrich layers and hemipelagic sediments are compared using the results of the PCA in **Fig. 4.12**. On the PC1/PC2 plot, "untypical" ODP samples (HL3 & 6) can be clearly distinguished from the "typical" HL samples but not from the hemipelagic sediments. Contrast in the biomarker composition of the sedimentary organic matter in the "typical" and "untypical" HLs indicates different sources of sediments.

The biomarker composition of the sediments in HLs 3 and 6 from the ODP 609 appear different from that in HL3 from SU90-09 (**Fig. 4.12** and **Table 4. 12**). HLs 3 & 6 from the former location contain less reworked organic matter with higher CPI, ACL and lower UCM. The concentration of n-alkanes in the "untypical" HL sediments there is lower than in HL3 from core SU90-09 (**Table 4.3** and **Table 4. 10**). HL3 sediments from core SU90-09 contain some features similar to those in prominent HLs, such as distribution of UCM with two humps in a chromatographic trace (**Fig. 4.10**) and relative abundances of the long-chain n-alkanes (**Fig. 4.11** and **Table 4.3**). In contrast, the "untypical" HLs from ODP 609 are markedly different from the "typical" ones. This indicates a different source of organic matter in the "untypical" HLs from the two locations. Less reworked character of organic matter in the ODP 609 layers may indicate predominance of aeolian over the IRD input or a different IRD source. In agreement with this, Villanueva *et al.* (1997) report differences in n-alkane distribution between cores SU90-39 (northeast of ODP609) and SU90-08 (just east of SU90-09) suggesting different sediment sources. Probably, HL3 sediments from the southern location combine contribution from several sources including some shared with the prominent HL sediments and also windborne organic matter.

4.5.3 Variability between prominent HLs from different areas of the ocean

Ten groups of samples were compared using MANOVA of PC1, PC2 and PC3 – five HLs and 2 precursor events from SU90-09, samples from MD95-2024, "typical" (HLs 1, 2, 4 & 5) and "untypical" (HL3 & 6) HLs from ODP 609. The results are

presented in **Table 4. 12.** and **Fig. 4.13.** The biomarker composition of HLs from core SU90-09 seems to differ significantly from that of the other two locations. For this core, the only P value outside 95% confidence interval was calculated for the HL1 precursor event and "typical" HLs from the ODP 609 core. This can be explained by the high variability within HL1 precursor. HLs from the southwestern Labrador Sea (MD95-2024) appear similar to the "typical" HLs from the North Atlantic ODP 609 core. The exception is HL4 in ODP 609. It is different from the rest of the "typical" ODP 609 samples in its higher UCM values (**App. 3**). The two samples from core ODP 609 collected from the carbonate-rich layers (225 - HL4 and 295 - HL5) are higher in their n-alkane concentrations (>3 μg/g) then the rest of HL samples from this core and are characterised by a more pronounced predominance of n-C_{29} over n-C_{27} alkane.

Table 4. 12 Comparison of HL samples from different areas of the ocean. Results of MANOVA of PC1, PC2 & PC3. Probability of one or more differences between the two-dimensional mean vectors.

	MD95 HLs1-6	ODP 609 HLs 1,2,4,5	ODP 609 HLs 3,6
SU90-09 HL1	0.0007	0.0184	0.0000
SU90-09 HL1pr	0.0147	**0.0976**	0.0000
SU90-09 HL2	0.0003	0.0019	0.0000
SU90-09 HL2pr	0.0002	0.0051	0.0000
SU90-09 HL3	0.0000	0.0000	0.0000
SU90-09 HL4	0.0041	0.0018	0.0000
SU90-09 HL5	0.0002	0.0007	0.0000
ODP HLs 1,2,4,5	**0.6480**		
ODP HLs 3,6	0.0000		

Multinomial logistic regression analysis of selected variables was carried out to evaluate the contribution of individual variables to the variability between HLs from different locations. The results are presented in **Table 4. 13**. The most significant difference between HLs from different locations lie in the amount of UCM and the relative abundance of porphyrins (*S/I*). These values are higher for most of the HL samples from SU90-09 than for HLs from the other locations. CPI

plays an important part in distinguishing between HL1 and HL2 of SU90-09 from the IRD layers in the MD95 core. However, it is important to note that HLs 1 and 2 in all the cores are characterised by lower CPI values than HLs 4 & 5 (**App. 3** and **Table 4.3**).

Table 4. 13 Comparison of HL samples from SU90-09 with HL samples from MD95-2024. Results of mlogit. Probability>F values. MD95- MD95-2024 HLs1-6, ODP typ – "typical" HLs 1, 2, 4, 5 from core ODP609.

Groups compared		CPI_{24-31}	C_{29}/C_{31}	ACL_{25-33}	UCM/TNA	S/I
MD95	SU90-09 HL1	**0.012**	0.231	**0.031**	0.080	0.058
MD95	SU90-09 HL1pr	0.157	**0.041**	**0.009**	**0.015**	**0.009**
MD95	SU90-09 HL2	**0.005**	0.952	0.599	**0.003**	**0.018**
MD95	SU90-09 HL2pr	0.286	0.760	0.326	**0.003**	**0.040**
MD95	SU90-09 HL3	0.484	0.478	0.125	**0.001**	**0.032**
MD95	SU90-09 HL4	0.141	0.330	0.956	0.148	**0.009**
MD95	SU90-09 HL5	0.786	0.385	0.260	0.685	**0.020**
ODP typ	SU90-09 HL1	0.295	0.134	0.433	0.237	**0.020**
ODP typ	SU90-09 HL1pr	0.992	**0.031**	**0.046**	**0.036**	**0.006**
ODP typ	SU90-09 HL2	0.165	0.452	0.698	**0.029**	**0.009**
ODP typ	SU90-09 HL2pr	0.648	0.642	0.963	**0.017**	**0.015**
ODP typ	SU90-09 HL3	0.441	0.874	0.550	**0.007**	**0.013**
ODP typ	SU90-09 HL4	0.552	0.782	0.535	0.505	**0.006**
ODP typ	SU90-09 HL5	0.182	0.980	0.126	0.737	**0.010**

Similarity in the biomarker composition of the "typical" HL sediments from cores ODP 609 and MD95-2024 indicates the same source of organic matter in the two locations. HLs from core MD95-2024 contain sediments from the Labrador Sea and Baffin Bay basins deposited mainly as spillover turbidites from the NAMOC and probably contain a combined biomarker signature from that area (Stoner *et al.*, 1996). Ice rafting was also named as an important mechanism of terrestrial sediment deposition in that location (Veiga-Pires & Hillaire-Marcel, 1999) N-alkane distribution in the HL2 sample from the western slope of the Labrador Sea core HU87-025-07P is similar to that in MD95-2024. This sample, however, is low in

relative abundance of porphyrins and UCM, especially at low molecular weight (**Fig.s 4.10 and 4.11**). Due to its location proximal to one of the secondary ice streams along the Labrador Sea margin, the biomarker content of this sample may be derived mostly from that outlet and not reflect the combined signal of all the sources in the region. It may, however, contain a true biomarker signature of the sediments in the NAMOC. That may indicate an additional North American source of IRD (Gulf of St. Lawrence or West Greenland?) in core MD95-2024 characterised by a distinctive UCM hump at low molecular weight and high abundance of porphyrins.

Similar to MD95-2024, IRD from North America appear to be the main source of terrigenous organic matter in the prominent Heinrich layers from core ODP 609. However, there is a difference in UCM distribution between the two cores: in most samples from core MD95-2024 UCM contains compounds characterised by low molecular weight, whereas the low molecular weight UCM hump in the samples from ODP 609 is less prominent and a secondary maximum at the retention time of n-C_{33} alkane is visible. Therefore, input from an additional source containing UCM of high molecular weight (Europe?) is likely. For the HLs from core SU90-09, a combination of several sources may explain the variability between and within prominent HLs. A North American signal is indicated by a UCM hump at low molecular weight and n-alkane envelope (**Fig.s 4.10 and 4.11**). There is some variation in the biomarker signature of HL sediments in MD95-2024, e.g. CPI is higher for the earlier HLs 4-6 than for the younger HLs 1-3. Similar tendency is observed in both ODP 609 and SU90-09 HLs biomarker fingerprints. However, sediments with high concentration of porphyrins, UCM with high molecular weight, and low CPI (in HLs1 and 2) must have originated elsewhere. The Gulf of St. Lawrence may be the source area of the sediments with low molecular weight UCM and high porphyrin content. High molecular weight UCM may have a European origin since it is present in the sediments from both ODP609 and SU90-09 and absent from MD95-2024.

4.5.4 Conclusions

The "untypical" HLs 3 and 6 in the two cores from the "IRD belt" (ODP 609 and SU90-09) differ significantly in the biomarker composition of their organic matter from the "typical" HLs 1, 2, 4 & 5 and are similar to the overlaying hemipelagic sediments. A combination of aeolian and ice rafted origins for these layers is proposed. In contrast, there is no significant difference between HLs 1, 2, 4 &5 and HLs3 & 6 samples from the southwestern Labrador Sea core MD95-2024.

The biomarker composition of sediments in the "untypical" HLs from ODP 609 appears different to that in HL3 from SU90-09 and may indicate a diminished IRD input in the former. HL3 sediments from core SU90-09 probably combine contributions from several sources.

The source of IRD in the prominent HLs from core ODP 609 is similar to that in MD95-2024 and indicates a predominantly North American origin. An additional source of IRD characterised by the presence of a mixture of highly branched aliphatic compounds of high molecular weight (chromatographic UCM) is proposed for HLs 1, 2, 4, and 5 in core ODP 609.

The biomarker composition of the HLs from core SU90-09 is probably a result of a combination of several sources including source(s) common with IRD layers from core MD95-2024. Origin of the additional sedimentary sources with high concentration of porphyrins, a mixture of highly branched aliphatic compounds (chromatographic UCM) of high molecular weight and n-alkane distribution with low CPI (in HLs1 and 2) is at least partially different from that in core ODP 609.

4.6 Provenance of IRD in the North Atlantic: Correlating sources and sinks

The biomarker composition of Heinrich layer sediments from different locations in the North Atlantic was compared with that of a number of potential sources as exemplified by glacigenic debris flow deposits (GDF) (See Chapter 3). Gas chromatograms of the saturated fraction and chain-length distribution of n-alkanes of the representative samples from HLs are presented in **Figs. 4.10 and 4.11** and from debris flows in **Figs. 4.14 and 4.15**. Due to the fact that the composition of the HL sediments is a result of complex input from a number of IRD sources (**Section 4.5**), simplification using PCA analysis proved unproductive when attempting to correlate sources and sinks of IRD. That is why various biomarker characteristics were considered individually.

4.6.1 A missing IRD source

The GC fingerprint of HL2 from the western slope of the Labrador Sea (core HU87-025-07P) is similar to that from the debris flow in the same location. This may indicate a predominantly local source of IRD in this Heinrich layer or the genuine composition of the IRD input from a number of sources in northern Canada. GC fingerprints of HLs from the other locations do not match those of any of the potential IRD sources analysed in this study. In fact, there is more similarity between HLs from cores MD95-2024, SU90-09 and the "typical" HLs from ODP 609 than between any of the HLs and debris flows. A unimodal chromatographic n-alkane distribution with maximum at n-C_{27} or n-C_{29} alkanes matches that of Labrador Sea (LS), Baffin Bay (BB) and North Sea Fan (NSF) debris flows (**Figs. 4.11 and 4.15**). A contribution from Europe in HLs from core MD95-2024 is unlikely. Therefore, n-alkane distribution at least for the sediments in that core, reflects that from North American sources. A mixed biomarker signal from the Labrador Sea and Baffin Bay GDF is probably responsible for the nature of the chromatographic n-alkane envelope for HL samples from the southwestern Labrador Sea and possibly the other two locations studied here (**Figs. 4.11 and 4.15**). However, GDF sediments from the North American sources used in this study contained very low amounts of

highly branched aliphatic compounds, and those are characterised by high molecular weight. The UCM hump at the low molecular weight region, prominent in the chromatographic traces of HL sediment extracts from MD95-2024, SU90-09 and "typical" HLs from ODP 609 (**Fig. 4.10**), was missing from those of LS and BB GDF (**Fig. 4.14**). It thus transpired that an important source of IRD containing UCM of low molecular weight had not been identified. However, chromatographic fingerprint containing such characteristic UCM signature was found to belong to several sediment samples from core POR18 (69°10.54'N, 51°49.38'W) from Disco Bugt in West Greenland (Lloyd *et al.*, in press). Thus it can be concluded that HLs in core MD95-2024 contain combined IRD from northern Canada and West Greenland.

4.6.2 Multiple sources of IRD in cores SU90-09 and ODP 609

The similarity of n-alkane distributions in prominent HL samples from cores SU90-09 and ODP 609 to those of the HLs from MD95-2024 indicates a shared source of IRD. A contribution from North American sources of IRD in the North Atlantic is in agreement with the established view on the provenance of IRD in HLs (e.g. Andrews & Tedesco, 1992; Bond *et al.*, 1992; Gwiazda *et al.*, 1996b; Hemming *et al.*, 1998). In addition to IRD input from West Greenland, a contribution of IRD from additional sources to HL sediments from cores SU90-09 and ODP 609 is evident.

ODP 609

Chromatographic fingerprints of the "typical" HLs from ODP 609 contain a less prominent hump of low molecular weight UCM but are characterised by overall higher UCM content with a secondary hump in the high molecular weight region. The addition of the more reworked organic matter is indicated by slightly lower CPI values for the HLs from ODP 609 than from MD95-2024. This may reflect a contribution from European ice sheets: Bear Island Fan (BIF), Scoresby Sund Fan (SSF) and debris flows from Svalbard contain highly degraded sedimentary organic matter with low CPI and high chromatographic UCM. The source of organic matter

in the "untypical" HLs from ODP 609 was not found in any of the potential sources analysed in this study. These sediments contain organic matter of low maturity more consistent with aeolian deposits than with IRD. This may indicate a diminished IRD input of IRD during HEs 3 and 6 at this location as was proposed by Gwiazda *et al.* (1996a) and Madureira *et al* (1997) based on the analyses of HL sediments from the nearby cores VM28-82 and T88-9P respectively. However, the possibility of IRD input should not be discarded. For instance, NSF debris flows contain young sedimentary organic matter. Yet, the biomarker signature of this source is different in relative abundances of long-chain n-alkanes (maximum at n-C_{27} alkane rather than n-C_{31}) and photosynthetic pigment content (the presence of chlorin peaks on the UV-VIS spectra of NSF sediments) from that of ODP 609 "untypical" HL sediments. Other possible European IRD sources are the British Isles and Fram Strait. There is evidence of input from these locations in the Sr-Nd isotopic composition of HL3 in several North Atlantic cores (Snoeckx *et al.*, 1999). These sources have not been analysed in present study.

SU90-09

HL sediments from core SU90-09 are characterised by higher relative abundance of porphyrins, higher chromatographic UCM and lower CPI values than those in MD95-2024 (**Table 4.3** and **Table 4. 10**). This indicates input of IRD from additional source/sources containing older, highly degraded organic matter. Such features are consistent with sedimentary organic matter from the Nordic Seas margins except for the North Sea Fan. However, if that were the case, the signature of mature highly degraded organic matter would be more pronounced in the HL sediments from ODP 609 because of its location further north. While CPI values for HLs from ODP 609 are indeed slightly lower than average for corresponding HLs from SU90-09 (**App. 3**), ODP 609 HLs contain significantly lower amounts of UCM and photosynthetic pigments than HL sediments from SU90-09.

In addition, sedimentary organic matter from HLs 1 and 2 precursor events whose enhanced European input is suggested by mineralogical and isotopic data (Grousset *et al.*, 2001), is characteristic of less mature sediments with higher CPI and

ACL than in the corresponding HLs. That may indicate some input from the Fennoscandian ice sheet. As in the NSF debris flow sediments, n-alkane distribution in the precursor events shows a maximum at n-C_{27} alkane. However, the UV-VIS spectra of the precursor events samples is low in Ni and VO porphyrins and did not contain chlorin peaks at 665 nm, characteristic of the NSF sediments although there is an increase in the relative abundance of porphyrins compared to ambient glacial sediments. Also, high amounts of UCM in the precursor event sediments imply a contribution from an additional source.

In core SU90-09, UCM input is decoupled from that of photosynthetic pigments. UCM is higher for the younger HLs 1, 2 and 3 than for the older HLs4 and 5, whereas these older layers are characterised by the highest relative abundance of porphyrins. Similar to the precursor events, HL3 and ambient glacial sediments from SU90-09 are the highest in UCM but low in Ni and VO porphyrins. Although *S/I* ratios >10 for these sediments indicate presence of porphyrins, they are probably not Ni and VO chelates. These may be Cu porphyrins brought by aeolian transport or from sea ice. Variation in the absolute abundance of Ni and VO porphyrins in core SU90-09 does not match that of relative abundance of porphyrins (**Fig. 4.2** and **Table 4.3**), supporting the existence of multiple sources of photosynthetic pigments.

The additional source of IRD is possibly the Gulf of St. Lawrence area. There is, for instance, petrographic evidence for ice rafting from several locations around the Gulf of St. Lawrence before and during HE1 and HE2 (Piper & Skene, 1998; Piper & DeWolfe, 2003). Mineralogical and isotopic evidence for input from this location in HLs in North Atlantic has been reported previously (Bond & Lotti, 1995; de Abreu *et al.*, 2003; Grousset *et al.*, 2001). However, no significant contribution from this source to the HLs in core MD95-2024 has been reported. HLs in that location contain carbonate-rich sediments from Northern Canada and the red sands of Gulf of St. Lawrence are deposited below HLs (Piper & Skene, 1998).

Recent findings show that the isotopic signature traditionally attributed to the Scandinavian source area may be of Gulf of St. Lawrence origin (Farmer *et al.*, 2003). If so, the precursor events may be not of European but of southern Laurentide provenance. That may be true also for HL3 in core SU90-09. Contrasts in the biomarker composition of HL3 and ambient glacial sediments from SU90-09 with

that of HLs 3 and 6 and ambient glacial sediments from ODP 609 support mostly North American origin of IRD in the former location.

The issue of post-depositional transformation of HL sediments has not been addressed in the present work. However, the biomarker composition of HL sediments should reflect not only a contribution from different sources of IRD but also the results of post-depositional transformation of the sediments, e.g. changes in the grain size distributions due to scouring by bottom currents. For instance, HLs from core ODP 609 are thinner than those from the nearby V28-82 and are characterised by higher detrital carbonate content and lower magnetic susceptibility (Hemming, 2004, and references therein). This may be a result of the partial loss of the fine grain size fraction, containing for example shale-derived sediments, from core ODP 609. These fine-grain sediments may have contained mature, biodegraded organic matter. Analysis of HL sediments from sites that have not have been affected by bottom-current processes, e.g. core V28-82 (McManus *et al.*, 1998), as well as analysis of different size fractions, could provide answer to this question.

4.6.3 Conclusions

To conclude, the main source of IRD in the prominent HLs from the two North Atlantic cores, ODP 609 and SU90-09, is a combination of inputs from Northern Canada and West Greenland. Prominent HLs from ODP 609 contain a minor proportion of sediments from an additional source or sources. Contribution from several other sources is more pronounced in the HLs from core SU90-09. These additional sources contain highly reworked organic matter with large amounts of mixed highly branched aliphatic compounds (chromatographic UCM) of high molecular weight, n-alkane distribution with low CPI, and high relative abundance of porphyrins. The variability between and within HLs in core SU90-09 is probably a result of variability in relative inputs from different IRD sources.

No significant input from the European ice sheets was detected in the two cores. Biomarker composition of the "untypical" HLs 3 and 6 from ODP 609 is more consistent with aeolian rather than IRD input. However, not all potential source areas were considered and samples from additional sources (i.e. British Isles and Fram Strait) need to be analysed to confirm or disprove this view.

A contribution from some IRD sources may be underrepresented in HL sediments from the sites affected by bottom-current activity due to winnowing of the fine grain size fraction.

4.7 Conclusions

- The biomarker composition of sediments deposited during prominent Heinrich events 1, 2, 4 and 5 in cores SU90-09 and ODP 609 is significantly different from that of overlaying hemipelagic sediments. Therefore prominent Heinrich events can be identified on sedimentary records based on the composition of the sedimentary organic matter. There is no significant difference between biomarker compositions of organic matter in HLs 3 and 6 and overlaying ambient sediments.
- Sediments deposited during Heinrich events in core SU90-09 contain highly reworked organic matter consistent with input from ancient sedimentary outcrops. Ice rafting is thought to have been the main process responsible for the formation of HLs in this core.
- Hemipelagic sediments in core SU90-09, deposited during the Holocene, prior to HL3 and overlaying HLs 4 and 5, contain younger organic matter consistent with aeolian input. Ambient sediments deposited between HLs 1 and 3 contain highly degraded organic matter probably of mixed ice rafted, sea ice and aeolian origin. This was interpreted as a result of the shift in the Polar Front location during MIS3.
- The biomarker composition of HL sediments from core SU90-09 varies between and within HLs. All five HLs analysed can be distinguished from one another on the basis of the biomarker composition of their sediments. Precursor events are recognised in the sedimentary record of HLs 1 and 2 but not HLs 4 and 5. Three steps can be distinguished in HLs 4 and 5 with the narrow middle step different from the periods above and below it, and two steps in HL1 and possibly in HL2.
- The "untypical" HLs 3 and 6 in cores ODP 609 and SU90-09 differ significantly in the biomarker composition of their organic matter from the "typical" HLs 1, 2, 4 & 5 indicating different sources of organic matter in "typical" and "untypical" HLs. In contrast, there is no significant difference between HLs 1, 2, 4 &5 and HLs3 & 6 samples from the southwestern Labrador Sea core MD95-2024.
- The "untypical" HLs 3 and 6 in cores ODP 609 differ significantly from HL3 in SU90-09 in the biomarker composition of their organic matter. The source

of organic matter in the former is attributed to aeolian input. A combination of aeolian and ice rafted origins is proposed for the latter.

- N-alkane distribution in core MD95-2024 was found consistent with combined input from Baffin Bay, Labrador Sea and West Greenland. Biomarker composition of the sediments in the prominent HLs from cores ODP 609 and SU90-09 is largely similar to that from core MD95-2024 implying contribution from North Canadian/West Greenland sources. However, biomarker signature of organic matter from several other sources is well pronounced in these cores. These additional sources contain highly reworked organic matter with large amounts of branched aliphatic molecules (chromatographic UCM) of high molecular weight, n-alkane distribution with low carbon preference index (CPI) and high relative abundance of porphyrins. No significant input from the European ice sheets was detected in the two cores.
- The variability in the biomarker composition between and within HLs is probably a result of variability in relative input from different IRD sources or different ice streams within the same source.
- Apart from variability in the contribution from different IRD sources, the dissimilarities between HLs from different areas of the ocean may be a result of post-depositional transformation of the sediments at some locations, e.g. changes in the grain size distributions due to scouring by bottom currents.

5. Summary, conclusions and future work

CONTENTS

5.1 Summary and conclusions

The aim of this project was to investigate the application of biomarkers to the study of provenance of allochthonous organic matter deposited in the North Atlantic during the last glacial period. In order to achieve this, the biomarker composition of the possible sources and sinks of the ice rafted debris (IRD) was described and compared. As a proxy for source of IRD, use of glacigenic debris flows (GDF) was proposed. Sinks were represented by Heinrich layer (HL) sediments from several deep-sea cores.

5.1.1 Use of biomarker composition of GDF to characterise sources of IRD

The first objective was to investigate the possibility of using the biomarker signatures of GDF as a source proxy for IRD in the North Atlantic. In order to do this, distribution of photosynthetic pigments, n-alkanes, highly branched aliphatic hydrocarbons (unresolved complex mixture (UCM) in the gas chromatogram) and long-chain alkenones in the GDF and overlying glacimarine and hemipelagic sediments from several locations on the North Atlantic continental margins was described and compared. Samples from four Trough Mouth Fans (TMFs) representing east Greenland (Scoresby Sund), the Fennoscandian Ice Sheet (North Sea Fan), the Barents Sea (Bear Island Fan) and Svalbard (Isfjorden and Bellsund TMFs) were considered. North American sources were represented by Baffin Bay and Labrador Sea GDF deposits.

Using biomarker analysis, a number of parameters were generated which were used to characterise and compare different types of sediments in the GDF deposits. Biomarker analysis provides a more detailed and more specific approach than analysis of bulk properties of the sediments.

The biomarker composition of GDF sediments is different from that of overlying hemipelagic and glacimarine sediments, indicating different sources of organic matter in the different types of sediments (**Section 3.4.2.2**). GDF sediments contain reworked organic matter, derived mainly from ancient sedimentary rocks as exemplified by the presence of metalloporphyrins (nickel and vanadyl chelates) and

mixtures of highly branched aliphatic molecules which are not resolved by gas chromatography and can be recognised on a chromatogram as a hump of unresolved complex mixture (UCM). On the other hand, organic matter in hemipelagic sediments is of much younger nature, mostly deposited as a result of aeolian and fluvial weathering of contemporary soils. Glacimarine sediments resulted from a mixed input of ice rafted and hemipelagic organic matter.

With very few exceptions, the GDF sediments from each TMF on the Nordic Seas continental margins are characterised by homogeneity of their biomarker composition within each core and within each TMF (**Section 3.4.2.1**). GDF sediments from North America are homogenous within each core. However, some variability was found between the two cores from Baffin Bay. For the most part, however, sediments from these two cores are more similar to each other in their biomarker composition than to any other GDF analysed. Only one core containing GDF from Labrador Sea was analysed.

The biomarker signatures of GDF sediments analysed in this study were found to be unique to each GDF deposit, and represent the combined signature of a variety of outcrops eroded by each ice stream (**Section 3.4.3.3**). Therefore, the biomarker composition of GDF can be used to constrain the sources of IRD in the North Atlantic.

The biomarker composition of a glacial till deposit off Scoresby Sund is largely similar to that of GDF sediments from that location. Hence glacial till sediments can probably be used as proxies for sources of IRD in areas where GDF did not form.

Other implications

GDF from NSF and Svalbard were found to contain long-chain alkenones and chlorins (**Section 3.3.3.3**). These compounds are usually associated with autochthonous input. Discovery of alkenones and chlorins in GDF sediments means that the presence of these compounds in the sediments deposited in glacial environments may be a result of allochthonous as well as autochthonous input. Therefore the use of these biomarkers to reconstruct palaeoceanographic conditions during glacial periods may result in incorrect estimations due to the allochthonous

contribution. However, a contribution of alkenones from NSF and Svalbard alone does not account for the unusually high sea surface temperatures calculated for the last glacial maximum in the Nordic Seas (Rosell-Mele & Comes, 1999). This probably indicates the existence of an additional source of allochthonous alkenones in the Nordic Seas. Circum-Arctic areas (Darby *et al.*, 2002) may present such source.

5.1.2 Sources of allochthonous organic matter in the North Atlantic

The second objective was to investigate the spatial and temporal variability of autochthonous and allochthonous inputs in the deep-sea sediments from several North Atlantic cores. Core SU90-09 (43°05N, 31°05W) was analysed at high resolution (every 0.5-5 cm). In addition, several samples of HL and hemipelagic sediments from another core in the "IRD belt", ODP 609 (49°52 N, 24°14 W), from southwestern Labrador Sea core MD95-2024 (50°12.26N, 45°41.14W), and from one HL2 sample from Labrador Sea core HU87-025-07P (57°04.37'N 50°12.25W) were analysed.

The biomarker composition of sediments deposited during prominent Heinrich events 1, 2, 4 and 5 in cores SU90-09 and ODP 609 is significantly different from that of overlaying hemipelagic sediments (**Section 4.3.2**). Therefore prominent Heinrich events can be identified on sedimentary records based on the composition of their organic matter. There is no significant difference between biomarker composition of organic matter in HLs 3 and 6 and overlaying ambient sediments. Sedimentary organic matter in both HL and hemipelagic sediments in all cores was found to be mostly of allochthonous origin. Sediments deposited during prominent Heinrich events in cores SU90-09 and ODP 609 contain highly reworked organic matter deposited as a result of ice rafting.

A shift in the location of the marine Polar Front during MIS3 is recorded in the biomarker composition of the ambient sediments (**Section 4.3.2**). In core SU90-09, background sediments overlying HLs 4, 5 and preceding HL3, as well as those deposited during the Holocene, contain younger organic matter as a result of aeolian

input from contemporary environments. Deposition of highly degraded organic matter probably of mixed ice rafted, sea ice and aeolian origin, is recorded in the biomarker composition of the ambient sediments overlaying HLs 1, 2 and 3. Their biomarker composition, however, is different from that of the "typical" HLs but not from that of HL3.

Core SU90-09 was studied at high resolution (**Section 4.4**). The biomarker composition of HL sediments in that core was found to vary between and within HLs. All five HLs analysed can be distinguished from one another based on the biomarker composition of their sedimentary organic matter. For the most part, the biomarker compositions of sediments in the older HLs 4 and 5 are more similar to one another than to the younger HLs 1 and 2. HLs 1 and 2 are similar in their n-alkane distributions but differ in other parameters. Precursor events are recognised in the sedimentary records of HL1 and HL2 but not HL4 and HL5. Three steps can be distinguished in HLs 4 and 5 with a narrow middle step different from the periods above and below it. There are two steps in HL1 and possibly in HL2.

Biomarker compositions of the "untypical" HLs 3 and 6 in the two cores from the "IRD belt" (ODP 609 and SU90-09) differ significantly from that of the "typical" HLs 1, 2, 4 & 5 and are similar to the overlying ambient sediments. In contrast, there is no significant difference between HLs 1, 2, 4 & 5 and HLs 3 & 6 in samples from the southwestern Labrador Sea core MD95-2024. It was concluded that an IRD contribution from North American sources did exist during HEs 3 and 6 but on a smaller scale, and icebergs from these sources did not reach the locations of cores SU90-09 and ODP 609. The "untypical" HLs 3 and 6 in core ODP 609 differ significantly from HL3 in SU90-09 in the biomarker composition of their organic matter. The source of organic matter in the former is attributed to aeolian input. A combination of aeolian, sea ice and ice rafted origins is proposed for the latter (**Section 4.5.2**).

The variability in the biomarker composition between and within HLs is probably a result of variability in relative input from different IRD sources or different ice streams within the same source. However, as well as variability in the sources of IRD, post-depositional transformation of HL sediments at some locations,

e.g. loss of fine grain size fraction due to scouring by bottom currents, may be responsible for variability in HLs from different areas of the ocean.

5.1.3 Correlation of sources and sinks of IRD in the North Atlantic

The third objective was to compare the allochthonous biomarker signatures in deep-sea sediments with those described in the possible source areas to ascertain the provenance of IRD during HEs.

Use of objective statistical methods such as cluster analysis for correlating sources and sinks of IRD in HLs proved unsuccessful due to the complex nature of the input of IRD in HLs. That is why correlation was limited to visual comparison of gas chromatographs, n-alkane distributions and values for individual variables.

The biomarker composition of HLs was compared with that of GDF sediments (**Section 4.6**). In core MD95-2024, a contribution from only North American sources was expected. In agreement with this assumption, the n-alkane distribution in this core was consistent with combined input from Baffin Bay and Labrador Sea. However, a mixture of highly branched aliphatic compounds (UCM on the chromatogram) of low molecular weight present in the sediments from core MD95-2024 was absent from the North American GDF analysed indicating input from an additional source. A similar chromatographic fingerprint was found to belong to several sediment samples from core POR18 (69°10.54'N, 51°49.38'W) from Disco Bugt in West Greenland (Lloyd *et al.*, in press). Thus it was concluded that HLs in core MD95-2024 contain combined IRD from North Canada and from West Greenland.

The biomarker composition of the sediments in the prominent HLs from cores ODP 609 and SU90-09 is largely similar to that from core MD95-2024 implying a contribution from north Canadian/West Greenland sources. However, biomarker signatures of organic matter from several other sources is well pronounced in these cores. These additional sources contain highly reworked organic matter with large amounts of branched aliphatic molecules (chromatographic UCM) of high molecular weight, n-alkane distribution with low carbon preference index (CPI) and

high relative abundance of porphyrins. No significant input was detected from the European ice sheets in the two cores.

5.2 Future work

5.2.1 Sources and sinks of IRD

Since the beginning of this project, knowledge on the location and nature of GDF deposits in the North Atlantic has improved considerably. Comparison of biomarker composition of potential sources and sinks of IRD in the North Atlantic show that not all sources of IRD were considered in this study. GDF deposits from Baffin Bay and the Labrador Sea need to be studied in more detail in order to address the problem of heterogeneity of GDF deposits in these areas. Sediments from other possible Laurentide Ice Sheet outlets (e.g. the Newfoundland slope and Laurentian Fan) may contain information on the "missing" sources of IRD. Input of IRD from circum-Arctic areas into the Nordic Seas and possibly the North Atlantic via Fram Strait has been reported (Darby *et al.*, 2002) and needs to be investigated.

The biomarker composition of sources of IRD from the same location may have differed through time due to change in the pathways of ice streams, or through weathering or exhaustion of erodible strata. That may have resulted in variability between HLs reflecting not a change in source area of IRD, but a change in the source material from the same area. Analysis of GDF deposited during different episodes of ice rafting may provide more accurate information on the changes through time in the composition of IRD transported into the ocean.

More HEs in different areas of the North Atlantic including Nordic Seas need to be studied at a high resolution in order to further elucidate the temporal and spatial variability of IRD inputs. Special attention should be paid to the likelihood of post depositional transformation of the HL sediments in the analysed cores.

5.2.2 Biomarker analysis

Use of even the simplest techniques (GC and UV-VIS spectrophotometry) allows clear distinction between the biomarker compositions of potential IRD sources. However, HLs were found to contain a combination of inputs from different sources of IRD that are likely to vary in the concentration of organic matter. That makes it difficult to assess the contribution from each source based on the distribution of

biomarkers ubiquitous in sediments from potential sources (i.e. n-alkanes and porphyrins). Use of Mass Spectrometry will broaden the spectrum of biomarkers used to construct signatures of individual sources and potentially can allow identification of specific biomarker compounds unique to each source.

Isotopic analysis of individual compounds (i.e. $\delta^{13}C$ composition and ^{14}C dating) will prove useful in distinguishing between autochthonous and allochthonous inputs of organic matter (e.g. alkenones and chlorins) in the deep-sea and GDF sediments.

Different rock types and therefore different outcrops eroded by ice streams are unevenly represented in different size fractions of IRD. Post depositional transformation of deep-sea sediments as a result of bottom-current activity may result in change of their grain size distribution (Hemming, 2004, and references therein). Biomarker fingerprinting of different particle size fractions from potential sources and sinks of IRD may prove useful in separating signals from different sources, and that may facilitate correlation between sources and sinks.

REFERENCES

Adams, J., Maslin, M., Thomas, E., (1999) Sudden climate transitions during the Quaternary. *Progress in Physical Geography*, 23(1), 1-36.

Aksu, A.E., (1984) Subaqueous debris flow deposits in Baffin Bay. *Geo-marine letters*, 4, 83-90.

Aksu, A.E., Hiscott, R.N., (1989) Slopes and Debris Flows on the high-latitude continental slopes off Baffin Bay. *Geology*, 17, 885-888.

Aksu, A.E., Hiscott, R.N., (1992) Shingled Quaternary debris flow lenses on the north-east Newfoundland Slope. *Sedimentology*, 39, 193-206.

Aksu, A.E., Piper, D.J., (1987) Late Quaternary sedimentation in Baffin Bay. *Canadian Journal Earth Sciences*, 24, 1833-1846.

Alley, R.B., Blankenship, D.D., Rooney, S.T., Bentley, C.R., (1989) Sedimentation beneath ice shelves - the view from Ice Stream B. *Marine Geology*, 85, 101-120.

Alley, R.B., Meese, D.A., Shuman, C.A., Gow, A.J., Taylor, K.C., Grootes, P.M., White, J.W.C., Ram, M., Waddington, E.D., Mayewski, P.A., Zielinski, G.A., (1993) Abrupt increase in Greenland snow accumulation at the end of the Younger Dryas event. *Nature*, 362, 527-529.

Anderson, R.S., Betancourt, J.L., Mead, J.I., Hevly, R.H., Adam, D.P., (2000) Middle- and late-Wisconsin paleobotanic and paleoclimatic records from the southern Colorado Plateau, USA. *Palaeogeography, Palaeoclimatology, Palaeoecology*, 155, 31-57.

Andrews, D.F., MacLean, B., (2003) Hudson Strait ice streams: a review of stratigraphy, chronology and links with North Atlantic Heinrich events. *Boreas*, 32, 4-17.

Andrews, J., Jennings, A., Kerwin, M., Kirby, M.E., Manley, W., Miller, G.H., Bond, G., MacLean, B., (1995) A Heinrich-like event, H-0 (DC-0): Source(s) for detrital carbonate in the North Atlantic during the Younger Dryas Chronozone. *Paleoceanography*, 10, 943-952.

Andrews, J.T., (1998) Abrupt changes (Heinrich events) in late Quaternary North Atlantic marine environments: a history and review of data and concepts. *Journal of Quaternary Science*, 13, 3-16.

Andrews, J.T., (2000) Explained and unexplained spacial and temporal variability in rates of marine sediment accumulation along the Northeast margin of the Laurentide ice sheet <= 14 Ka. *Journal of Sedimentary Research*, 70, 782-787.

Andrews, J.T., Cooper, T.A., Jennings, A.E., Stein, A.B., Erlenkeuser, H., (1998) Late Quarternary iceberg-rafted detritus events on the Denmark Strait-Southeast Greenland continental slope (~65N):rekated to North Atlantic Heinrich events? *Marine Geology*, 149, 211-228.

Andrews, J.T., Erlenkeuser, H., Tedesco, K., Aksu, A.E., Jull, A.J.T., (1994) Late quaternary (Stage 2 and 3) meltwater and Heinrich events, northwest Labrador Sea. *Quaternary Research*, 41, 26-34.

Andrews, J.T., Geirsdottir, A., Jennings, A.E., (1989) Late Quaternary Spatial and Temporal Changes in Clay-Size and Silt-Size Mineral Assemblages of Fiord and Shelf Cores, Western Baffin-Bay, Northwest North-Atlantic. *Continental Shelf Research*, 9(5), 445-463.

Andrews, J.T., Jennings, A.E., (1987) Influence of Sediment Source and Type on the Magnetic- Susceptibility of Fjord and Shelf Deposits, Baffin-Island and Baffin-Bay, Nwt. *Canadian Journal of Earth Sciences*, 24(7), 1386-1401.

Andrews, J.T., Tedesco, K., (1992) Detrital carbonate-rich sediments, northwestern Labrador Sea:Implications for ice-sheet dynamics and iceberg rafting (Heinrich) events in the North Atlantic. *Geology*, 20, 1087-1090.

Baker, E.W., Lauda, J.W., (1986) Porphyrins in the geological record. In: R.B. Jones (Ed.), *Biological markers in the sedimentary record.* (Ed. by R.B. Jones), pp. 125-226. Elsevier.

Baker, E.W., Palmer, S.E., (1979) Chlorophyll diagenesis in IPOD Leg 47A, Site 397 core samples. In: U. von Rad, W.B.F. Ryan, e. al. (Eds.), *Init. Rep. Deep-Sea Drill. Proj., 47 Pt.1* (Ed. by U. von Rad, W.B.F. Ryan, e. al.), pp. 547-551. U.S. Government Printing Office, Washington.

Baker, P.A., Rigsby, C.A., Seltzer, G.O., Fritz, S.C., Lowenstein, T.K., Bacher, N.P., Veliz, C., (2001) Tropical climate changes at millennial and orbital timescales on the Bolivian Altiplano. *Nature*, 409, 698-701.

Bard, E., Rostek, F., Turon, J.L., Gendreau, S., (2000) Hydrological impact of Heinrich events in the subtropical northeast Atlantic. *Nature*, 289:, 1321-1324.

Barnabas, I.J., Dean, J.R., Fowlis, I.A., Owen, S.P., (1995) Extraction of Polycyclic Aromatic Hydrocarbons From Highly Contaminated Soils Using Microwave Energy. *The Analyst*, 120, 1897-1904.

Baumann, K.-H., Lackshewitz, K.S., Mangerud, J., Spielhagen, R.F., Wolf-Welling, T.C.W., Henrich, R., Kassens, H., (1995) Reflection of Scandinavian Ice Sheet fluctuations in norwegian Sea sediments during the past 150,000 years. *Quaternary Research*, 43, 185-197.

Benson, L., Barber, D., Andrews, J.T., Taylor, H., Lamothe, P., (2003) Rare-earth elements and Nd and Pb isotopes as source indicators for Labrador Sea clay-size sediments during Heinrich event 2. *Quaternary Science Reviews*, 22(8-9), 881-889.

Blanco, E.V., Mahia, P.L., Lorenzo, S.M., Rodriguez, D.P., Fernandez, E.F., (2000) Optimization of microwave-assisted extraction of hydrocarbons in marine sediments: comparison with the Soxhlet extraction method. *Fresenius Journal of Analytical Chemistry*, 366, 283–288.

Bond, G., Broecker, W., Johnsen, S., McManus, J., Labeyrie, L., Jouzel, J., Bonani, G., (1993) Correlations between climate records from North Atlantic sediments and Greenland ice. *Nature*, 365, 143-146.

Bond, G., Heinrich, H., Broecker, W., Labeyrie, L., McManus, J., Andrews, J., Huon, S., Jantschik, R., Clasen, S., Simet, C., Tedesco, K., Klas, M., Bonani, G., Ivy, S., (1992) Evidence for massive discharges of icebergs into the North Atlantic ocean during the last glacial period. *Nature*, 360, 245-249.

Bond, G.C., Lotti, R., (1995) Iceberg discharges into the North Atlantic on millennial time scales during the last glaciation. *Science*, 267, 1005-1010.

Bond, G.C., Showers, W., Elliot, M., Evans, M., Lotti, R., Hajdas, I., Bonani, G., Johnson, J.A., (1999) The North Atlantic's 1-2 kyr rythm: Relation to Heinrich events, Dansgaard/Oeschger and the Little Ice Age. In: C.D. Clark (Ed.), *Mechanisms of Global Climate Changes at Millenial Timescales, 112, Geophys Monogr. Ser.* (Ed. by C.D. Clark), pp. 35-58. AGU, Washington D.C.

Boon, J.J., de Lange, F., Schuyl, P.J.W., de Leeuw, J.W., Schenck, P.A., (1977) Organic geochemistry of Walvis Bay diatomaceous ooze. II Occurrence and

significance of the hydroxy fatty acids. In: R. Campos, J. Goni (Eds.), *Advances in Organic Geochemistry, 1975* (Ed. by R. Campos, J. Goni), pp. 255-272. Enadimsa, Madrid.

Boulton, G.S., Smith, G.D., Jones, A.S., Newsome, J., (1985) Glacial Geology and Glaciology of the Last Mid-Lattitude Ice Sheets. *Journal of Geological Society: London*, 142, 265-273.

Bout-Roumazeiles, V., Cortijo, E., Labreyie, L., Debrabant, P., (1999) Clay mineral evidence of nepheloid layer contributions to the Heinrich layers northwest Atlantic. *Palaeogeography, Palaeoclimatology, Palaeoecology*, 146, 211-228.

Brassell, S.C., (1993) Application of Biomarkers for delineating marine paleoclimatic fluctuations during the pleistocene. In: M.H. Engel, A. Macko (Eds.), *Organic Geochemistry* (Ed. by M.H. Engel, A. Macko), pp. 699-738. Plenum Press, New York.

Brassell, S.C., Brereton, R.G., Eglinton, G., Grimalt, J., Liebezeit, G., Marlowe, I.T., Pflaumann, U., Sarnthein, M., (1986a) Palaeoclimatic signals recognized by chemometric treatment of molecular stratigraphic data. *Organic Geochemistry*, 10, 649-660.

Brassell, S.C., Eglinton, G., (1986) Molecular geochemical indicators in sediments. In: M.Sohn (ed.) Marine Organic Geochemistry. *Amer.Chem.Soc.Symp.Ser.*, 305, 10-32.

Brassell, S.C., Eglinton, G., Marlowe, I.T., Pflaumann, U., Sarnthein, M., (1986b) Molecular stratigraphy: a new tool for climatic assessment. *Nature*, 320, 129-133.

Brassell, S.C., Eglinton, G., Maxwell, J.R., Philp, R.P., (1978) Natural background of alkanes in the aquatic environment. In: O. Hutzinger, L.H. van Lelyveld, B.C.J. Zoeteman (Eds.), *Aquatic pollutants: transformation and biological effects* (Ed. by O. Hutzinger, L.H. van Lelyveld, B.C.J. Zoeteman), pp. 69-86. Pergamon Press, Oxford.

Brault, M., Simoneit, B.R.T., Marty, J.C., Saliot, A., (1988) Hydrocarbons in waters and particulate material from hydrothermal environments at the East Pacific Rise, 13°N. *Organic Geochemistry*, 12, 209-219.

Bray, E.E., Evans, E.D., (1961) Distribution of n-paraffins as a clue to recognition of source beds. *Geochimica et Cosmochimica Acta*, 22, 2-15.

Brincat, D., Yamada, K., Ishiwatari, R., Uemura, H., Naraoka, H., (2000) Molecular-isotopic stratigraphy of long-chain n-alkanes in Lake Baikal Holocene age sediments. *Organic Geochemistry*, 31, 287-294.

Broecker, W.S., (1994) Massive iceberg discharges as triggers for global climate change. *Nature*, 372, 421-424.

Broecker, W.S., Bond, G., Klas, M., Clark, E., McManus, J., (1992) Origin of the northern Atlantic Heinrich events. *Climate Dynamics*, 6, 265-273.

Butt, F.A., Elverhøi, A., Solheim, A., Forsberg, C.F., (2000) Deciphering Late Cenozoic development of the western Svalbard Margin from ODP Site 986 results. *Marine Geology*, 169, 373-390.

Callot, H.J., (1991) Geochemistry of chlorophylls. In: H. Scheer (Ed.), *Chlorophylls* (Ed. by H. Scheer), pp. 339-364. Boca Raton, CRC Press.

Callot, H.J., Ocampo, R., Albrecht, P., (1990) Sedimentary porphyrins: correlation with biological precursors. *Energy and Fuels*, 4, 635-639.

Calvo, E., Villanueva, J., Grimalt, J.O., Boelaert, A., Labeyrie, L., (2001) New insights into the glacial latitudinal temperature gradients in the North Atlantic.

Results from U-37(K ') sea surface temperatures and terrigenous inputs. *Earth and Planetary Science Letters*, 188(3-4), 509-519.

Camel, V., (2000) Microwave-assisted Solvent Extraction of Environmental Samples. *Trends in Analytical Chemistry*, 19, 229-248.

Carro, V., Saavedra, Y., Garcia, I., Llompart, M., (1999) Optimisation of Microwave Assisted Solvent Extraction of Polychlorinated Biphenyls from Marine Sediments. *Journal of Microcolumn Separations*, 11, 544-549.

Cayre, O., Lancelot, Y., Vincet, E., (1999) Paleoceanographic reconstructions from planctonic foraminifera off the Iberian Margin: temperature, salinity, and Heinrich events. *Paleoceanography*, 14, 384-396.

Chapman, M.R., Shackleton, N.J., Duplessy, J.-C., (2000) Sea surface temperature variability during the last glacial¯interglacial cycle: assessing the magnitude and pattern of climate change in the North Atlantic. *Palaeogeography, Palaeoclimatology, Palaeoecology*, 157, 1-25.

Charles, C.D., Lynch-Stieglitz, J., Ninnemann, U.S., Fairbanks, R.G., (1996) Climate connections between the hemisphere revealed by deep sea sediment core/ice core correlations. *Earth and Planetary Science Letters*, 142, 19-27.

Chee, K.K., Wong, M.K., Lee, H.K., (1996) Optimization Of Microwave-Assisted Solvent Extraction Of Polycyclic Aromatic Hydrocarbons In Marine Sediments Using A Microwave Extraction System With High-Performance Liquid Chromatography-Fluorescence Detection And Gas Chromatography-Mass Spectrometry. *Journal of chromatography*, 723, 259-271.

Chen, M.-T., Wang, C.-H., Huang, C.-Y., Wang, P., Wang, L., Sarnthein, M., (1999) a late Quaternary pl,anktonic foraminifer faunal record of rapid climatic changes from the South China Sea. *Marine Geology*, 156, 85-108.

Comet, P.A., Eglinton, G., (1987) The use of lipids as facies indicators. In: J. Brooks, A.J. Fleet (Eds.), *Marine Petroleum Source Rocks*, *Geological Society Special Publication* (Ed. by J. Brooks, A.J. Fleet). Blackwell, Oxford.

Conte, M.H., Volkman, J.K., Eglinton, G., (1994) Lipid Biomarkers of the Haptophyta.*The Systematics Association Special Volume*. In: B.S.C. Leadbeater (Ed.), *The Haptophyte Algae*, *51* (Ed. by B.S.C. Leadbeater), pp. 351-377. Clarendon Press, Oxford.

Cortijo, E., Labeyrie, L., Vidal, L., Vautravers, M., Chapman, M., Duplessy, J.-C., Elliot, M., Arnold, M., Turon, J.-L., G., A., (1997) Changes in sea surface hydrology associated with Heinrich event 4 in the North Atlantic Ocean between 40° and 60°N. *Earth and Planetary Science Letters*, 146, 29-45.

Cortijo, E., Labeyrie, L., Elliot, M, Balbon, E & Tisnerat, N., (2000) Rapid climatic variability of the North Atlantic Ocean and global climate: a focus of the IMAGES program. *Quaternary Science Reviews*, 19, 227-241.

Cranwell, P.A., (1973) Chain-length distribution of n-alkanes from lake sediments in relation to post-glacial environmental change. *Freshwater Biology*, 3, 259-265.

Crucifix, M., Berger, A., (2002) Simulation of ocean-ice sheet interactions during the last deglaciation. *Paleoceanography*, 17.

Damste, J.S.S., Rijpstra, I.C., Reichart, G.-J., (2002) The influence of oxic degradeation on the sedimentary biomarker record II. Evidence from Arabian Sea sediments. *Geochimica et al Cosmochimica Acta*, 66, 2737-2754.

Dansgaard, W., Johnsen, S.J., Clausen, H.B., Dahl-Jensen, D., Gundestrup, N.S., Hammer, C.U., Hvidberg, C.S., Steffensen, J.P., Sveinbj"rnsdottir, A.E.,

Jouzel, J., Bond, G., (1993) Evidence for general instability of past climate from a 250-kyr ice-core record. *Nature*, 364, 218-220.

Darby, D.A., Bischof, J.F., Spielhagen, R.F., Marshall, S.A., Herman, S.W., (2002) Arctic ice export events and their potential impact on global climate during the late Pleistocene. *Paleoceanography*, 17(2), art. no.-1025.

Davis, J.C., (1986) *Statistics and Data Analysis in Geology*. Wiley, New York, NY.

de Abreu, L., Shackleton, N.J., Schonfeld, J., Hall, M., Chapman, M., (2003) Millennial-scale oceanic climate variability off the Western Iberian margin during the last two glacial periods. *Marine Geology*, 196(1-2), 1-20.

de Leeuw, J.W., van de Meer, F.W., Rijpstra, W.I.C., Schenck, P.A., (1980) On the occurrence and sctrutural identification of long chain unsaturated ketones and hydrocarbons in sediments. In: J.R. Maxwell (Ed.), *Advances in Organic Geochemistry 1979* (Ed. by J.R. Maxwell), pp. 211-217. Pergamon, Oxford.

Derenne, S., Largeau, C., Berkaloff, C., (1996) First example of an algeanan yielding aromatic-rich pyrolysate: possible geochemical implications on marine kerogen formation. *Organic Geochemistry*, 24, 617–627.

Dokken, T.M., Hald, M., (1996) Rapid climatic shifts during isotope stages 2-4 in the polar north Atlantic. *Geology*, 24, 599-602.

Dolphin, D., (1978) *The porphyrins*. Academic Press.

Dowdeswell, J.A., Evernøi, A., Andrews, J.t. & Hebbeln, D., (1999) Asynchronous Deposition of Ice-Rafted Layers in the Nordic Seas and North Atlantic Ocean. *Nature*, 400, 348-351.

Dowdeswell, J.A., Kenyon, N.H., Elverhoi, A., Laberg, J.S., Mienert, J., Siegert, M.J., (1996) Large-scale sedimentation on the glacier-influenced Polar North Atlantic margins: long-range side-scan sonar evidence. *Geophysical Research Letters*, 23, 3535-3538.

Dowdeswell, J.A., Kenyon, N.H., Laberg, J.S., (1997) The glacier-influenced Scoresby Sund Fan, East Greenland continental margin: evidence from GLORIA and 3.5 kHz records. *Marine Geology*, 143, 207-221.

Dowdeswell, J.A., Maslin, M.A., Andrews, J.T., McCave, I.N., (1995) Iceberg production, debris rafting, and the extent and thickness of "Heinrich layers" (H1, H2) in North Atlantic sediments. *Geology*, 23, 301-304.

Dowdeswell, J.A., O Cofaigh, C., Kenyon, N.H., Rosell-Mele, A., (2000) Geophysical and geological investigations of sedimentation and ice-ocean variability on Arctic continental margins. Cruise report. RRS James Clark Ross - Cruise JR-51. Bristol Glaciology Centre, Bristol.

Dowdeswell, J.A., Siegert, M.J., (1999) Ice-sheet numerical modeling and marine geophysical measurement of glacier-derived sedimentation on the Eurasian Arctic continental margins. *Geological Society of America Bulletin*, 111(7), 1080-1097.

Eglinton, G., Bradshaw, S.A., Rosell, A., Sarnthein, M., Pflaumann, U., Tiedemann, R., (1992) Molecular record of secular sea surface temperature changes on 100-year timescales for glacial terminations I, II and IV. *Nature*, 356, 423-426.

Eglinton, G., Calvin, M., (1967) Chemical fossils. *Scientific American*, 261, 32-43.

Eglinton, G., Hamilton, R.J., (1967) Leaf epicuticular waxes. *Science*, 156, 1322-1335.

Eglinton, G., Maxwell, J.R., Evershed, R.P., (1985) Red pigments in petroleum exploration. *Interdisciplinary Science Reviews*, 10, 222-236.

Elliot, M., Labreyie, L., Bond, G., Cortijo, E., Turton, J.L., Tinserat, N., Duplessy, J.C., (1998) Millennial-scale Iceberg discharges in the Irminger Basin during the last glacial period: Relationship with the Heinrich Events and environmental settings. *Paleoceanography*, 13, 433-446.

Elverhøi, A., Dokken, T.M., Hebbeln, D., Spielhagen, R.F., Svendsen, J.I., Sørflaten, M., Rørnes, A., Hald, M., Forsberg, C.F., (1995a) The growth and decay of the late Wiechselian Ice Sheet in Western Svalbard and adjacent areas based on provenance studies of marine sediments. *Quaternary Resaerch*, 44(303-316).

Elverhøi, A., Norem, H., Anderson, E.S., Dowdeswell, J.A., Fossen, I., Haflidason, H., Kenyon, N.H., Laberg, J.S., King, E.L., Sejrup, H.P., Solheim, A., Vorren, T.O., (1997) On the origin and flow behavior of submarine slides on deep-sea fans along the Norwegian-Barents Sea Continental margin. *Geo-Marine Letters*, 17, 119-125.

Elverhøi, A., Svendsen, J.I., Solheim, A., Andersen, E.S., Milliman, J., Mangerud, J., Hooke, R.L., (1995b) Late Quaternary Sediment Yield from the High Arctic Svalbard Area. *Journal of Geology*, 103(1), 1-17.

Eskilsson, C.S., Björklund, (2000) Analytical-scale Microwave-assisted Extraction. *A Journal of Chromatography*, 902, 227-250.

Fagel, N., Hillaire-Marcel, C., Robert, C., (1997) Changes in the Western Boundary Undercurrent outflow since the Last Glacial Maximum, from smectite/illite ratios in deep Labrador Sea sediments. *Paleoceanography*, 12, 79-96.

Fagel, N., Innocent, C., Gariepy, C., Hillaire-Marcel, C., (2002) Sources of Labrador Sea sediments since the last glacial maximum inferred from Nd-Pb isotopes. *Geochimica et Cosmochimica Acta*, 66(14), 2569-2581.

Fahl, K., Stein, R., (1999) Biomarkers as organic-carbon source and environmental indicators in the Late Quaternary Arctic Ocean: problems and perspectives. *Marine Chemistry*, 63, 293-309.

Farmer, G.L., Barber, D., Andrews, J., (2003) Provenance of Late Quaternary ice-proximal sediments in the North Atlantic: Nd, Sr and Pb isotopic evidence. *Earth and Planetary Science Letters*, 209(1-2), 227-243.

Farrimond, P., Eglinton, G., Brassell, S.C., (1986) Alkenones in Cretaceous black shales, Blake-Bahama Basin, wesatern North Atlantic. *Organic Geochemistry*, 10, 897-903.

Ficken, K.J., Farrimond, P., (1995) Sedimentary lipid geochemistry of Framvaren: impacts of a changing environment. *Marine Chemistry*, 51(1), 31-43.

Font, N., Hernandez, F., Hogendoorn, E.A., Baumann, R.A., van Zoonen, P., (1998) Microwave-Assisted Solvent Extraction And Reversed-Phase Liquid Chromatography-UV Detection For Screening Soils For Sulfonylurea Herbicides. *A Journal of Chromatography*, 798, 179-186.

Francois, R., Bacon, M.P., (1994) Heinrich events in the North Atlantic: radiochemical evidence. *Deep-Sea Research I*, 41(315-334).

Fronval, T., Jansen, E., Bloemendal, J., Johnsen, S., (1995) Oceanic evidence for coherent fluctuations in Fennoscandian and Laurentide ice sheets on millenium timescales. *Nature*, 374, 443-446.

Ganzler, K., Salgo, A., Valko, K., (1986) Microwave Extraction - A Novel Sample Preparation Method for Chromatography. *A Journal of Chromatography*, 371, 299-306.

Gelpi, E., Schneider, H., Mann, J., Oro, J., (1970) Hydrocarbons of geochemical significance in microscopic algae. *Phytochemistry*, 9, 603-612.

Greenwood, P.F., Arouri, K.R., Logan, G.A., Summons, R.E., (2004) Abundance and geochemical significance of C2n dialkylalkanes and highly branched C3n alkanes in diverse Meso- and Neoproterozoic sediments. *Organic Geochemistry*, 35(3), 331-346.

Grimm, E., Jacobson, G.L., Watts, W.A., Hansen, B.C.S., Maasch, K.A., (1993) A 50,000-year record of climate oscillations from Florida and its temporal correlation with the Heinrich Events. *Science*, 261, 198-200.

Grousset, F.E., Cortijo, E., Huon, S., Herve, L., Richter, T., Burdloff, D., Duprat, J., Weber, O., (2001) Zooming in on Heinrich layers. *Paleoceanography*, 16(3), 240-259.

Grousset, F.E., Labeyrie, L., Sinko, J.A., Cremer, M., Bond, G., Duprat, J., Cortijo, E., Huon, S., (1993) Patterns of Ice-rafted Detritus in the Glacial North Atlantic (40-50°N). *Paleoceanography*, 8, 175-192.

Grousset, F.E., Pujol, C., Labeyrie, L., Auffret, G.A., Boelaert, A., (2000) Were the North Atlantic Heinrich events triggered my the behavior of the European ice sheets? *Geology*, 28, 123-126.

Gunn, G.E., Best, A.I., (1998) A new automated nondestructive system for high resolution multi-sensor core logging of open sediment cores. *Geo-marine letters*, 18(70-77).

Gwiazda, R.H., Hemming, S.R., Broecker, W.S., (1996a) Provenance of icebergs during Heinrich event 3 and the contrast to their sources during other Heinrich episodes. *Paleoceanography*, 11, 371-378.

Gwiazda, R.H., Hemming, S.R., Broecker, W.S., (1996b) Tracking the sources of icebergs with lead isotopes: the proveneance of ice-rafted debris in Heinrich layer 2. *Paleoceanography*, 11, 77-93.

Harris, P.G., Zhao, M., Rosell-Melé, A., Tiedemann, R., Sarnthein, M., Maxwell, J.R., (1996) Chlorin accumulation rate as a proxy for Quaternary marine primary productivity. *Nature*, 383, 63-65.

Hasty, E., Revetz, R., (1995) Total Petroleum Hydrocarbon Determination by Mycrowave Solvent Extraction. *American Laboratories*, 66-67.

Heinrich, H., (1988) Origin and consequences of cyclic ice rafting in the Northeast Atlantic Ocean during the past 130,000 years. *Quaternary Research*, 29, 143-152.

Hemming, N.G., (2004) Heinrich events: Massive Late Pliestocene detritus layers of the North Atlantic and their global climate imprint. *Review of Geophysics*, 42(RG1005), 1-43.

Hemming, S.R., Broecker, W.S., Sharp, W.D., Bond, G.C., Gwiazda, R.H., McManus, J.F., Klas, M., Hajdas, I., (1998) Provenance of Heinrich layers in core V28-82, northeastern Atlantic: $^{40}Ar/^{39}Ar$ ages pf ice-rafted hornblende, Pb isotopes in feldspar grains, and Nd-Sr-Pb isotopes in the fine sediment fraction. *Earth and Planetary Science Letters*, 164, 317-333.

Hemming, S.R., Gwiazda, R.H., Andrews, J.T., Broecker, W.S., Jennings, A.E., Onstott, T.C., (2000) $^{40}Ar/^{39}Ar$ and Pb-Pb study of individual hornblende and feldspar grains from southeastern Buffin Island glacial sediments: implications for the provenance of the Heinrich layers. *Canadian Journal of Earth Science*, 37, 879-890.

Hemming, S.R., Hajdas, I., (2003) Ice-rafted detritus evidence from 40Ar/39Ar ages of individual hornblende grains for evolution of the eastern margin of the Laurentide ice sheet since 43 14C ky. *Quaternary International*, 99-100, 29-43.

Hemming, S.R., Vorren, T.O., Kleman, J., (2002) Provinciality of ice rafting in the North Atlantic: application of Ar-40/Ar-39 dating of individual ice rafted hornblende grains. *Quaternary International*, 95-6, 75-85.

Heslop, D., Show, J., Bloemendal, J., Chen, F., Wang, J., Parker, E., (1999) Sub-Millennial Scale Variations in East Asian Monsoon Systems Recorded by Dust Deposits from the North-wetern Shinese Loess. *Physical Chemistry of Earth (A)*, 24, 785-792.

Hesse, R., Khodabakhsh, S., (1998) Depositional facies of late Pleistocene Heinrich events in the Labrador Sea. *Geology*, 26, 103-106.

Hesse, R., Khodabakhsh, S., Klaucke, I., Ryan, W.B.F., (1997) Assimetrical turbid surface-plume deposition near ice-outlets of the Pleistocene Laurentide ice sheet in the Labrador Sea. *Geo-Marine Letters*, 17, 179-187.

Hesse, R., Klauck, I., Khodabakhsh, S., Piper, D.J., (1999a) Continental slope sedimentation adjacent to an ice margin. III. The upper Labrador Slope. *Marine Geology*, 155, 249-276.

Hesse, R., Klaucke, I., (1995) A continuous along-slope seismic profile from the Upper Labrador Slope. In: K.T. Pickering, R.N. Hiscott, N.H. Kenyon, F.R. Lucchi, R.D. Smith (Eds.), *Atlas of Deep Water Environments: Architectural style in turbidite systems* (Ed. by K.T. Pickering, R.N. Hiscott, N.H. Kenyon, F.R. Lucchi, R.D. Smith), pp. 18-22. Chapman & Hall, London.

Hesse, R., Klaucke, I., Khodabakhsh, S., Piper, D.J., (1999b) Continental slope sedimentation adjacent to an ice margin. III. The upper Labrador Slope. *Marine Geology*, 155, 249-276.

Hesse, R., Rakofsky, A., Chough, S.K., (1990) The centeral Labrador Sea: facies and dispersal patterns of clastic sediments in a small ocean basin. *Marine and Petroleum Geology*, 7, 13-28.

Hillaire-Marcel, C., de Vernal, A., Bilodeau, G., Wu, G., (1994) Isotope stratigraphy, sedimentation rates, deep surculation, and carbonate events in the Labrador Sea during the last ~200 ka. *Canadian Journal Earth Sciences*, 31, 63-89.

Hinrichs, J., Schnetger, B., Schale, H., Brumsack, H.-J., (2001) A high resolution study of NE Atlantic sediments at station Bengal: geochemistry and early diagenesis of Heinrich layers. *Marine Geology*, 177, 79-92.

Hiscott, R.N., Aksu, A.E., (1994) Submarine debris flows and Continental slope evolution in front of Quaternary ice sheets, Baffin Bay, Canadian Arctic. *American Association of Petroleum Geologists Buletin*, 78(3), 445-460.

Hiscott, R.N., Aksu, A.E., Mudie, P.J., Parsons, D.F., (2001) A 340,000 year record of ice rafting, palaeoclimatic fluctuations, and shelf-crossing glacial advances in the southwestern Labrador Sea. *Global and Planetary Change*, 28(1-4), 227-240.

Hölemann, J.A., Henrich, R., (1994) Allochtonous versus autochtonous organic matter in Cenozoic sediments of the Norwegian Sea: Evidence for the onset of glaciations in the northern hemisphere. *Marine Geology*, 121, 87-103.

Hulbe, C.L., MacAyeal, D.R., Denton, G.H., Kleman, J., Lowell, T.V., (2004) Catastrophic ice shelf breakup as the source of Heinrich event icebergs. *Paleoceanography*, 19(PA1004, doi:10.1029/2003PA000890).

Huon, S., Grousset, F.E., Burdloff, D., Bardoux, G., Mariotti, A., (2002) Sources of fine-sized organic matter in North Atlantic Heinrich Layers: [delta]13C and [delta]15N tracers. *Geochimica et Cosmochimica Acta*, 66(2), 223-239.

Innocent, C., Fagel, N., Hillaire-Marcel, C., (2000) Sm-Nd isotope systematics in deep-sea sediments: clay-size versus coarser fractions. *Marine Geology*, 168(1-4), 79-87.

Innocent, C., Fagel, N., Stevenson, R.K., Hillaire-Marcel, C., (1997) Sm-Nd signature of modern and late Quaternary sediments from the northwest North Atlantic: Implications for deep current changes since the Last Glacial Maximum. *Earth and Planetary Science Letters*, 146(3-4), 607-625.

Jansen, E., Raymo, M.E., Blum, P., party, T.L.s.s., (1996) *Proceedings of the Ocean Drilling Program, Initial Reports*. College Station, TX.

Jayaraman, S., Pruell, R.J., McKinney, R., (2001) Extraction of organic contaminants from marine sediments and tissues using microwave energy. *Chemosphere*, 44, 181-191.

Jeffrey, S.W., Mantoura, R.F.C., Wright, S.W., (1997) *Phytoplankton pigments in oceanography*. UNESCO, Paris.

Kaufmann, B., Christen, P., (2002) Recent extraction techniques for natural products: microwave-assisted extraction and pressurised solvent extraction. *Phytochemical Analysis*, 13, 105–113.

Keely, B.J., Harris, P.G., Popp, B.N., Hayes, J.M., Meischner, D., Maxwell, J.R., (1994) Porphyrin and chlorin distributions in a Late Pliocene lacustrine sediment. *Geochimica et Cosmochimica Acta*, 58, 3691-3701.

Kenig, F., Sinninghe Damste, J.S., Kock-van Dalen, A.C., Rijpstra, W.I.C., Huc, A.Y., de Leeuw, J.W., (1995) Occurrence and origin of mono-, di-, and trimethylalkanes in modern and Holocene cyanobacterial mats from Abu Dhabi, United Arab Emirates. *Geochimica et Cosmochimica Acta*, 59, 2999–3015.

King, E.L., Haflidason, H., Sejrup, H.P., Lovlie, R., (1998) Glacigenic debris flows on the North Sea Trough Mouth Fan during ice stream maxima. *Marine Geology*, 152(1-3), 217-246.

King, E.L., Sejrup, H.P., Haflidason, H., Elverhøi, A., Aarseth, I., (1996) Quaternary seismic stratigraphy of the North Sea Fan: glacially-fed gravity flow aprons, hemipelagic sediments, and large submarine slides. *Marine Geology*, 130, 293-315.

Kirby, M.E., Andrews, J.T., (1999) Mid-Wisconsin Laurentide Ice Sheet growth and decay: Implications for Heinrich events 3 and 4. *Paleoceanography*, 14, 211-223.

Knutz, P.C., Austin, W.E.N., Jones, E.J.W., (2001) Millennial-scale depositional cucles related to British Ice Sheet variability and Notrth Atlantic paleocirculation since 45 kyr B.P., Barra Fan, U.K. margin. *Paleoceanography*, 16, 54-64.

Koç, N., Jansen, E., (1994) Response of the high-latitude Northern Hemisphere to orbital climate forcing: evidence from the Nordic Seas. *Geology*, 22, 523-526.

Kornilova, O., Rosell-Melé, A., (2003) Application of microwave-assisted extraction to the analysis of biomarker climate proxies in marine sediments. *Organic Geochemistry*, 34, 1517-1523.

Krabbe, H., (1996) Biomarker distribution in the lacustrine shales of the Upper Triassic-Lower Jurassic Kap Stewart Formation, Jameson Land, Greenland. *Marine and Petroleum Geology*, 13(7), 741-754.

Laberg, J.S., Vorren, T.O., (1995) Late Weichselian submarine debris flow deposits on the Bear Island Trough Mouth Fan. *Marine Geology*, 127(1-4), 45-72.

Laberg, J.S., Vorren, T.O., (1996) The Middle and Late Pliestocene evolution of the Bear Island Trough Mouth Fan. *Global and Planetary Change*, 12, 309-330.

Laberg, J.S., Vorren, T.O., (2000) Flow behaviour of the submarine glacigenic debris flows on the Bear Island Trough Mouth Fan, western Barents Sea. *Sedimentology*, 47, 1105-1117.

Landvik, J., Bondevik, S., Elverhoi, A., Fjeldskaar, W., Mangerud, J., Salvigsen, O., Siegert, M.J., Svendsen, J.I., Vorren, T.O., (1998) The last glacial maximum of Svalbard and the Barents Sea area: ice sheet extent and configuration. *Quaternary Science Reviews*, 17, 43-75.

LeBlanc, G., (1999) Microwave-accelerated techniques for solid sample extraction. *Current Trends and Developments in Sample Preparation LC-GC*, 17, S30–S37.

Lebreiro, S.M., Moreno, J.C., McCave, I.N., Weaver, P.P.E., (1996) Evidence for Heinrich layers off Portugal (Tore Seamount 39N,12W). *Marine Geology*, 131, 47-56.

Letellier, M., Budzinski, H., (1999) Microwave assisted extraction of organic compounds. *Analusis*, 27, 259-271.

Letellier, M., Budzinski, H., Bellock, J., Connan, J., (1999) Focussed Microwave-assisted Extraction of Polyciclic Aromatic Hydrocarbons from Sediments and Sourse Rocks. *Organic Geochemistry*, 30, 1353-1365.

Lewan, M.D., (1984) Factors controlling the proportionality of vanadium to nickel in crude oils. *Geochimica et al Cosmochimica Acta*, 48, 2231-2238.

Lin, H.-L., Lai, C.-T., Ting, H.-C., Wang, L., Sarnthein, M., Hung, J.-J., (1999) Late Pleistocene nutrients and sea surface productivity in the South China Sea: a record of teleconnections with Northern hemisphere events. *Marine Geology*, 156, 197-210.

Linthout, K., Troelstra, S.R., Kuijpers, A., (2000) Provenance of Coarse Ice-Rafted Detritus near the SE Greenland Margin. *Geologie en Mijnbouw / Netherlands Journal of Grosciences*, 79, 109-121.

Llompart, M.P., Lorenzo, R.A., Cela, R., Ken, L., Belanger, J.M.R., Pare, J.R.J., (1997) Evaluation of Supercritical Fluid Extraction, Microwave-Assisted Extraction And Sonication In The Determination Of Some Phenolic Compounds From Various Soil Matrices. *A Journal of Chromatography*, 774, 243-251.

Lloyd, J.M., Kroon, D., Boulton, G.S., Laban, C., Fallick, A., (1996) Ice rafting history from Spitsbergen ice cap over the last 200kyr. *Marine Geology*, 131, 103-121.

Lloyd, J.M., Park, L.A., Kuijpers, A., Moros, M., Early Holocene palaeoceanography and deglacial chronology of Disko Bugt, West Greenland. *Submitted and accepted in Quaternary Science Reviews.*

Lopez-Avila, V., Young, R., Kim, R., Beckert, W.F., (1995) Accelerated Extraction of Organic Pollutants Using Microwave Energy. *Journal of Chromatographic Science*, 33, 481-484.

Lopez-Avila, V., Young, R., Teplitski, N., (1996) Microwave-Assisted Extraction as an Alternative to Soxlet, Spnication and Supercritical Fluid Extraction. *Journal of AOAC International*, 79, 142-156.

MacAyeal, D.R., (1993) Binge/purge oscillations of the Laurentide ice sheet as a cause of the North Atlantic's Heinrich events. *Paleoceanography*, 8, 775-784.

Madureira, L.A.S., Conte, M.H., Eglinton, G., (1995) Early diagenesis of lipid biomarker compounds in North Atlantic sediments. *Paleoceanography*, 10, 627-642.

Madureira, L.A.S., van Kreveld, S.A., Eglinton, G., Conte, M.H., Ganssen, G., van Hinte, J.E., Ottens, J.J., (1997) Late Quaternary high-resolution biomarker and other sedimentary climate proxies in a northeast Atlantic core. *Paleoceanography*, 12, 255-269.

Manighetti, B., McCave, I.N., (1995) Depositional fluxes, palaeoproductivity, and ice rafting in the NE Atlantic over the past 30 ka. *Paleoceanography*, 10, 579-592.

Marlowe, I., (1984) Lipids as palaeoclimatic indicators. University of Bristol.

Marlowe, I.T., Green, J.C., Neal, A.C., Brassell, S.C., Eglinton, G., Course, P.A., (1984) Long chain (n-C_{37}-C_{39}) Alkenones in the Prymensiophyceae. Distribution of Alkenones and lipids and their Taxonomic significance. *British Phycology Journal*, 19, 203-216.

Marshall, J., Clarke, G.K.C., (1997) A continuum mixture model of ice stream thermomechanics in the Laurentide Ice Sheet 2: application to the Hudson Strait ice stream. *Journal of Geophysical Research*, B102, 20615-20637.

Maslin, M.A., (1995) Changes in North Atlantic Deap-Water formation associated with the Heinrich Events. *Naturwissenschaften*, 82, 330-333.

Maslin, M.A., Shackleton, N.J., Pflaumann, U., (1995) Surface water temperature, salinity and density changes in the NE Atlantic during the last 45,000 years: Heinrich events, deep water formation and climatic rebounds. *Paleoceanography*, 10, 527-544.

McCaffrey, M.A., Farrington, J.W., Repeta, D.J., (1991) The organic geochemistry of Peru margin surface sediments: II. Paleoenvironmental implications of hydrocarbon and alcohol profiles. *Geochimica et Cosmochimica Acta*, 55, 483-498.

McCave, I.N., (1995) Sedimentary precesses and the creation of the stratigraphic record in the Late Quaternary North Atlantic Ocean. *Phil.Trans.R.Soc.Lond.B*, 348, 229-241.

McManus, J.F., Anderson, R.F., Broecker, W.S., Fleisher, M.Q., Higgins, S.M., (1998) Radiometrically determined sedimentary fluxes in the sub-polar North Atlantic during the last 140,000 years. *Earth and Planetary Science Letters*, 155, 29-43.

Meglen, R.R., (1992) Examining large databases: a chemometric approach using principal component analysis. *Marine Chemistry*, 39, 217-237.

Mienert, J., Chi, J., (1995) Astronomical time-scale for phisical property records from Quaternary sediments of the northern North Atlantic. *Geologische Rundschau*, 84, 67-88.

Miles, J.A., (1994) *Illustrated Glossary of Petroleum Geochemistry.* Clarendon Press, Oxford.

Miller, J.C., Miller, J.N., (1993) *Statistics for Analytical Chemistry.* Ellis Horwood and Prentice Hall, London.

Molins, C., Hogendoorn, E.A., Heusinkveld, H.A.G., Van Zoonen, P., Baumann, R., (1997) A Microwave Assisted Solvent Extraction (Mase) of Organochlorine Pesticides from Soil Samples. *International Journal Of Environmental Analytical Chemistry*, 68, 155-169.

Muller, P.J., Kirst, G., Ruhland, G., von Storch, I., Rosell-Mele, A., (1998) Calibration of the alkenone paleotemperature index U-37(K ') based on core-

tops from the eastern South Atlantic and the global ocean (60 degrees N-60 degrees S). *Geochimica Et Cosmochimica Acta*, 62(10), 1757-1772.

Muller, R.A., MacDonald, G.J., (1995) Glacial Cycles and Orbital Inclanation. *Nature*, 377, 107-108.

Nam, S.-I., Stein, R., Grobe, H., Hubberten, H., (1995) Late Quaternary glacial-interglacial changes in sediment composition at the East Greenland continental margin and their paleoceanographic implications. *Marine Geology*, 122, 243-262.

O Cofaigh, C., Taylor, J., Dowdeswell, J.A., Pudsey, C.J., (2003) Palaeo-ice streams, trough mouth fans and high-latitude continental slope sedimentation. *Boreas*, 32, 37-55.

O Cofaigh, C., Taylor, J., Dowdeswell, J.A., Rosell-Mele, A., Kenyon, N.H., Evans, J., Mienert, J., (2002) Sediment reworking on high-latitude continental nargins and its implications for palaeoceanographic studies: insights from the Norwegian-Greenland Sea. In: C. O Cofaigh (Ed.), *Glacier-influenced sedimentation on high-latitude continental margins., 203* (Ed. by C. O Cofaigh), pp. 325-348. Geological Society of London, Special Publications, London.

Paillard, D., Cortijo, E., (1999) A simulation of the Atlantic meridional circulation during Heinrich event 4 using reconstructed sea surface temperatures and salinities. *Paleoceanography*, 14, 716-724.

Paillard, D., Labeyrie, L., (1994) Role of the termohaline circulation in the abrupt warming after Heinrich events. *Nature*, 372, 162-164.

Pastor, A., Vázquez, E., Ciscar, R., de la Guardia, M., (1997) Efficiency of the Microwave-assisted Extraction of Hydrocarbons and Pesticides from Sediments. *Analytica Chimica Acta*, 344, 241-149.

Peters, K.E., Moldowan, J.M., (1993) *The biomarker guide.* Prentice-Hall, London.

Peters, K.E., Snedden, J.W., Sulaeman, A., Sarg, J.F., Enrico, R.J., (2000) A new geochemical-sequence stratigraphic model for the Mahakam Delta and Makassar Slope, Kalimantan, Indonesia. *American Association of Petroleum Geologists Buletin*, 84(1), 12-44.

Piper, D.J., Skene, K.I., (1998) Latest Pleistocene ice-rafting events on the Scotian Margin (eastern Canada) and their relationship to Heinrich events. *Paleoceanography*, 13, 205-214.

Piper, D.J.W., DeWolfe, M., (2003) Petrographic evidence from the eastern Canadian margin of shelf-crossing glaciations. *Quaternary International*, 99-100, 99-113.

Porter, S.C., An, Z.S., (1995) correlation betwen climate vents in the north Atlantic and China during the last glaciation. *Nature*, 375, 305-308.

Poynter, J., Eglinton, G., (1990) Molecular composition of three sediments from Hole 717C: The Bengal fan. *Proc.Ocean Drill.Prgr.*, 116, 155-161.

Poynter, J.G., Farrimond, P., Robinson, N., Eglinton, G., (1989) Aeolian-derived higer plant lipids in the marine sedimentary record: Links with paleoclimate. In: M. Sarnthein (Ed.), *Paleoclimatology and Paleometerology: Modern and past patterns of global athmospheric transport* (Ed. by M. Sarnthein), pp. 345-462. Kluwer Academic, Hingham, Mass.

Prahl, F., Carpenter, R., (1984) Hydrocarbons in Washington coastal sediments. *Estuarine, Coastal and Shelf Science*, 17, 703-720.

Prahl, F.G., Wakeham, S.G., (1987) Calibration of unsaturation patterns in long-chain ketone compositions for palaeotemperature assessment. *Nature*, 320, 367-369.

Prokopenko, A.A., Williams, D.F., Karabanov, E.B., Khursevich, G.K., (2001) Continental response to Heinrich events and Bond cycles in sedimentary record of Lake Baikal, Siberia. *Global and Planetary Change*, 28(1-4), 217-226.

Rahman, A., (1995) Reworked nannofossils in the North Atlantic Ocean and subpolar basins: implications for Heinrich events and oceanic circulation. *Geology*, 23, 487-490.

Rashid, H., Hesse, R., Piper, D.J.W., (2003a) Distribution, thickness and origin of Heinrich layer 3 in the Labrador Sea. *Earth and Planetary Science Letters*, 205(3-4), 281-293.

Rashid, H., Hesse, R., Piper, D.J.W., (2003b) Evidence for an additional Heinrich event between H5 and H6 in the Labrador Sea. *Paleoceanography*, 18.

Rashid, H., Hesse, R., Piper, D.J.W., (2003c) Origin of unusually thick Heinrich layers in ice-proximal regions of the northwest Labrador Sea. *Earth and Planetary Science Letters*, 208(3-4), 319-336.

Repeta, D.J., Eglinton, G., Lee, C., (1992) Marine Organic Geochemistry: window to the past. *Oceanus*, 35.

Requejo, A.G., Allan, J., Creaney, S., Gray, N.R., Cole, K.S., (1992) Aryl isopreneoids and diaromatic carotenoids in Palaeozoic sorce rocks and oils from the Western Canada and Willston Basins. *Organic Geochemistry*, 19, 245-264.

Revel, M., Sinko, J.A., Grousset, F.E., Biscaye, P.E., (1996) Sr and Nd isotopes as tracers of North Atlantic lithic particles: paleoclimatic implications. *Paleoceanography*, 11, 95-113.

Robinson, S.R., Maslin, M.A., McCave, I.N., (1995) Magnetic susceptibility variations in Upper Pleistocene deep-sea sediments of the NE Atlantic: Implications for ice rafting and paleocirculation at the last glacial maximum. *Paleoceanography*, 10, 221-250.

Rosell-Melé, A., Carter, J., Parry, A., Eglinton, G., (1995) <<Atlantic Core-top Calibration of the UK37 in Sediment Samples. *Anaitical Chemistry*, 67, 1283-1289.

Rosell-Mele, A., Comes, P., (1999) Evidence for a warm Last Glacial Maximum in the Nordic seas or an example of shortcomings in U-37(K)' and U-37(K) to estimate low sea surface temperature? *Paleoceanography*, 14, 770-776.

Rosell-Mele, A., Jansen, E., Weinelt, M., (2002) Appraisal of a molecular approach to infer variations in surface ocean freshwater inputs into the North Atlantic during the last glacial. *Global and Planetary Change*, 34(3-4), 143-152.

Rosell-Melé, A., Koç, N., (1997) Paleoclimatic significance of the stratigraphic occurrence of photosynthetic biomarker pigments in the Nordic seas. *Geology*, 25, 49-52.

Rosell-Melé, A., Maslin, M., Maxwell, J.R., Schaeffer, P., (1997) Biomarker evidence for "Heinrich" events. *Geochimica et Cosmochimica Acta*, 61, 1671-1678.

Rosell-Melé, A., Weinelt, M., Koç, N., Jansen, E., Sarnthein, M., (1998) Variability of the Arctic front during the last climatic cycle: application of a novel molecular proxy. *Terra Nova*, 10, 86-89.

Ruddiman, W.F., (1977) Late Quaternary deposition of ice-rafted sand in the subpolar North Atlantic (lat 40ø-65øN). *Geological Society of America Bulletin*, 88, 1813-1827.

Rühlemann, C., Mulitza, S., Müller, P.J., Wefer, G., Zahn, R., (1999) Warming of the tropical Atlantic Ocean and lowdown of thermohaline circulation during the last deglaciation. *Nature*, 402, 511-514.

Saettem, J., Pool, D.A.R., Ellingsen, K.L., Sejrup, H.P., (1992) Glacial geology of outer Bjornoyrenna, Southwestern Barents Sea. *Marine Geology*, 103, 15-51.

Schulz, H.M., Schoner, A., Emeis, K.C., (2000) Long-chain alkenone patterns in the Baltic Sea - an ocean-freshwater transition. *Geochimica et Cosmochimica Acta*, 64, 469-477.

Scourse, J.D., Hall, I.R., McCave, I.N., Young, J.R., Sugdon, C., (2000) The origin of Heinrich layersL evidence from H2 for European precursor events. *Earth and Planetary Science Letters*, 182, 187-195.

Sigmond, E.M.D., (1992) Bedrock map of Norway and adjacent ocean areas. Scale 1:3 million. Geological Survey of Norway.

Silgoner, I., Krska, R., Lombas, E., Gans, O., Rosenberg, E., Grasserbauer, M., (1998) Microwave Assisted Extraction Of Organochlorine Pesticides From Sediments And Its Application To Contaminated Sediment Samples. *Fresenius' Journal of Analytical Chemistry*, 362, 120-124.

Simoneit, B.R.T., (1977) Organic matter in eolian dusts over the Atlantic Ocean. *Marine Chemistry*, 5, 443-464.

Simoneit, B.R.T., Mazurek, M.A., (1982) Organic matter in the troposphere- II Natural Backgraound of biogenic lipids matter in aerosoles over the rural western United States. *Atmospheric environment*, 16, 2139-2159.

Smelror, M., (1999) Pliocene-Pliestocene and redeposited kinoflagellate systs from the western Svalbqard Margin (Site 986): biostratigraphy, pleoenvironments and sediment provenance. In: T.D. Herbert (Ed.), *Proc. ODP, Scientific Results., 162* (Ed. by T.D. Herbert), pp. 83-97. Ocean Drilling Program, College Station, TX.

Snoechx, H., Grousset, F.E., Revel, M., Boelaert, A., (1999) European contribution of ice-rafted sand to Heinrich layers H3 and H4. *Marine Geology*, 158, 197-208.

Snoeckx, H., Grousset, F.E., Revel, M., Boelaert, A., (1999) European contribution of ice-rafted sand to Heinrich layers H3 and H4. *Marine Geology*, 158, 197-208.

Stoker, M.S., (1995) The influence of glacigenic sedimentation on slope-apron development on the continental margin off Northwest Britain. In: R.A. Scrutton, M.S. Stoker, G.B. Shimmeld, A. Tudhope (Eds.), *The Tectonics, Sedimentation and Palaeoceanography of the North Atlantic #region, 90, Geological society special publication* (Ed. by R.A. Scrutton, M.S. Stoker, G.B. Shimmeld, A. Tudhope), pp. 159-177.

Stokes, C., Clark, C., (2001) Palaeo-ice streams. *Quaternary Science Reviews*, 20, 1437-1457.

Stoner, J.S., Channell, J.E.T., Hillaire-Marcel, C., (1996) The magnetic signature of rapidly deposited detrital layers from the deep Labrador Sea: Relationship to North Atlantic Heinrich layers. *Paleoceanography*, 11, 309-325.

Stoner, J.S., Channell, J.E.T., Hillaire-Marcel, C., (1998) A 200 ka geomagnetic chronostratigraphy for the Labrador Sea: Indirect correlation of the sediment record to SPECMAP. *Earth and Planetary Science Letters*, 159(3-4), 165-181.

Stoner, J.S., Channell, J.E.T., Hillaire-Marcel, C., Kissel, C., (2000) Geomagnetic paleointensity and environmental record from Labrador Sea core MD95-2024: global marine sediment and ice core chronostratigraphy for the last 110 kyr. *Earth and Planetary Science Letters*, 183(1-2), 161-177.

Summerhayes, C.P., Kroon, D., Rosell-Mel,, A., Jordan, R.W., Schrader, H.J., Hearn, R., Grimalt, J.O., Eglinton, G., (1995) Variability in the Benguela Current upwelling system over the past 70,000 years. *Progress in Oceanography*, 35, 207-251.

Sundararaman, P., Gallegos, E.J., Baker, E.W., Slayback, J.R.B., Johnston, M.R., (1984) Hydrogen chemical ionization tandem mass spectroemtry of metalloporphyrins. *Analytical Chemistry*, 56, 2552-2556.

Tamburini, F., Huon, S., Steinmann, P., Grousset, F.E., Adatte, T., Fllmi, K.B., (2002) Dysaerobic conditions during Heinrich events 4 and 5: Evidence from phosphorus distribution in a North Atlantic deep-sea core. *Geochimica et Cosmochimica Acta*, 66(23), 4069-4083.

Taylor, J., Dowdeswell, J.A., Kenyon, N.H., O Cofaigh, C., (2002) Late Quaternary architecture of trough-mouth fans:debris flows and suspended sediments on the Norwegian margin. In: C. O Cofaigh (Ed.), *Glacier-Influenced Sedimentation on High-Latitude Continental Margins., 203* (Ed. by C. O Cofaigh), pp. 55-71. Geological Society, London, Special publications., London.

Taylor, K.C., Lamorey, G.W., Doyle, G.A., Alley, R.B., Grootes, P.M., Mayewski, P.A., White, J.W.C., Barlow, L.K., (1993) The 'flickering switch' of late Pleistocene climate change. *Nature*, 361, 432-436.

Ternois, Y., Kawamura, K., Keigwin, L., Ohkouchi, N., Nakatsuka, T., (2001) A biomarker approach for assessing marine and terrigenous inputs to the sediments of Sea of Okhotsk for the last 27,000 years. *Geochimica et Cosmochimica Acta*, 65(5), 791-802.

Thomson, J., Higgs, N.C., Clayton, T., (1995) A geochemical criterion for the recognition of Heinrich events and estimation of their depositional fluxes by the $(^{230}Th_{excess})_0$ profiling method. *Earth and Planetary Science Letters*, 135, 41-56.

Thomson, J., Nixon, S., Summerhayes, C.P., Schönfeld, J., Zahn, R., Grootes, P.M., (1999) Implications for sedimentation changes on the Iberian margin over the last two glacial/interglacial transitions from $(^{230}Th_{excess})_0$ systematics. *Earth and Planetary Science Letters*, 165, 255-270.

Thouveny, N., Moreno, E., delanghe, D., Candon, L., Lancelot, Y., Shackleton, N.J., (2000) Rock magnetic detection of distal ice-rafted debries: clue for the identification of Heinrich layers on the Portuguese margin. *Earth and Planetary Science Letters*, 180, 61-75.

Tissot, B.P., Welte, D.H., (1984) *Petroleum Formation and Occurrence*. Springer-Verlag, New York.

Tomaniová, M., Hajšlová, J., Kocourek, V., Holadová, K., Klímová, I., (1998) Microwave-assisted Solvent Extraction - a New Method for Isolation of Polynuclear Aromatic Hydrocarbons from Plants. *A Journal of Chromatography*, 827, 21-29.

van Kreveld, S., (2000) Potential links between surging ice sheets, circulation changes and the dansgaard-Oeschger cycles in the Irminger Sea 60-18 kyr. *Paleoceanography*, 15(425-442).

Vance, D., Archer, C., (2002) Isotopic constraints on the origin of Heinrich event precursors. *Geochimica et al Cosmochimica Acta*, 66(Suppl.1), A798.

Veiga-Pires, C.C., Hillaire-Marcel, C., (1999) U and Th isotope cinstraints on the duration of Heinrich eventa H0-H4 in the southeastern Labrador Sea. *Paleoceanography*, 14, 187-199.

Vidal, L., Labeyrie, L., Cortijo, E., Arnold, M., Duplessy, J.-C., Michel, E., Becqué, S., van Weering, T.C.E., (1997) Evidence for changes in the North Atlantic Deep Water linked to meltwater surges during the Heinrich events. *Earth and Planetary Science Letters*, 146, 13-27.

Villanueva, J., Gromalt, J.O., Cortijo, E., Vidal, L., Labeyrie, L., (1997) A biomarker approach to the organic matter deposited in the North Atlantic during the last climatic cycle. *Geochimica et Cosmochimica Acta*, 61, 4633-4646.

Voelker, A., Sarnthein, M., Grootes, P., Erlenkeuser, H., Laj, C., Mazaud, A., Nadeau, M.-J., Schleicher, M., (1998) Correlation of marine ^{14}C ages from the Nordic Seas with the GISP2 isotope recird: Implications for ^{14}C calibration beyond 25 ka BP. *Radiocarbon*, 40(1-2), 517-534.

Volkman, J., Holdsworth, D.G., Neill, G.P., Bavor, H.J.J., (1992) Identification of natural, anthropogeic and petroleum hydrocarbons in aquatic sediments. *The Science of the Total Environment*, 112, 203-219.

Volkman, J.K., Eglinton, G., Corner, E.D.S., Sargent, J.R., (1980) Novel unsaturated straight-chain C37-C39 methyl and ethyl ketones in marine sediments and coccolithophore Emiliana huxleyi. In: J.R. Maxwell (Ed.), *Advances in Organic Geochemistry 1979* (Ed. by J.R. Maxwell), pp. 219-227. Pergamon, Oxford.

Vorren, T.O., Laberg, J.S., (1997) Trough mouth fans - palaeoclimate and ice-sheet monitors. *Quaternary Science Reviews*, 16, 856-881.

Vorren, T.O., Lebesbye, E., Andereassen, K., Larsen, K.-B., (1989) Glacigenic sediments on a passive continental margin as exemplified by the Barents Sea. *Marine Geology*, 85, 251-272.

Wagner, T., Henrich, R., (1994) Organo- and Lithofacies of glacial-interglacial deposits in the Norwegian-Greenland Sea: Responses to paleoceanographic and paleoclimatic changes. *Marine Geology*, 120, 335-364.

Wagner, T., Hölemann, J.A., (1995) Deposition of organic matter in the Norwegian-Greenland Sea during the past 2.7 million years. *Quaternary Resaerch*, 44, 355-366.

Wang, D., Hesse, R., (1996) Continental slope sedimentation adjacent to an ice-margin. II. Glaciomarine depositional facies on Labrador Slope and glacial cycles. *Marine Geology*, 135, 65-96.

Yokoyama, Y., Esat, T.M., Lambeck, K., (2001) Coupled climate and sea-level changes deduced from Huon Peninsula coral terraces of the last ice age. *Earth and Planetary Science Letters*, 193, 579-587.

Zaragosi, S., Eynaud, F., Pujol, C., Auffret, G.A., Turon, J.-L., Garlan, T., (2001) Initiation of the European deglaciation as recorded in the northwestern Bay of Biscay slope environments (Meriadzek Terrace and Trevelyan Escarpment): a multy-proxy approach. *Earth and Planetary Science Letters*, 188, 493-507.